UTILIZATION OF CO_2 FOR PRESSURE MAINTENANCE AND IMPROVING OIL RECOVERY IN HEAVY OIL RESERVOIRS

A Thesis

Submitted to the Faculty of Graduate Studies and Research

In Partial Fulfillment of the Requirements

For the Degree of

Master of Applied Science

In

Petroleum Systems Engineering

University of Regina

By

Sixu Zheng

Regina, Saskatchewan

July, 2012

UNIVERSITY OF REGINA

FACULTY OF GRADUATE STUDIES AND RESEARCH

SUPERVISORY AND EXAMINING COMMITTEE

Sixu Zheng, candidate for the degree of Master of Applied Science in Petroleum Systems Engineering**,** has presented a thesis titled, ***Utilization of CO_2 for Pressure Maintenance and Improving Oil Recovery in Heavy Oil Reservoirs,*** in an oral examination held on June 22, 2012. The following committee members have found the thesis acceptable in form and content, and that the candidate demonstrated satisfactory knowledge of the subject material.

External Examiner:	Dr. Hussameldin Ibrahim, Industrial Systems Engineering
Supervisor:	Dr. Daoyong Yang, Petroleum Systems Engineering
Committee Member:	Dr. Farshid Torabi, Petroleum Systems Engineering
Committee Member:	*Dr. Fanhua Zeng, Petroleum Systems Engineering
Chair of Defense:	Dr. Zhou Zhang, Faculty of Business Administration

*Not present at defense

ABSTRACT

Tremendous resources of heavy oil are located in Western Canada, i.e., Alberta and Saskatchewan, most of which are contained in thin payzones. Thermal-based techniques have conventionally been utilized to enhance heavy oil recovery. However, characteristics of these thin reservoirs result in excessive heat losses to adjacent formations, leading to thermal-based techniques ineffective and uneconomical in such heavy oil formation. Although pressure maintenance via gas injection has been applied in light and medium oil reservoirs, few attempts have been made to evaluate performance of CO_2 injection for such purpose in a heavy oil reservoir. It is of practical and fundamental importance to evaluate suitability of pressure maintenance and improving heavy oil recovery with CO_2 injection in thin payzones where other enhanced oil recovery (EOR) techniques are not applicable.

In this thesis study, techniques have been developed to experimentally and numerically evaluate performance of CO_2 injection in heavy oil reservoirs for the purpose of pressure maintenance and improving oil recovery. Experimentally, a three-dimensional (3D) displacement model consisting of five vertical wells and three horizontal wells is used to evaluate the performance of waterflooding-CO_2 injection, waterflooding and CO_2-alternating-water (CO_2 WAG), and continuous CO_2 injection processes, respectively. Three well configurations have been designed to examine their effects on heavy oil recovery. The corresponding initial oil saturation, oil production rate, water cut, oil recovery and residual oil saturation distribution are examined under various operating conditions. Subsequently, numerical simulation is performed to match the experimental measurements and optimize the operating parameters.

It is found that utilization of CO_2 for pressure maintenance is beneficial for heavy oil recovery and that well configuration plays a crucial role in enhancing oil recovery. The well configurations with horizontal well(s) are found to control a larger reservoir area and initiate a better sweep efficiency, leading to higher oil recovery. There exists an excellent agreement between the numerically simulated and experimentally measured oil recovery, demonstrating that numerical simulation has captured the overall mechanisms of both the waterflooding-CO_2 injection process and waterflooding-CO_2 WAG process. The optimum WAG ratio is determined to be 0.75 and 1.00 for two CO_2 WAG processes, respectively.

To facilitate screening a right candidate for pressure maintenance with CO_2 injection in heavy oil reservoirs, screening criteria associated with reservoir temperature, pressure, API gravity, oil saturation, net pay thickness and permeability have been developed. The central composite design (CCD) technique is successfully used to design reservoir simulation strategies. Three response surface models with good statistics have been developed based on the simulation results. Pressure and API gravity are found to be the most influential reservoir properties on the performance of CO_2 injection in heavy oil reservoirs. It is convenient and efficient to screen and rank the candidate reservoirs on the basis of oil recoveries that are evaluated through the newly proposed response surface models.

ACKNOWLEDGEMENTS

I sincerely wish to acknowledge my academic supervisor, Dr. Daoyong (Tony) Yang, for his excellent guidance, continuous encouragement, and strong support throughout the course of this thesis study.

I also wish to acknowledge the following individuals and organizations for their support and encouragement during my MASc study at the University of Regina.

- My past and present research group members: Dr. Mohamed Arhuoma, Dr. Heng Li, Dr. Shengnan Chen, Mr. Chuck Egboka, Mr. Huazhou Li, Mr. Yin Zhang, Mr. Feng Zhang, Mr. Chengyao Song, Ms. Min Yang, Ms. Xiaoli Li, Ms. Ping Yang, and Mr. Deyue Zhou for their useful technical discussions and assistance;
- Natural Sciences and Engineering Research Council of Canada (NSERC) for the Discovery Grant and the Collaborative Research and Development (CRD) Grant, respectively;
- Petroleum Technology Research Center (PTRC) for the research fund to Dr. Daoyong (Tony) Yang;
- Faculty of Graduate Studies and Research (FGSR) at the University of Regina for awarding the Teaching Assistantship (2010 Fall), the Graduate Scholarship (2011 Fall);
- Many friends who have extended their encouragement and friendship to me during my study in Regina.

DEDICATION

To my beloved parents, Mrs. Xiuxia Zhang and Mr. Jiuxing Zheng, for their continuous support and unconditional love.

TABLE OF CONTENTS

LIST OF TABLES

LIST OF FIGURES

NOMENCLATURE

Notations

a_i , a_{ii} , a_{ij}	Coefficients of response surface model as defined in Equation [4.1]
a_0	Intercept term of response surface model as defined in Equation [4.1]
A	Computed intercept of best-fit line for Equation [2.2]
A_o	Oil API gravity, °API
b	Computed slope of best-fit line for Equation [2.2]
GOR	Gas-oil ratio, scf/STB
k	Absolute permeability, mD
k_H	Horizontal permeability, mD
k_V	Vertical permeability, mD
k_{rg}	Relative permeability to gas for the liquid-gas system
k_{rw}	Relative permeability to water for the water-oil system
k_{rog}	Relative permeability to oil for the liquid-gas system
k_{row}	Relative permeability to oil for the water-oil system
P	Pressure, MPa
P_i	Initial reservoir pressure, kPa

R_s	CO_2 solubility, mol%
R_{sc}	CO_2 solubility, scf/bbl
S_g	Gas saturation, %
S_w	Water saturation, %
S_{oi}	Initial oil saturation, %
S_{wi}	Initial water saturation, %
SF	Swelling factor
SG	Specific gravity
T	Temperature, °C
T_r	Reduced temperature
V_{m1}	Molar volume of CO_2 saturated oil at saturation temperature and atmospheric pressure
V_{m2}	Molar volume of CO_2 saturated oil at saturation temperature and saturation pressure
V_O	Volume fraction of oil in the mixture, %
V_S	Volume fraction of solvent in the mixture, %
MW	Oil molecular weight, g/mol
x_i	Linear term of response surface model as defined in Equation [4.1]

x_i^2 Quadratic term of response surface model as defined in Equation [4.1]

x_{ni} Normalized value for parameter i as defined in Equation [4.2]

x_{oi} Original value for parameter i as defined in Equation [4.2]

$x_i x_j$ Interaction term of parameters i and j for response surface model as defined in Equation [4.1]

$x_{oi,max}$ Maximum original value for parameter i as defined in Equation [4.2]

$x_{oi,min}$ Minimum original value for parameter i as defined in Equation [4.2]

Greek letters

α Empirical constant

γ_o Oil specific gravity

γ_s Solvent specific gravity

δ Binary interaction coefficient

μ_m Mixture viscosity, mPa·s

μ_o Oil viscosity, mPa·s

μ_s Solvent viscosity, mPa·s

ϕ Porosity, %

ω Acentric factor

Subscript

n	Normalized
o	Original

CHAPTER 1 INTRODUCTION

1.1 Heavy Oil Resources and Recovery Techniques

Since conventional oil reserves are depleting in many countries and the global energy consumption is still increasing, heavy oil resources have drawn much more attention to sustain the global energy demands. Heavy oil not only accounts for more than double the conventional oil resources in the world, but also offers potentiality to satisfy current and future oil demand (Speight, 2009). Heavy oil is characterized by high viscosities and low API gravities compared with that of the conventional oils. Due to its high viscosity and fast depletion of reservoir pressure, it is a great challenge to recover such heavy oil resources economically and effectively.

Western Canada (i.e., Alberta and Saskatchewan) holds tremendous heavy oil and bitumen resources with an estimated original-oil-in-place (OOIP) of 5.7 billion m^3 in Alberta (AEUB, 2007) and 3.4 billion m^3 in Saskatchewan (Saskatchewan Energy and Resources, 2008), respectively. Three of the most important deposits in Alberta are the Athabasca Wabiskwa-McMurray, the Cold Lake Clearwater and Peace River Bluesky-Gething deposits (ERCB, 2011). In Saskatchewan, the heavy oil is found in the sands of Bakken formation (Mississippian) and the Mannville group (Lower Cretaceous). In geography, these deposits are situated in west-central Saskatchewan (Wilson and Bennett, 1985).

Generally, two approaches have been used for recovery of heavy oil and bitumen: open pit mining and in-situ methods, depending upon the depth of the deposit (ERCB, 2009). Open pit mining method is used to recover the crude bitumen reserves that occur

near the surface. In this way, overburden is removed, oil sand is mined, and bitumen is extracted from the sand in facilities using hot water. Although open pit mining has high recovery efficiency, mining susceptible reserves only occupy approximately 5% of Canadian heavy oil and bitumen deposits (Das and Butler, 1994). In contrast with open pit mining technique, the in-situ recovery method is applicable to the heavy oil reserves at a greater depth. In addition, it is more economical and environmentally friendly because the in-situ recovery method disturbs less land and averts sand disposal. Therefore, considerable research interest has been focused on in-situ recovery processes.

In general, in-situ recovery processes are classified into two categories: thermal recovery processes and no-thermal recovery processes. The key to producing heavy oil is to reduce oil viscosity, accomplishing by thermal recovery processes which use heat to achieve heavy oil/bitumen viscosity reduction in-situ (Farouq Ali, 2002). Thermal recovery processes include the cyclic steam stimulation (CSS) process (Vittoratos *et al*., 1990; Denbina *et al*., 1991), steam flooding, steam-assisted gravity drainage (SAGD) process (Butler *et al.*, 1981), and in-situ combustion (ISC) process. Thermal recovery techniques seem to be effective as the oil viscosity is very sensitive to temperature. Among the many thermal-based methods proposed for heavy oil recovery, by far the most successful ones are based on steam injection in some form (Farouq Ali, 2002). However, tremendous heavy oil reserves are contained in thin payzones with thickness of less than 10 m or even less than 5 m (Srivastava *et al*., 1999), resulting in thermal-based processes ineffective or uneconomical due to excessive heat losses to overburden and underburden or adjacent aquifer. Due also to the burning of fuels for steam generation, a relatively high environmental footprint also restricts the application of thermal recovery

processes. Meanwhile, great water consumption is another major restriction for the thermal-based processes in some areas.

In comparison with thermal-based recovery processes, no-thermal recovery techniques have been investigated and applied in the past few decades because of their less energy consumption and good applicability to thin formations. The cold heavy oil production with sand (CHOPS) is one of the no-thermal in-situ recovery processes, in which heavy oil and bitumen are produced with sand under solution-gas drive by using progressive cavity pumps (Smith, 1988). CHOPS is an option for unconsolidated sand formation with good gas-oil ratio (GOR), but the effects of dilation caused by sand production may make it difficult to conduct follow-up approaches, such as steam injection (Farouq Ali, 2002).

Recently, solvent-based no-thermal recovery processes have attracted increasing interests in enhancing heavy oil recovery. Such processes include vapour extraction (VAPEX) process (Butler and Mokrys, 1991; Mokrys and Butler 1993; Das, 1998; Boustani and Maini, 2001; Samane *et al*., 2009), cyclic solvent injection (Lim *et al*., 1995; Li *et al*., 2008), CO_2 injection (Ala and Earlougher, 1981; Dyer and Farouq Ali, 1989), and light hydrocarbon flooding (Garcia and Meneven, 1983; Wu and Kantzas, 2008). The primary oil recovery mechanism in these processes is to reduce the heavy oil viscosity through solvent dissolution rather than heat. The major technical challenges associated with thermal recovery processes, such as heat losses, water consumption, and produced water treatment, are avoided in solvent-based recovery processes (Das and Butler, 1998). In addition, utilization of CO_2 for heavy oil recovery can not only improve oil recovery but also achieve great environmental benefits due to the storage of CO_2 in reservoirs.

1.2 Importance of Utilization of CO_2 Injection in Heavy Oil Reservoirs

In Western Canada, most of heavy oil reserves are contained in thin formations and the primary oil recovery is very low (Dyer and Farouq Ali, 1989; Srivastava *et al*., 1999). Due to the nature of such resources, it is required to implement one or combination of secondary or tertiary oil recovery techniques in order to continue economic production of these oil resources. Although waterflooding is a widely used recovery approach in conventional oil reservoirs, it yields early breakthrough and low oil recovery in heavy oil reservoirs due to adverse mobility ratio of injected water to heavy oil. Thermal-based recovery processes expose the apparent weaknesses, such as excessive heat losses and great water consumption, in thin heavy oil reservoirs. VAPEX evolves from the SAGD concept, in which solvents (e.g., butane and propane) rather than steam are injected (Das and Butler, 1998). As with SAGD, thin thickness weakens the role of gravity drainage during VAPEX process. Furthermore, relatively low reservoir temperature and expensive solvents make VAPEX not economically or technically feasible in thin heavy oil reservoirs. By contrast, CO_2 shows a considerable potential of recovering thin heavy oil reservoirs.

A number of laboratory studies and field tests have been conducted to explore the feasibility of CO_2 in enhancing oil recovery processes, and satisfactory results are acquired in light and medium oil reservoirs (Holm, 1959; Menzie and Nielsen, 1963; Mungan, 1981; Lin, 1983; McDonald *et al*., 1985; Srivastava and Huang, 1997; Pyo *et al.*, 2003). Due to the characteristics of high viscosity and low API gravity, it is difficult to achieve miscibility between the injected CO_2 and heavy oil. Although it is less effective, immiscible CO_2 injection can still contribute to increasing oil recovery by initiating

viscosity reduction, oil swelling, interfacial tension reduction, solution-gas drive and blowdown recovery (Holm and O'Brien, 1971; Jha, 1986; Rojas and Farouq Ali, 1988).

The solubility of CO_2 in crude oil is higher than that of natural gas and air, while CO_2 dissolves readily in heavy oil and bitumen, which is beneficial for oil recovery (Beecher and Parkhurst, 1926; Rojas and Farouq Ali, 1988). Compared with CO_2, ethane and propane can be used as solvents to reduce oil viscosity; however, their respective vapor pressures are relatively low. In addition, ethane and propane are expensive commodities. Therefore, CO_2 is considered to be a more promising agent for enhancing oil recovery in heavy oil reservoirs. Pressure maintenance via gas injection has been applied in light and medium oil reservoirs; however, few attempts have been made to evaluate performance of CO_2 injection for such purpose in a heavy oil reservoir. It is of practical and fundamental importance to evaluate suitability of pressure maintenance and improving heavy oil recovery with CO_2 injection in thin payzones where other enhanced oil recovery (EOR) techniques are not applicable.

1.3 Purpose of This Thesis Study

The purpose of this thesis study is to comprehensively investigate the suitability of utilization of CO_2 for pressure maintenance and improving oil recovery in heavy oil reservoirs. The primary objectives of this study include:

1) To investigate the effect of CO_2 pressure maintenance on ultimate oil recovery in heavy oil reservoirs through a three-dimensional (3D) physical model consisting of five vertical wells and three horizontal wells.

2) To design different well configurations and examine the effect of well configuration on pressure maintenance with CO_2 injection.
3) To evaluate performance of CO_2 flooding in a waterflooded reservoir, continuous CO_2 flooding and water-alternating-CO_2 flooding processes, respectively.
4) To perform numerical simulation to match the experimental displacement measurements so that processes of pressure maintenance with CO_2 injection can be optimized.
5) To develop screening criteria for screening right reservoir candidates for pressure maintenance with CO_2 injection in heavy oil reservoirs.

1.4 Outline of the Thesis

This thesis is composed of five chapters. More specifically, Chapter 1 is an introduction to the thesis topic together with its major research objectives and scope. Chapter 2 provides an updated literature review on the approaches of pressure maintenance in heavy oil reservoirs. It also includes the main mechanisms associated with CO_2 EOR in heavy oil reservoirs. Chapter 3 presents experimental and numerical determination of oil recovery by using pressure maintenance with CO_2 injection under various well configurations. Chapter 4 details the methodology for developing response surface models, and further the screening criteria for pressure maintenance with CO_2 injection in heavy oil reservoirs. Finally, Chapter 5 summarizes the major scientific findings of this study and provides some recommendations for future research.

CHAPTER 2 LITERATURE REVIEW

Reservoir pressure is a crucial factor that plays a vital role in oil recovery, though it will inevitably decrease as fluid production continues. In order to achieve a high oil recovery, especially in heavy oil reservoirs, it is necessary to maintain reservoir pressure during production process. Due to high viscosity, flow resistance of heavy oil in the formation is extremely high, while the initial reservoir pressure is relatively low and insufficient to compensate the loss of energy, leading to dramatic pressure depletion in a short period during exploitation. Thus, a large amount of heavy oil cannot be efficiently and economically recovered due to the depleted formation pressure.

Although reservoir pressure depletes naturally during production process, it has been well-recognized that pressure maintenance is an effective approach to extend the reservoir lifespan and thus improve the ultimate oil recovery. Bennett (1938) defined pressure maintenance as the practice of returning gas from flush production to the formation for the purpose of keeping reservoir pressure and energy as near initial conditions as possible. Gradually, pressure maintenance has been considered in its broad aspects, in which reservoir pressure is fully or partially maintained by injecting fluid(s) to increase oil recovery (Horner, 1945; Patton, 1947; Loomis and Shea, 1951; Paul, 1951; Kelly and Kennedy, 1965; Crawford, 1967; Boutette *et al*., 1990; David, 2004; Romanov and Zolnikova, 2008). In the past few decades, the following techniques have been investigated and implemented to maintain reservoir pressure.

2.1 Water Injection

Water injection has been used to maintain reservoir pressure and improve oil recovery in many light and medium oil reservoirs (Horner, 1945; Rogan and Smith, 1965; Park, 1966; Boutette *et al*., 1990; Sommerauer and Petersen, 2003; Guan *et al*., 2006). It is found that pressure depletion is successfully controlled by waterflooding and subsequently incremental production is achieved. In heavy oil reservoirs, water injection is often implemented, at least initially, either along with or after primary recovery, in order to re-pressurize the reservoir and displace oil to the producing wells (Mai, 2009).

In Saskatchewan and Alberta, water injection into heavy oil reservoirs has been operating for up to 50 years (Miller, 2005). As summarized by Adams (1982), waterflooding in Lloydminster heavy oil reservoirs showed a consistent performance with an ultimate oil recovery of some 9.5% of the original oil in place (OOIP) at 95% water cut. In practice, waterflooding initiated wormhole generation, aggravated areal sweep problem and severe channelling, demonstrating by the tracer tests. Smith (1992) discussed the water injection projects in Wainwright and Wildmere oilfields in which the unclean water plugged the formation. Such plugging segregates the reservoir into a high pressure zone near the injector(s) and a low pressure region in the rest of the pattern so that pressure maintenance of most of the reservoir cannot be accomplished. In addition, several production mechanisms were proposed as follows (Smith, 1992):

1) Pressure support of the injected water drives both phases independently toward a pressure sink at the producer;

2) Multi-phase expansion and flow in the formation. The gas bubble can block small pore throats, resulting in displacement of the flow either from a small to a large pore or from a water filled pore to an oil/gas filled one;
3) Water injection can be used to control GOR by preventing the continuous gas phase from developing, thereby making full use of the energy that comes from the expansion of an oil phase;
4) The imbibition process that water is imbibed into the matrix from the fractures and oil flows into fractures is similar to that of the naturally fractured reservoirs; and
5) Weak emulsion or micro-emulsion is formed as a result of native surfactants and in-situ foam formation, imposing a positive impact on oil transportation and displacement improvement.

Based on field cases and experimental studies, extensive efforts have been made to evaluate performances of water injection in heavy oil reservoirs (Forth *et al*., 1996; Kantzas and Brook, 2004; Turta *et al*., 2006). The corresponding findings are listed as follows:

1) Pressure maintenance in most of heavy oil reservoirs cannot be well accomplished by water injection;
2) Heavy oil waterfloodings exhibit very poor sweep efficiency, while water fingering and channelling are the conspicuous problems;
3) Converting producers to injectors, changing injection/production rates, and drilling infill wells will likely improve sweep efficiency; and

4) It is difficult to forecast performance of waterflooding projects in heavy oil reservoirs, while the most reliable method is to compare the candidate reservoir to an existing project with similar reservoir rock and fluid properties.

It is well-recognized that water breakthrough occurs very early during waterflooding in heavy oil reservoirs due to the adverse mobility ratio. Water channels lead to poor sweep efficiency and high water cut (Mai, 2009). If untreated, the injected water can damage formations, leading to a low injectivity around the wellbore of injector (Smith, 1992). Therefore, it is difficult to achieve good performance of pressure maintenance by water injection in heavy oil reservoirs.

2.2 Gas Injection

Pressure maintenance by gas injection has been proposed and implemented in oilfields since 1903. Bennett (1938) summarized the early projects of pressure maintenance by gas injection, in which the gas from flush production was re-injected into the formation for the purpose of keeping reservoir pressure as near initial conditions as possible. The early return of gas into the formation through its continuous injection not only effectively controls pressure drop, but also greatly increases oil recovery. The review of the performance of thirty years experience in the Hilbig Field demonstrated that pressure maintenance by gas injection yielded satisfactory results during the early life of the oilfield (Kelly and Kennedy, 1965). The desirable results of gas injection in light and medium oil reservoirs prompt the application of gas injection in heavy oil reservoirs for pressure maintenance purpose.

Several kinds of gases have been investigated and used to perform injection in heavy oil reservoirs, such as light hydrocarbons (i.e., methane and ethane), nitrogen, fuel gas, rich air (30% to 40% oxygen), and carbon dioxide (Bennett, 1938; Klins and Farouq Ali, 1982; Garcia and Meneven, 1983; Spivak and Chima, 1984; Jha and Chakma, 1991; Olenick *et al*., 1992; Zhang *et al*., 2000; Dong and Huang, 2002; Kuhlman, 2004; Dong *et al*., 2006; Sahin *et al*., 2007).

The most common way to categorize gas injection is based on miscibility, i.e., the minimum miscibility pressure (MMP), which is defined as the minimum pressure at which reservoir crude oil is miscible with the injected fluid(s). When the reservoir pressure is maintained equal to or higher than the MMP, the gas is considered to be miscible with the formation oil. Gas injection processes are more effective when the injected gas is near or completely miscible with the oil in the reservoirs. The miscible gas flooding is a complex process, which is dominated by several factors, such as reservoir temperature, pressure and fluid properties. Ideally, the miscibility can eliminate the interfacial tension (IFT), thus the capillary forces that trap the oil in the small pores disappear, leading to a significant increase in oil recovery (Arshad *et al*., 2009).

Although it is difficult to achieve miscibility during the process that gas injection is primarily intended for pressure maintenance, the injected gas contributes to an increase in productivity by increasing reservoir pressure and displaces oil from formation to producers. Furthermore, the dissolution of injected gas is beneficial for enhancing oil recovery. A large reduction in the viscosity of crude oil occurs as it is saturated with gas (e.g., CO_2) at increasing pressure (Holm and Josendal, 1974). When the gas dissolves in

oil, an increase in liquid volume (i.e., swelling effect) will occur. More oil, especially in small pores and end pores, could be mobilized due to the swelling effect.

The overall efficiency of the gas injection process depends on both the microscopic and the macroscopic sweep efficiencies. More specifically, the mobility ratio controls the areal sweep efficiency in a reservoir, while the vertical sweep efficiency is controlled by the density difference between the injected and displaced fluids. The overall poor volumetric sweep efficiency is the main concern in a gas injection project. It is critical to control the displacement front for a successful gas injection process due to its unfavourable mobility ratio.

Numerous efforts have been made to improve the displacement fronts in a gas injection process. Foams can be used to perform mobility control in a gas flooding process, leading to a higher foam resistance in formations with a higher permeability (Zhu *et al*., 1998). This will be beneficial for mitigating the fluid channelling in fractures and high permeability channels. Enick *et al*. (2000) designed and synthesized the direct thickeners for dense carbon dioxide, inducing a significant increase in gas viscosity to improve the gas-oil mobility ratio. The effects of coupling immiscible CO_2 and polymer injection on heavy oils were also investigated (Zhang *et al*., 2010). It is found that the coupled CO_2 and polymer injection process has much better gas utilization than the water-alternating-CO_2 process.

Gas injection has a great potential to successfully maintain reservoir pressure and improve oil recovery, especially in water-sensitive, tight and thin reservoirs (Dello *et al*., 1996; Singhal *et al*., 2008). Due to the low viscosity and high mobility ratio of gas to liquid, gas fingering and channelling tends to occur in heavy oil reservoirs. As such,

mobility ratio control is the main concern in gas injection, while displacement front stability is the key to the successful projects of pressure maintenance with gas injection.

2.3 Water-alternating-gas (WAG) Processes

Pressure maintenance by gas injection shows a strong ability to achieve higher oil recovery compared to water injection because of higher microscopic displacement efficiency. The problem, however, is the high mobility of the gas that limits the vertical and the areal sweep efficiencies. In recent years, the so-called WAG process has attracted increasing interest. The WAG process is a cyclic method of injecting alternating cycles of gas followed by water and repeating this process over a number of cycles. WAG injection combines the improved microscopic displacement efficiency of the gas flooding with improved macroscopic sweep efficiency by injecting water.

Christensen *et al*. (2001) presented a comprehensive review of field experience on WAG processes. Because of failure to maintain sufficient pressure, meaning loss of miscibility, real field cases may oscillate between miscible and immiscible flooding during the life of the oil production. There have been numerous immiscible or miscible WAG processes with favourable performance, such as the Kuparuk field (Shi *et al*., 2008), Neuquen Basin (Righi and Pascual, 2007), Weyburn field (Asghari *et al*., 2007), and Pubei Oilfield (Yang *et al*., 2000). WAG processes have been mainly applied to maintain the reservoir pressure with the improved frontal stability. It may be appropriate in some reservoirs that are not suitable for miscible gas injection because of elevated temperature, low fracturing pressure and high MMP. As for improving heavy oil recovery with immiscible WAG injection, nitrogen in the injected gas did not have a detrimental

effect on oil recovery compared with that of pure CO_2, while the co-injection of a surfactant (foam) solution with CO_2 could improve the oil recovery, possibly due to a better sweep efficiency (Zhang *et al*., 2006).

The performance of a WAG process is significantly affected by reservoir heterogeneity, rock wettability, fluid properties, miscibility conditions, trapped gas, injection techniques and well operational parameters. Not only is performance of the WAG process largely affected by the injection parameters, including WAG ratio (i.e., water slug size to gas slug size), injection rate and cycle time, but also by the production parameters, including production rate and bottomhole pressure at the producer (Surguchev *et al*., 1992; Chen *et al*., 2010). Pariani *et al*. (1992) stated that high stratified reservoirs tended to have early gas breakthrough and high recycle rates. Decrease in the gas-water ratio (GWR) can be used to control gas breakthrough and recover incremental oil economically.

Certain efforts have been made to study the influence of wettability on WAG processes (Wang and Locke, 1980; Huang and Holm, 1988; Sohrabi *et al*., 2001; Tehrani *et al*., 2001). The largest amount of oil trapping occurs during the CO_2 WAG flood of preferentially water-wet reservoirs, while better oil recovery is achieved during WAG process when the reservoir is at mixed-wet and preferentially oil-wet states (Huang and Holm, 1988).

In particular, as one of crucial factors, WAG ratio affects the oil recovery and has its optimum value in a hydrocarbon reservoir. An improved oil recovery in a miscible CO_2-WAG process is achieved due to an increase in sweep efficiency and the highest oil recovery is achieved when the overall WAG ratio for the entire reservoir reaches 0.5

(Chen *et al*., 2010). As for the CO_2-WAG application in a heavy oil reservoir, a high rather than low WAG ratio is recommended, while a WAG ratio of 4:1 or 5:1 is found to be the optimum value (Rojas and Farouq Ali, 1986).

2.4 Mechanisms Associated with CO_2 Injection in Heavy Oil Reservoirs

In the early days, gas injection was primarily intended to maintain reservoir pressure with the purpose of increasing initial productivity due to increased reservoir pressure (Jha and Chakma, 1991). Although carbon dioxide (CO_2) is considered as the main anthropogenic greenhouse gas which causes the global warming, it shows a great potential to enhance oil recovery. Early works indicate that the solubility of CO_2 in crude oil is higher than that of natural gas and air and that CO_2 dissolves readily in heavy oil and bitumen, increasing oil volume while reducing its viscosity (Beecher and Parkhurst, 1926; Rojas and Farouq Ali, 1988).

Holm and Josendal (1974) summarized the mechanisms of CO_2 displacing oil from porous rocks: 1) promoting oil swelling, 2) reducing oil viscosity, 3) increasing oil density, 4) being highly soluble in water, 5) exerting an acidic effect on rock, and 6) vaporizing and extracting light components of crude oil. Heavy oil is characterized by high viscosity and low API gravity so that it is difficult for CO_2 to achieve miscibility with heavy oil. However, immiscible CO_2 injection can still contribute to oil recovery through several mechanisms, such as viscosity reduction, swelling effect, interfacial tension reduction, and blowdown recovery (Jha, 1986; Rojas and Farouq Ali, 1988). Therefore, the injected CO_2 not only acts a pressure maintenance agent, but also enhances oil recovery during pressure maintenance processes in heavy oil reservoirs.

2.4.1 Viscosity reduction

It will dissolve into crude oil when CO_2 is injected into a reservoir. Due to the dissolution of CO_2, the viscosity of crude oil is reduced, depending on pressure, temperature and properties of the oil. It is found that the oil viscosity is linearly decreased with CO_2 concentration (Srivastava *et al*., 2000; Enayati *et al*., 2008). For a given CO_2 concentration, viscosity is decreased with an increase in pressure at the first stage, and then increased slightly (Hao *et al*., 2004). Spivak and Chima (1984) asserted that the process of immiscible CO_2 flooding in heavy oil reservoirs can be considered as a process of viscosity reduction, while the presence of nitrogen along with CO_2 made less viscosity reduction of the oil due to the decreased solubility of CO_2 in oil in the presence of N_2. Viscosity reduction was also evaluated and analyzed by other researchers (Kantar *et al*., 1985; Huang *et al*., 1987; Hatzignatiou and Lu, 1994). It is observed that dissolution of CO_2 in oil causes a reduction in viscosity, contributing largely to improve flow properties and to enhance oil recovery. It is important to quantify viscosity reduction prior to evaluating the potential of heavy oil reservoirs with CO_2 injection.

In order to estimate the viscosity change of oil due to dissolution of gas, several correlations have been developed. Lederer (1933) presented an equation for mixture viscosity,

$$\ln \mu_m = \frac{V_s}{\alpha V_o + V_s} \ln \mu_o + \left(1 - \frac{V_s}{\alpha V_o + V_s}\right) \ln \mu_s \qquad [2.1]$$

where μ_m is mixture viscosity, μ_s is solvent viscosity, μ_o is oil viscosity, V_s and V_o are volume fractions of solvent and oil in the mixture, respectively, and α is an empirical constant in the range of 0 to 1.

Chew and Connally Jr. (1959) presented a correlation for the effect of dissolved gas on the oil viscosity,

$$\mu_m = A(\mu_o)^b \qquad [2.2]$$

where μ_o is viscosity of the dead oil at the reservoir temperature and atmospheric pressure, mPa·s. *A* and *b* are the computed intercepts and slopes of the best-fit line, respectively. The temperature of the data that are used to obtain the correlation is in the range of 22.22 to 144.44ºC; while the lowest and highest bubble point pressures are 132 psi and 5645 psi, respectively.

In 1965, Simon and Graue (1965) developed a graphical correlation, where the CO_2-dead oil viscosity was a function of the saturation pressure and initial oil viscosity at 48.89ºC. This correlation is the first calculation method, aiming at CO_2-crude oil system, but the graphical method is not convenient for computer calculation in addition to a large deviation with experimental data.

Lobe (1973) proposed the following mixing rule for calculating the viscosity of a solvent-diluted crude oil,

$$\mu_m = V_s\mu_s \exp(V_o\alpha_o) + V_o\mu_o \exp(V_s\alpha_s) \qquad [2.3a]$$

where

$$\alpha_o = 0.27\ln\left(\frac{\mu_o}{\mu_s}\right) + \left[1.3\ln\left(\frac{\mu_o}{\mu_s}\right)\right]^{0.5} \qquad [2.3b]$$

$$\alpha_s = -1.7\ln\left(\frac{\mu_o}{\mu_s}\right) \qquad [2.3c]$$

where V is the volume fraction, subscript s is the lower viscosity component (e.g., solvent), and subscript o is the higher viscosity component (e.g., oil).

Beggs and Robinson (1975) developed a correlation that neglected the dependence of oil viscosity on both composition and pressure. The correlation is presented as follows:

$$\mu_m = A\left(10^X - 1\right)^B \quad [2.4a]$$

where

$$X = 10^{\left(3.0324 - 0.02023 A_o\right)} \left(1.8T + 32\right)^{-1.163} \quad [2.4b]$$

$$A = 10.715\left(GOR + 100\right)^{-0.515} \quad [2.4c]$$

$$B = 5.44\left(R_s + 150\right)^{-0.338} \quad [2.4d]$$

where A_o is oil API gravity, °API, T is temperature, °C, and GOR is dissolved gas-oil ratio, scf/STB. The solution GOR is from 20 to 2,070 scf/STB, oil gravity is between 16 and 58ºAPI. The lowest and highest pressures are 0 psi and 5,250 psi, respectively, while the temperature is in the range of 2.11 to 146.11ºC.

In 1982, Mehrotra and Svrcek (1982) presented a correlation for CO_2-saturated bitumen as follows.

$$\log\log(\mu_m) = a_1 + a_2 T + a_3 P + \frac{a_4}{T + 273.16} P \quad [2.5]$$

where T is temperature, °C, P is pressure, MPa, and the empirical constants: $a_1 = 0.815991$, $a_2 = 0.0044495$, $a_3 = 0.076639$, and $a_4 = 34.5133$.

Shu (1984) extended the Lederer equation to higher viscosity ratios by using a generalized expression for the empirical constant α, which was expressed as a function of the component viscosities and densities on the basis of the experimental data for mixtures of heavy oils with light petroleum fractions,

$$\alpha = \frac{17.04\left(\gamma_o - \gamma_s\right)^{0.5237} \gamma_o^{3.2745} \gamma_s^{1.6316}}{\ln\left(\mu_o / \mu_s\right)} \qquad [2.6]$$

where γ_s and γ_o are specific gravities of the solvent and heavy oil, respectively. This correlation is examined with heavy oil/bitumen-solvent blending data with an excellent prediction of the mixture viscosities. However, this developed correlation is limited to organic solvents (e.g., kerosene) and cannot be extended to CO_2-heavy oil systems where CO_2 density may be higher than that of heavy oil at high pressures.

Quail *et al*. (1987) modified the Beggs-Robinson equation to fit the Saskatchewan heavy oil. Chung *et al*. (1988) obtained a modified α correlation that was a function of temperature, pressure and specific gravity of heavy oil. A generalized viscosity equation was proposed by Puttagunta *et al*. (1991) based on the Saskatchewan heavy oil database. Emera and Sarma (2008) used a genetic algorithm (GA)-based technique to develop the correlations to predict the CO_2-oil viscosity for both dead and live oils.

Viscosity is one of the most crucial properties that affect the CO_2 flooding efficiency. Viscosity reduction due to the dissolution of CO_2 is desirable for heavy oil recovery because of the reduced flow resistance of heavy oil and improved mobility ratio. Although the existing correlations can be used to determine oil viscosity, most of which

are applicable to certain kinds of oil and limited to certain conditions of pressures and temperatures.

2.4.2 Swelling effect

The dissolution of CO_2 into heavy oil causes an increase in the oil volume. The degree of swelling depends on pressure, temperature, crude oil composition and the mole fraction of CO_2 present in the crude oil. The relative permeability to oil will increase to some extent due to the swelling of reservoir oil. The importance of oil swelling was stated for two reasons: 1) the residual oil left in the reservoir is inversely proportional to the swelling factor; that is, the greater the swelling, the less the stock tank oil abandoned in the reservoir, 2) the swollen oil droplets will force water out of the pore spaces, creating the drainage rather than imbibitions process for water-wet systems (Mangalsingh and Jagai, 1996).

In 1963, Welker and Dunlop (1963) defined swelling factor (SF) as the volume of crude oil saturated with CO_2 at reservoir pressure and temperature divided by the volume of crude oil at atmospheric pressure (0.1 MPa) and reservoir temperature. This definition has become a norm in petroleum industry since its introduction. The swelling of heavy oil is mainly attributed to the dissolution of CO_2 into oil. Thereby, a strong dependence of the swelling factor on solubility is expected. The correlations presented by Welker and Dunlop (1963) can be used to predict CO_2 solubility and oil swelling if the dead state gravity and viscosity of the oils are known. The swelling data were correlated as a linear function of solubility at 26.67ºC. The function is presented as follows:

$$SF = 1.0 + (0.35R_{sc})/1000 \quad [2.7]$$

where R_{sc} is the solubility that could be determined from the correlation.

It is pointed out that swelling factor is a function of not only the amount of dissolved CO_2, but also the size of the oil molecules (Simon and Graue, 1965). The relationship among swelling factor, mole faction of the dissolved CO_2, and molecular size was correlated in a graphic form. As such, their correlations are not suitable for computer calculation or reservoir simulation studies. Furthermore, these correlations are not applicable for impure CO_2 or mixture gases, while there is no theoretical basis for extrapolation to other systems because their correlations are completely empirical.

It has been shown by Teja and Sandler (1980) that the swelling factor can be calculated by molar volume and molar solubility in the following form,

$$SF = \frac{V_{m2}}{V_{m1}} \times \frac{1}{1 - R_s} \quad [2.8]$$

where V_{m1} is the molar volume of CO_2-saturated oil at saturation temperature and atmospheric pressure, V_{m2} is the molar volume of CO_2 saturated oil at saturation temperature and saturation pressure, and R_s is the CO_2 solubility in mole percentage.

Mullken and Sandler (1980) treated the crude oil as a single pseudocomponent and characterized it with specific gravity and Watson K_w factor. They firstly calculated the solubility of CO_2 in crude oil and density of the mixture using Peng-Robinson equation of state (PR EOS) and then obtained the swelling factor of CO_2 saturated-oil with Equation [2.8]. A binary interaction coefficient formula was obtained by regressing the CO_2

solubility data,

$$\delta = 0.5010 - 0.3576T_r - 0.18285SG - 0.0961\omega \quad [2.9]$$

where δ is the binary interaction coefficient between CO_2 and oil, T_r, SG, and ω are the reduced temperature, specific gravity and acentric factor of crude oil, respectively. These parameters are calculated from the Lee-Kesler correlation (1976). Such a method shows a very accurate prediction of the swelling factor of various oils dissolved with CO_2, but the data range is narrow and the oil type is limited due to the fact that it is based on the same data used by Simon and Graue (1965).

Emera and Sarma (2008) proposed a swelling factor correlation as a function of the CO_2 solubility and oil molecular size. The oil is classified as the heavy oil if molecular weight (MW) $\geq$300, and light oil if MW <300, respectively.

For heavy oil ($MW \geq 300$):

$$SF = 1 + 0.3302Y - 0.8417Y^2 + 1.5804Y^3 - 1.074Y^4 - 0.0318Y^5 + 0.21755Y^6 \quad [2.10a]$$

where

$$Y = 1000.0 \times \left[\left(\left(\frac{\gamma}{MW} \right) \times R_s^{\,2} \right)^{\exp\left(\frac{\gamma}{MW}\right)} \right] \quad [2.10b]$$

For light oil (MW <300):

$$SF = 1 + 0.48411Y - 0.9928Y^2 + 1.6019Y^3 - 1.2773Y^4 + 0.48267Y^5 - 0.06671Y^6 \quad [2.10c]$$

where γ is oil specific gravity, MW is the oil molecular weight, R_s is the CO_2 solubility, mole fraction.

The Emera-Sarma correlation covers a wider range of oil gravity, pressure up to 34.5 MPa, oil *MW* greater than 490, oil viscosities up to 12,000 mPa·s, and temperature up to 140ºC. The GA-based correlation is empirical and lacking theoretical support. Sankur *et al*. (1986) carried out a laboratory experiment for a heavy oil-CO_2 system. At 48.89ºC and bubble point pressure, the swelling factors of oil with 20 mole%, 40 mole% and 60 mole% CO_2 are found to be 1.034, 1.080 and 1.195, respectively. The results show that the swelling of oil primarily depends on concentration of the dissolved gas.

Bon and Sarma (2004) conducted PVT tests with low viscosity oil (50ºAPI) at 137.22ºC. The relative volume was found to be a function of pressure for the increasing amount of gas injected, while the swelling at saturation pressure was measured to be 1.15, 1.42 and 1.97 at CO_2 concentration of 20, 40 and 60 mole%, respectively. Similar experiments were carried out by Hao *et al*. (2004), the swelling factor was as high as 1.4 in the test. Monger (1987) investigated the effects of contaminant gases (N_2, CH_4, H_2S and SO_2) on swelling factor of the CO_2-oil systems. For any given mixtures, the maximum swelling occurred at the bubble point. The mixture of CO_2 and SO_2 caused the greatest degree of swelling compared to other mixtures. This indicates that the mixture of CO_2 and SO_2 has the largest potential to enhance oil recovery.

By using the axisymmetric drop shape analysis (ADSA) for the pendant drop case, Yang and Gu (2004) observed the phenomenon of oil swelling when the crude oil is made in contact with CO_2, while the oil swelling process is indicated by the slowly increased volume of the oil drop and its equator diameter. The oil swelling factors of carbon dioxide, methane, ethane, propane, and their mixtures in heavy oil were determined (Yang and Gu, 2006). It is shown that propane has the largest oil swelling effect among

the four pure solvents (CO_2, CH_4, C_2H_6 and C_3H_8). In addition, significant amount of solvent mixture is dissolved into the heavy oil at their respective dew-point pressure, swelling the oil to a large extent.

The existing experimental results demonstrate that dissolution of CO_2 can cause the oil swelling and thus contributes to enhancing oil recovery. It is found that swelling effects are different due to the different amounts of CO_2 dissolved, while the swelling factor is increased with an increasing dissolution of CO_2 in certain pressure range (Dyer *et al*., 1994). It is worthwhile noting that EOS modeling of the CO_2-heavy oil systems provides an integrated method for predicting CO_2 solubility, mixture density, swelling factor, and even mixture viscosity.

2.4.3 Interfacial tension reduction

Although it is difficult to achieve miscibility between CO_2 and heavy oil, CO_2 can still decrease the interfacial tension (IFT). Reduction of interfacial tension leads to an increased capillary number and subsequently enhances oil recovery. Gasem *et al*. (1993) presented the smoothed low IFT data of CO_2/synthetic oil and CO_2/reservoir oil systems in the near-critical region. For heavy oil at moderate pressures (4.0-6.0 MPa) and temperatures (20-25ºC) with dissolved CO_2 of 50-100 m^3/m^3, a 30% reduction of interfacial tension can be observed (Mangalsingh and Jagai, 1996). The ADSA for pendant case was used to measure the interfacial tension of CO_2/heavy oil system at a temperature of 25ºC and pressures of 1.1 to 5.2 MPa (Yang and Gu, 2006). It is shown that the interfacial tension of CO_2/heavy oil system decreases linearly with the pressure in

the tested pressure range. The dissolved CO_2 acts as a surface-active agent, which induces the interfacial tension reduction.

The linear gradient theory (LGT) model, the simplified linear gradient theory (SLGT) model, the corresponding-states (CS) correlation, and the parachor method were extended to calculate the interfacial tensions of crude oil and gas condensate systems (Zuo and Stenby, 1998). To the exclusion of the near-critical region, the interfacial tensions calculated by all the models except the CS correlation were in a good agreement with the measured IFT data for several crude oil and CO_2-oil systems, while the SLGT model and the parachor model yielded better performance than that of the LGT model and CS correlation. The experimental measurements also indicated the addition of rich solvent(s) (e.g., C_3H_8 and *n*-C_4H_{10}) to the CO_2 stream resulted in an obvious reduction of IFT between CO_2 and Lloydminster heavy oil, while a mechanistic parachor theoretical model with the optimized parachor of Lloydminster heavy oil and the mass-transfer exponent was successfully used to qualitatively reproduce the measured IFTs between solvent(s) and heavy oil in the liquid-vapour phase region (Li *et al*., 2012).

IFT is one of the most important phase behaviour properties that affect CO_2 flooding efficiency (Yang and Gu, 2005). The dissolution of CO_2 reduces IFT of heavy oil, which contributes to heavy oil recovery because more residual oil can be displaced if the viscous forces acting on the trapped residual oil blobs to exceed the capillary retained forces (Chatzis and Morrow, 1984). Due to the interfacial tension reduction, pressure maintenance with CO_2 injection is favourable for enhancing oil recovery in heavy oil reservoirs.

2.4.4 Blowdown recovery

Blowdown recovery following an immiscible CO_2 flooding is very effective in recovering additional oil. Up to 30% of the initial oil-in-place may be recovered via solution gas drive mechanism during blowdown process (Jha, 1986). CO_2 is a gas that possesses a good ability to dissolve into oil, while energy stored by CO_2 when it goes into solution with an increase in pressure is released after flooding and continues to drive the oil to the producers (Mangalsingh and Jagai, 1996).

When some heavy oil reservoirs are produced by solution-gas drive, they show a higher than expected production rate, lower produced GOR, and a relatively higher recovery (Akin and Kovscek, 2002). In the Mead-Strawn field, CO_2 was injected during the process of water-alternating-CO_2 until 1968. Since the CO_2-waterflooded project was terminated, oil production lasted 5 more years by solution gas drive from the CO_2 remaining in the reservoir (Holm and O'Brien, 1971).

Rojas and Farouq Ali, (1986) studied the blowdown recovery as a function of pressure and found that high expansion of CO_2 at pressure below 1.0 MPa was the production mechanism of the blowdown phase of the floods, while most of the recovery was obtained at pressure below 1.0 MPa. Smith (1988) pointed out the high efficiency of solution gas drive in viscous oil due to: 1) a significant reduction oil viscosity because small gas bubbles were formed in the oil, 2) simultaneous flow of continuous oil phase and discontinuous gas phase in the form of tiny bubbles, and (3) high fluid compressibility resulting from high gas bubble density in the oil.

Akin and Kovscek (2002) conducted the core-scale experiments of solution-gas driving heavy oil with the help of X-ray computerized-tomography. The effect of gravity

segregation was observed, while a continuous gas phase accumulated at the top of the sandpack by gravity segregation. The influence of pressure decline rate and pressure gradient on solution gas drive in heavy oil were investigated (Sheikha and Pooladi-Darvish, 2009). It is indicated that the effect of pressure gradient on gas mobility and oil recovery is much more pronounced than that of pressure decline rate. Although mechanisms of solution gas drive in heavy oil reservoirs are not very well understood, the consensus has been reached on the following aspects (Holm and O'Brien, 1971; Smith, 1988; Bora *et al*., 2000; Firoozabadi, 2001; Akin and Kovscek, 2002; Sheikha and Pooladi-Darvish, 2009): 1) formation of small gas bubble in oil significantly reduces the oil viscosity, 2) high oil viscosity coupled with high flow velocity keeps the gas dispersed in the oil, and 3) recovery efficiency of solution gas drive is high in heavy oil due to very low gas mobility.

Blowdown recovery is a function of oil viscosity, gas saturation, pressure gradient and pressure decline rate in heavy oil. Furthermore, gravity segregation will occur in reservoirs during the blowdown process, while expansion of gas phase on the top of reservoir can provide the energy for draining oil.

2.5 Summary

Due to the adverse mobility ratio, pressure maintenance cannot be well accomplished by water injection in heavy oil reservoirs. Gas (e.g., CO_2) injection has recently attracted an increasing interest in pressure maintenance and improving oil recovery, while most of CO_2 injection projects are implemented in light or medium reservoirs. In addition to energy support, CO_2 injection contributes to oil recovery in

heavy oil reservoirs, resulting from viscosity reduction, swelling effect, interfacial tension reduction, and blowdown recovery through an immiscible process. The performance of pressure maintenance and improving oil recovery with CO_2 injection in heavy oil reservoirs has not been well investigated, though few attempts have been made to evaluate the effects of well configurations during the process of CO_2 injection. It is of practical and fundamental importance to evaluate suitability of pressure maintenance and improving oil recovery with CO_2 injection in heavy oil reservoirs.

CHAPTER 3 PRESSURE MAINTENANCE AND OIL RECOVERY

In this chapter, an experimental system is developed to examine the performance of pressure maintenance with CO_2 injection in a heavy oil reservoir. The major component of this experimental system is a three-dimensional (3D) displacement model consisting of five vertical wells and three horizontal wells. The performance of pressure maintenance with CO_2 injection has been examined under various well configurations (Zheng *et al.*, 2011). Subsequently, numerical simulation is performed to match the results of experimental displacements so that the processes of CO_2 injection with the purpose of pressure maintenance are evaluated and optimized (Zheng and Yang, 2012).

3.1 Experimental

3.1.1 Materials

The heavy oil sample and reservoir brine are collected from Lashburn area, Canada. The initial reservoir temperature is 21.0°C and pressure is 3500 kPa. The density of oil sample is measured to be 976.0 kg/m^3 at 15.6°C and atmospheric pressure. Viscosity of the oil sample is measured to be 5861 mPa·s at 20.0°C and atmospheric pressure with a Brookfield DV-II+ Programmable Viscometer (Brookfield Engineering Laboratories, USA). The asphaltene content of the heavy oil sample is measured to be 14.4 wt% (*n*-pentane insoluble).

The compositional analysis of heavy oil example is tabulated in Table 3.1. As can be seen from Table 3.1, there are no hydrocarbon components lighter than C_9 in this

Table 3.1 Compositional analysis results of oil sample

Carbon number	wt%	Carbon number	wt%	Carbon number	wt%
C_1	0.00	C_{11}	1.26	C_{21}	2.39
C_2	0.00	C_{12}	1.54	C_{22}	1.44
C_3	0.00	C_{13}	1.95	C_{23}	1.98
C_4	0.00	C_{14}	2.18	C_{24}	1.67
C_5	0.00	C_{15}	2.55	C_{25}	1.66
C_6	0.00	C_{16}	2.29	C_{26}	1.70
C_7	0.00	C_{17}	2.29	C_{27}	1.72
C_8	0.00	C_{18}	2.60	C_{28}	1.75
C_9	0.96	C_{19}	2.23	C_{29}	1.50
C_{10}	0.99	C_{20}	2.02	C_{30+}	61.33

heavy oil, while the heavy components of C_{30+} account for 61.33 wt%. Density of reservoir brine is measured to be 1051.7 kg/m^3 at 20.0°C, while ions of chloride, sodium, calcium, and magnesium are the dominant components. The brine viscosity is measured to be 1.03 mPa·s at 20.0°C. According to the compositional analysis of the reservoir brine, synthetic brine is prepared and used in this study (see its composition in Table 3.2).

In this study, research grade CO_2 with a purity of 99.998% is purchased from the Praxair, Canada. Densities of CO_2 at different pressures and temperatures are calculated by using the CMG WinProp module (Version 2009.11, Computer Modelling Group Ltd., Canada) with the Peng-Robinson equation of state (Peng and Robinson, 1976). The Ottawa sand #710 (Bell & Mackenzie, Co., Ltd) is used to pack the 3D displacement model and its screen analysis is listed in Table 3.3.

3.1.2 Experimental setup

Figure 3.1 shows a schematic diagram of the experimental setup used for evaluating performance of pressure maintenance with CO_2 injection under different well configurations. The entire setup can be divided into three sub-systems, i.e., fluid supply system, 3D displacement system, and fluid production system. The fluid supply system is used to supply both CO_2 and brine. A CO_2 cylinder, a gas regulator, and a digital pressure gauge are used to provide continuous CO_2 supply to the physical model, while the injection pressure is controlled by the gas regulator. The synthetic brine is introduced from transfer cylinders to the physical model by using a high pressure syringe pump (500HP, Teledyne ISCO Inc., USA) at a constant flow rate. A digital image of the entire experiment system is shown in Figure 3.2.

Table 3.2 Composition of synthetic brine

Component	Concentration, mg/l
Chloride	43677
Sodium	24700
Calcium	1500
Magnesium	850
Potassium	413

Table 3.3 Typical screen analysis of Ottawa sand #710

USA Standard Sieve Size		Retained, wt%
Mesh	mm	
40	0.425	Trace
50	0.300	0.3
70	0.212	7.0
100	0.150	52.0
140	0.106	32.0
200	0.075	8.0
270	0.053	0.7

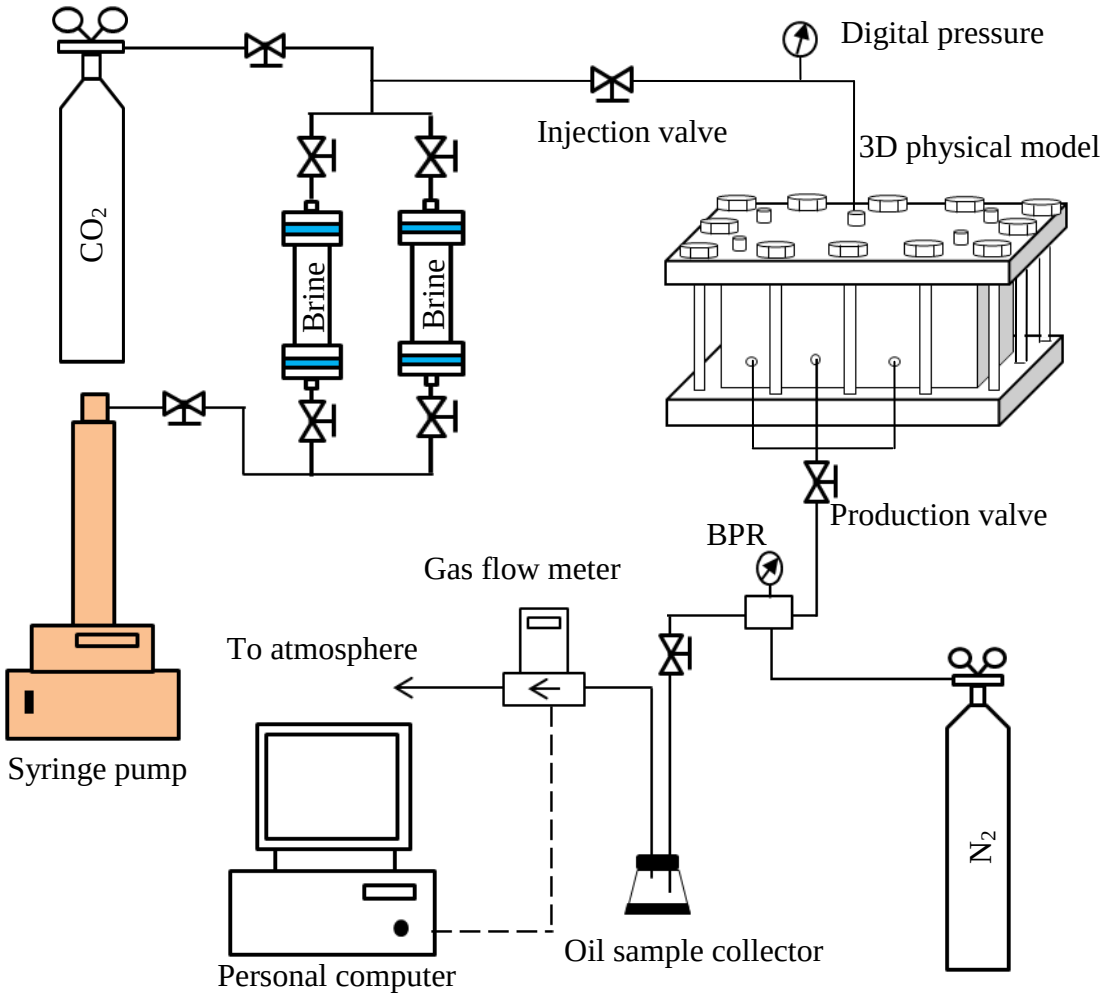

Figure 3.1 Schematic diagram of the experimental setup used for evaluating performance of pressure maintenance with CO_2 injection under different well configurations.

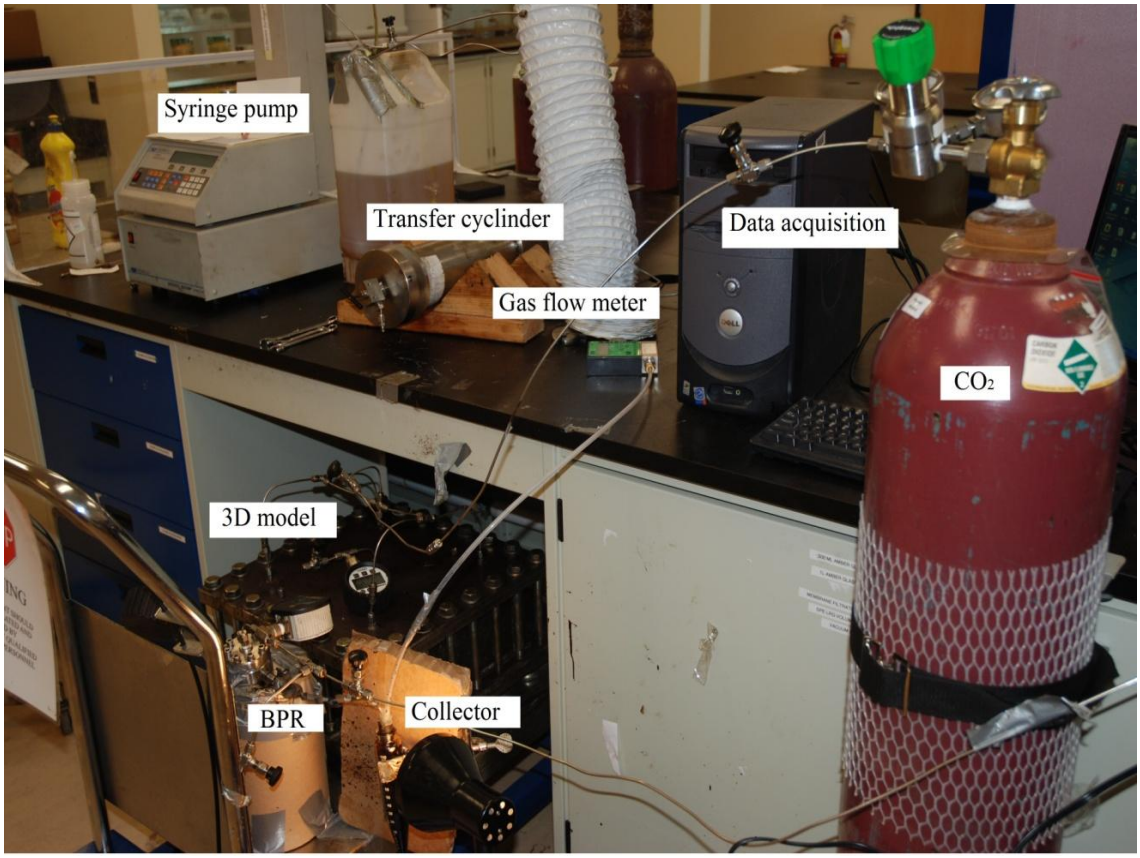

Figure 3.2 A digital image of the experimental setup.

The major component of this experimental setup is a 3D displacement model consisting of five vertical wells and three horizontal wells, which has an effective volume of 304 mm × 304 mm × 127 mm. The physical model is made of steel, and the thickness of wall is 25.4 mm. A total of 28 bolts are used to fasten the steel lid and a piece of rubber gasket is applied for sealing the model. The maximum operating pressure of this 3D displacement system is 6.0 MPa at room temperature. Three parallel horizontal wells are located at bottom of the void space, while five vertical wells are distributed as a conventional five-spot well pattern in the model. The well distribution of this physical model can be seen from Figure 3.3. This 3D displacement model can be used to perform experiments under five-spot, line drive, and other well patterns associated with horizontal wells. All the wells have a diameter of 6.35 mm, around each of which the small holes are perforated to allow fluids to flow. The wells are wrapped with a 250-mesh wire-screen (Ferrier Wire Goods, Canada) to prevent sand production during the tests.

The production system is comprised of a digital pressure gauge, a back pressure regulator (BPR) (EB1HP1, Equilibar, USA), an oil sample collector, and a gas flow meter (XFM17S, Aalborg, USA). During each test, the BPR is used to maintain a pre-specified pressure inside the physical model, on which the reference pressure is exerted with a nitrogen cylinder. The produced liquids are collected by conical-bottom glass centrifuge tubes (Kimble, USA), while the produced gas is measured through the gas flow meter before being exhausted to the atmosphere. The produced CO_2 flow rate and its accumulative volume are logged and stored automatically in a computer at a preset time interval during each test.

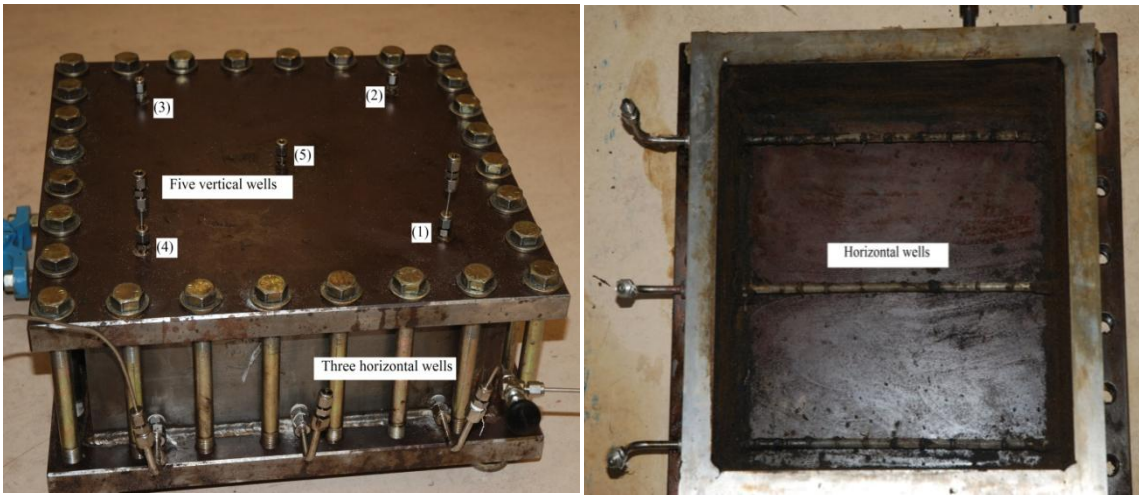

(a) **(b)**

Figure 3.3 Well distribution of the physical model: **(a)** vertical wells, and **(b)** horizontal wells.

3.1.3 Experimental preparations

Sand-packing: The physical model is placed horizontally before the void space is filled with the Ottawa sand. Once being fully packed, the physical model is covered and tightened by the steel lid with the rubber gasket in place. Then the physical model is shaken with a pneumatic vibrator (NP 35, Northern Vibrator, USA) for at least 10 h. While removing the lid and adding more sand to the formed void space in the model, the model is covered, sealed, tightened, and shaken again. The same process is normally repeated 4-5 times until no more void space is observed at the top of the physical model. Finally, leakage test is conducted for 30 minutes with nitrogen at pressures up to 5.0 MPa.

Porosity measurement: The imbibition method is used to measure porosity of the sandpack physical model with satisfactory accuracy (Dong and Dullien, 2006). The specific procedures are briefly described as follows. The sealed physical model is first connected to a vacuum pump (M12C, Fisher Scientific, Canada) for evacuation during which the injection valve is left open, while the production valve is kept tightly closed. Secondly, the production valve is submerged into a container filled with the synthetic brine whose weight and density are known. Thirdly, the injection valve is closed, while the production valve is opened to allow brine to imbibe into the model and saturate the sandpack. Fourthly, weight of the remaining brine sample in the container is measured. Finally, total volume of brine is calculated based on the weight difference of water measured before and after imbibition, and then porosity of the sandpack is calculated. The measured porosities of six tests are listed in Table 3.4, showing that the measured porosities of six tests vary in the range of 33.1-34.2%. Similar porosities can be achieved by using the same Ottawa sand and following the same packing procedure.

Table 3.4 The properties of the 3D physical model at six displacement scenarios

Scenario No.	ϕ , %	k , mD	S_{oi} , %
#1	34.2	1700	95.5
#2	33.2	1600	96.5
#3	33.3	1800	93.9
#4	33.1	1700	93.1
#5	33.5	1800	92.5
#6	33.3	1800	94.5

Note:

ϕ : Porosity

k : Absolute permeability

S_{oi} : Initial oil saturation

Permeability determination: The model is placed in horizontal position to measure the absolute permeability. Two diagonally opposite vertical wells are used to inject and produce the synthetic brine, respectively. During the test, different flow rates and cumulative produced volume are measured at corresponding injection pressures. Then, the CMG IMAX module (Version 2009.11, Computer Modelling Group Ltd., Canada) is used to determine absolute permeability by history matching the production data. The absolute permeabilities of six scenarios are also shown in Table 3.4.

Initial oil saturation measurement: After absolute permeability has been determined, the heavy oil sample is introduced to the physical model through its three bottom horizontal wells at a rate of 0.4-0.6 cm^3/min from a transfer cylinder by using a syringe pump. At the same time, all the other ports located in the lid are left open to release fluids from the physical model. The injection is terminated when no further water production is observed from the open ports. This means that the model has been saturated with heavy oil sample to ensure reasonable initial oil saturation under irreducible water saturation. The volume of the heavy oil used to saturate the model is then recorded. The initial oil saturation is calculated to be the ratio of the saturated oil volume to the pore volume of the sandpack model. After initial oil saturation being established, the experimental model is left undisturbed for 24 h to equilibrate the distribution of fluid.

Effects of temperature on the relative permeability endpoints have been previously studied. It is found that irreducible water saturation increases, while residual oil saturation decreases with temperature (Poston *et al*., 1970; Weinbrandt *et al*., 1975; Maini and Okazawa, 1987; Etminan *et al*., 2008). In order to obtain similar initial oil saturation for all scenarios, displacement of water with heavy oil is conducted at the same

temperature of 21.0°C. The properties of 3D displacement model for all tests are summarized in Table 3.4.

Asphaltene content measurement: Precipitation of asphaltene from the original heavy oil sample has been determined by using the standard ASTM D2007-03 method (ASTM D2007-03, 2007). More specifically, one volume of the heavy oil sample is poured into a beaker and mixed with 40 volumes of liquid *n*-pentane that is used as a precipitant. The mixture is stirred by using a magnetic stirrer (120SQ, Fisher Scientific, USA) for 12 h and then filtered through filter paper with 2 μm pore size. Prior to filtering the oil-precipitant mixture, the filter paper is weighed with an electronic balance (SP2001, Ohaus Corporation, USA). The filtration is terminated until the mixed fluids after passing through the filter paper remain colorless. The filter cake is formed at end of the filtration, which is primarily composed of asphaltene. The filter paper with the precipitated asphaltene is gently dried at T =100.0°C in an oven until the total weight does not change from the reading of the electronic balance. According to the weight change of the filter paper measured before and after filtration, the asphaltene content of the oil sample is calculated accordingly.

Residual oil saturation measurement: Once a blowdown recovery is completed, residual oil saturation has been measured. From top to bottom, the sandpack is divided into four layers and marked as Layers #1 to #4 in sequence, each of which is about 3.0 cm thick. Mixtures of sand and reservoir fluids are collected from 13 locations in each layer to measure the residual oil saturation. Firstly, the weight of each collected sample that contains sand, residual oil, and water is measured. Secondly, the collected sample is heated in an oven at 100.0°C for 4 h to ensure water is completely evaporated. Then the

remaining sand-oil mixture is weighed. It should be noted the heavy oil sample used in this study does not have any hydrocarbon components lighter than C_9 whose normal boiling point temperature is 143.0°C. As such, hydrocarbon components will not be distilled when the heating temperature is set to be 100.0°C for evaporating water. Thirdly, toluene and kerosene are used as solvents to completely remove the residual heavy oil in the sample. Finally, the sand is heated in the oven at 110°C and then weighed until it is completely dried. Consequently, residual oil saturation is calculated based on the weight differences, porosity of the sandpack model, oil density and sand density.

3.1.4 Experimental scenarios

In this study, effects of well configuration on pressure maintenance with CO_2 injection are examined by configuring the five vertical and three horizontal wells. Three well configurations are designed: (a) four vertical injectors and one vertical producer (Five-spot), (b) four vertical injectors and one horizontal producer (4VI-HP), and (c) one horizontal injector and one horizontal producer (HI-HP). The schematic diagram of these three well configurations is shown in Figure 3.4. Based on these well configurations, waterflooding-CO_2 injection process, waterflooding-CO_2 water-alternating-gas (WAG) process, and continuous CO_2 injection are designed and implemented, respectively. In total, six experimental scenarios are designed and performed. The experimental conditions of these six scenarios are summarized and listed in Table 3.5. Waterflooding is first implemented in Scenarios #1 to #5, respectively, and then followed by continuous CO_2 injection or CO_2 WAG, respectively. During waterflooding process, synthetic brine

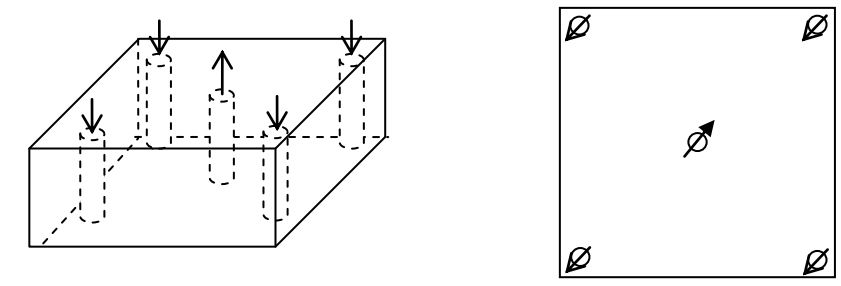

(a)

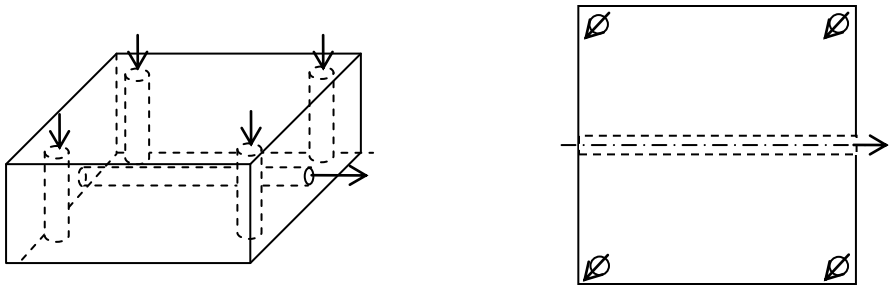

(b)

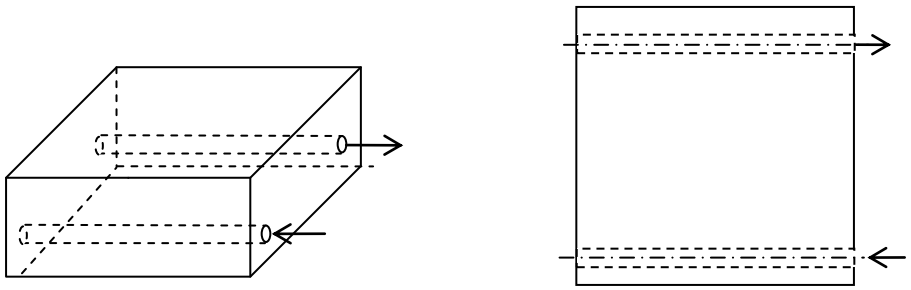

(c)

Figure 3.4 Schematic diagram of well configuration: **(a)** four vertical injectors and one vertical producer (Five-spot); **(b)** four vertical injectors and one horizontal producer (4VI-HP); **(c)** one horizontal injector and one horizontal producer (HI-HP).

Table 3.5 Well configurations and displacement types

Scenario No.	Well Configuration	Displacement Type
#1	Five-spot	Waterflooding-CO_2 injection
#2	4VI-HP	Waterflooding-CO_2 injection
#3	HI-HP	Waterflooding-CO_2 injection
#4	HI-HP	Waterflooding-CO_2 WAG process
#5	4VI-HP	Waterflooding-CO_2 WAG Process
#6	Five-spot and 4VI-HP	Continuous CO_2 injection

is injected into the 3D displacement model at a constant rate of 2.0 cm^3/min by using the syringe pump. For CO_2 injection process, CO_2 is injected from a CO_2 cylinder to the 3D displacement model through the injector(s), while a gas regulator connected with the cylinder is used to control the pre-specified injection pressure. The BPR is used to maintain the pressure inside the physical model at the preset pressure. Once a sufficient pressure drop is achieved, fluids start producing and filling the oil sample collector. The produced gas is flashed off from the oil sample collector and then measured by using the gas flow meter. All the flow rates and accumulative gas volume are recorded and stored automatically in a computer at a preset time interval.

3.2 Reservoir Simulation

The use of computer simulation in petroleum engineering started in the area of reservoir fluid flow where it was called reservoir simulation (Settari, 1993). Reservoir simulation plays a crucial role in forecasting the production behaviour of oil and gas fields, optimizing the reservoir development schemes, and evaluating the distribution of remaining oil through history matching. As opposed to only one reservoir life, the reservoir simulator can simulate many lives for the reservoir under different scenarios, and thus provides a very powerful tool to optimize reservoir operations (Satter *et al*., 1993). Furthermore, reservoir simulation is well-known for its cost-effective ability to evaluate reservoir performance under various operation conditions and thus determine the optimum strategy without equipment investment and operation costs.

To better understand the main mechanisms of pressure maintenance and improving oil recovery with CO_2 injection in heavy oil reservoirs, numerical simulation has been

performed to history match the experimental measurements of the waterflooding and CO_2 injection processes for Scenarios #1 to #5. There are few field cases to implement continuous CO_2 injection staring from primary production. Scenario #6 (continuous CO_2 injection) is an experimental attempt, while history matching for Scenario #6 is not conducted in this study due to the change of well configuration and oil distribution. More specifically, a three-dimensional model with Cartesian grids is built based on the scale of physical model, and then history matching is conducted to match the experimental results of each scenario with the IMEX simulator (Version 2009.11). Finally, the history matched models are used to optimize the reservoir performances under various operation conditions.

3.2.1 Model initialization

Simulator determination: The compositional analysis results of the heavy oil sample used in this study show that there are no components lighter than C_9, while the heavy components account for a large proportion. The operating pressure (lower than 4.0 MPa) is far below the MMP of 15.5 MPa at the temperature of 21.0°C which is calculated by the CMG WinProp module (Version 2009.11). Therefore, neither light components extraction nor the miscible flooding has been achieved under the experimental conditions in this study.

Black oil type models do a credible job on representing the fingering phenomenon, while not representing the compositional effects (Todd, 1979). After a black oil reservoir simulator was used to simulate the immiscible CO_2 application in the Bati Raman heavy oil reservoir, the field results indicated that the simulation model was successful in

predicting the immiscible CO_2 flooding performance (Karaoguz *et al*., 1989; Spivak *et al*., 1989). Also, the CO_2 immiscible WAG process in a heavy oil reservoir was successfully simulated by using a black oil simulator (Cobanoglu, 2001).

IMEX (Version 2009.11) is a full featured black oil simulator that models the flow of gas, gas-water, oil-water, and oil-water-gas in hydrocarbon reservoirs. Besides, IMEX is an effective tool for a broad range of reservoir management issues, such as primary depletion, water and gas injection, and WAG processes. Therefore, IMEX simulator is selected for simulating the displacement mechanisms that govern waterflooding and immiscible CO_2 injection processes in this study.

***Gridblock*:** A Cartesian 3D reservoir model is built for history matching the experimental tests. A grid system of 13×13×6 gridblocks is used in the numerical model to represent the physical model of 304 mm in length, 304 mm in width, and 127 mm in thickness. A total of 1014 gridblocks with 6 vertical layers are used in this simulation model. With regard to the well configuration in the physical model for each experimental scenario, the injector(s) and producer(s) are accordingly configured. For example, the grid system and well position for Scenario #2 are shown in Figure 3.5. Wells #1, #2, #3, and #4 are four vertical injectors and Well #5 is a horizontal producer.

***Initial conditions*:** The key initial conditions of physical model are listed in Table 3.6. These physical properties are used as the input variables in the numerical models. Homogeneous porosity distribution is assumed in the 3D model since the sand is screened in a narrow range. As mentioned previously, the heavy oil is saturated into the physical model at a low flow rate (0.6-0.9 cm^3/min), leading to a uniform initial oil/water saturation. In addition, due to a relatively high porosity and permeability, capillary

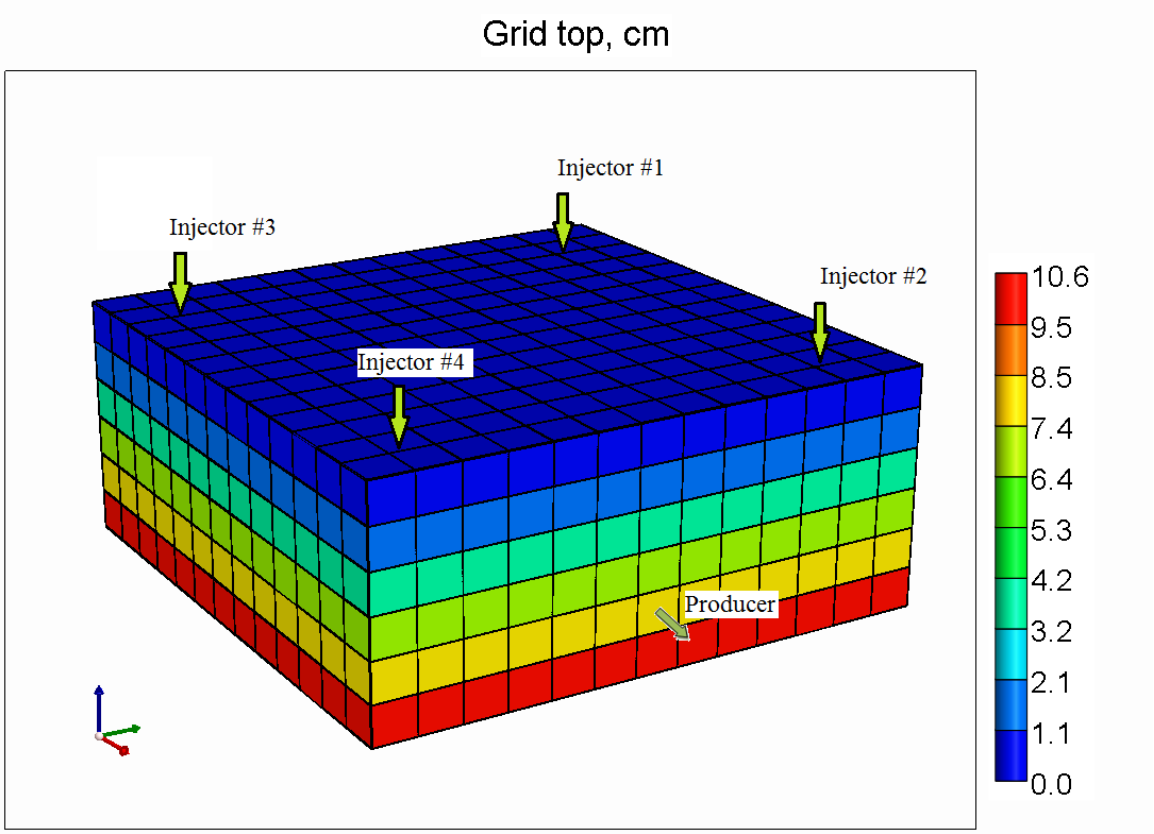

Figure 3.5 3D view of the simulation model of Scenario #2.

Table 3.6 Initial conditions of physical models for six scenarios

Scenario No.	P_i, kPa	T, °C	S_{oi}, %	S_{wi}, %	k_H, mD	k_V, mD	ϕ, %
#1	3500	21.0	95.5	4.5	1700	1700	34.2
#2	3500	21.0	96.5	3.5	1600	1600	33.2
#3	3500	21.0	93.9	6.1	1800	1800	33.3
#4	3500	21.0	93.1	6.9	1700	1700	33.1
#5	3500	21.0	92.5	7.5	1800	1800	33.5
#6	3500	21.0	94.5	5.5	1700	1700	33.3

Note:

P_i: Initial reservoir pressure

T: Reservoir temperature

S_{oi}: Initial oil saturation

S_{wi}: Initial water saturation

k_H: Horizontal permeability

k_V: Vertical permeability

ϕ: Porosity

pressure is assumed to be negligible.

3.2.2 History matching

History matching is a difficult inverse problem with the aim of finding a model such that the discrepancy between the performance of the simulated model and the production history of a reservoir is minimized (Tavassoli *et al*., 2004). In order to validate the numerical model and determine the main mechanisms of pressure maintenance and improving oil recovery with CO_2 injection in a heavy oil reservoir, history matching needs to be conducted to match the experimental results.

Since the experiments are completed under a controlled bottomhole pressure at the producer(s), this bottomhole pressure is treated as a known input for history matching. For waterflooding, water is injected at a constant rate through a syringe pump. CO_2 injection pressure is controlled by the gas regulator, while gas flow rate is measured using the gas flow meter during CO_2 injection processes. Thus, these two parameters are treated as known variables for history matching as well.

3.3 Results and Discussion

3.3.1 Waterflooding-CO_2 injection processes

Waterflooding: Waterflooding is first initiated for Scenarios #1 to #3, respectively. Following waterflooding with a specific well configuration, CO_2 is injected into the 3D model to examine effect of well configuration on pressure maintenance and oil recovery. Oil recovery for these three scenarios during waterflooding is shown in Figure 3.6. As

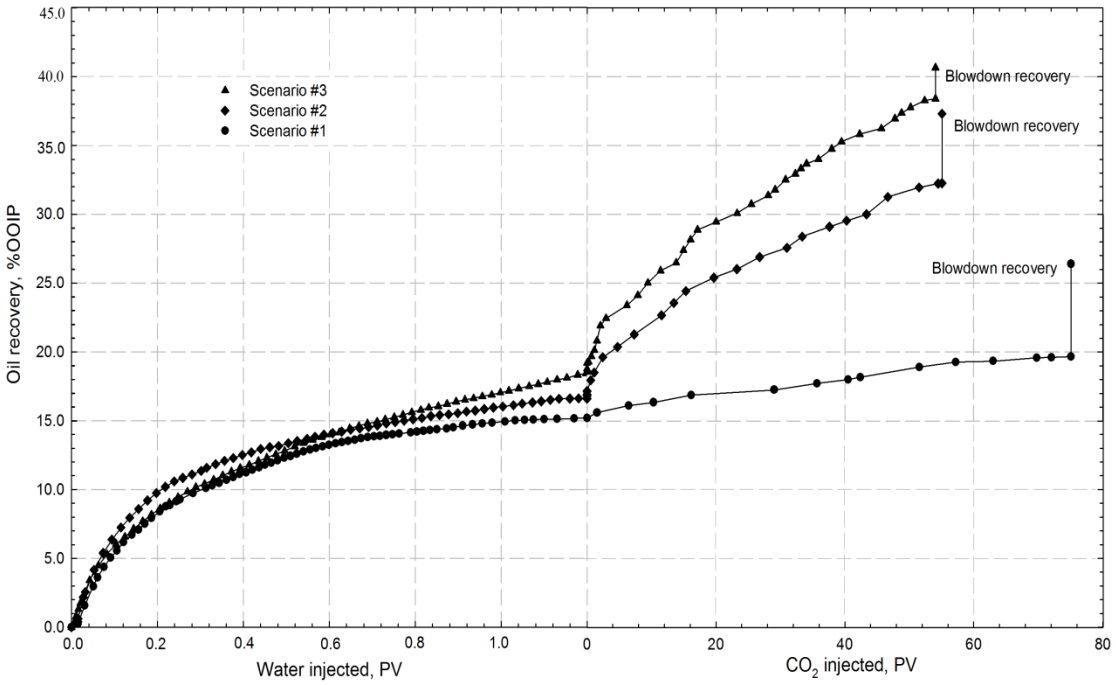

Figure 3.6 Oil recoveries during displacement experiments for Scenarios #1, #2, and #3, respectively.

can be seen, oil recovery is measured to be 14.9%, 16.1%, and 17.1% after 1.0 pore volume (PV) water injection for Scenarios #1, #2, and #3, respectively. The oil recoveries are not high during waterflooding for these three scenarios. This is due mainly to the fact that the heavy oil sample is dramatically viscous than the injected water, leading to a high mobility ratio of water to heavy oil. Consequently, viscous fingering is severe during waterflooding, resulting in a very early water breakthrough and low displacement efficiency.

Figure 3.7 shows water cut in the produced liquid during displacement processes of three scenarios, respectively. For light and medium oil waterfloods, as water is injected, oil is continuously produced until breakthrough, and a relatively high recovery factor can be achieved prior to breakthrough (Hadia *et al*., 2007). As shown in Figure 3.7, however, it is obvious that breakthrough occurs very early in a heavy oil waterflooding process, while water cut increases sharply to a high value at the early stage. Water cut approaches to about 80% at 0.2 PV of injected water, and then is measured to be 97.6%, 95.8%, and 93.1% at 1.0 PV of injected water for Scenarios #1, #2, and #3, respectively. It can be found from Figures 3.6 and 3.7 that considerable heavy oil is still produced at high water cuts, though early water breakthrough has already occurred. This is ascribed to the fact that water prefers to flow through the low resistance pathways that are generated by water after its breakthrough. The injected water is then able to mobilize the contacted oil and displace it to the producer along these paths (Mai, 2009; Zheng *et al*., 2011).

As shown in Figure 3.6, oil recovery for Scenarios #1 and #3 remains close at the early stage, while Scenario #2 yields a higher oil recovery. With a further increase of water injection, the well configurations associated with horizontal well (i.e., Scenarios #2

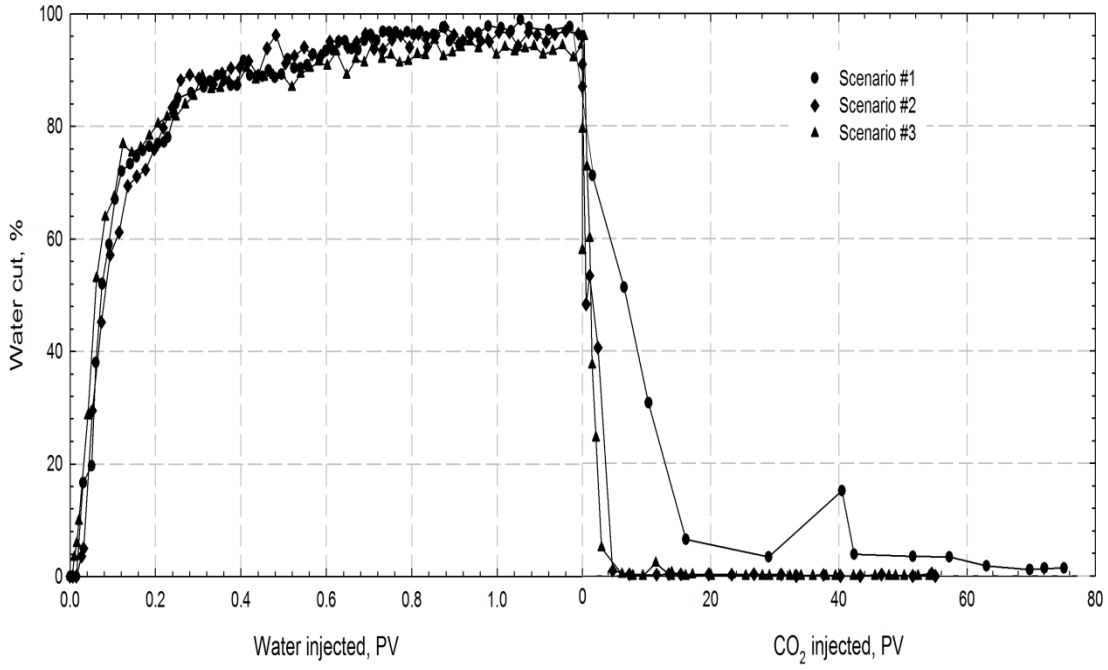

Figure 3.7 Water cut during displacement experiments for Scenarios #1, #2, and #3, respectively.

and #3) achieve much higher oil recovery than that of conventional five-spot configuration (Scenario #1).

The highest oil recovery is found to be 18.5% at 1.2 PV of water injection for Scenario #3. This can be attributed to the fact that a horizontal injector and a horizontal producer are used in Scenario #3, which facilitates achieving a better sweep efficiency.

CO_2 injection: After waterflooding with a specific well configuration, CO_2 is injected to examine effect of well configurations on pressure maintenance and oil recovery for Scenarios #1 to #3, respectively. During CO_2 injection processes, BPR is used to maintain the pressure of the physical model at 3860 kPa that is higher than the original reservoir pressure of 3500 kPa, while the CO_2 injection pressure of 3900 kPa is controlled through a gas regulator connected with the CO_2 cylinder.

It is experimentally found that gas breakthrough occurs early after CO_2 injection is initiated for all three scenarios. This is attributed to the low resistance channels generated during waterflooding and the high mobility ratio of CO_2 to reservoir fluids (water and heavy oil), both of which lead to severe CO_2 fingering. Such early CO_2 breakthrough indicates that viscous forces dominate the immiscible CO_2 injection and there exists relatively minor effect of mass transfer between CO_2 and heavy oil (Rojas and Farouq Ali, 1986; Tüzünoğlu and Bagci, 2000; Bagci, 2007).

As can also be seen in Figure 3.7, water cut declines sharply for all three scenarios during CO_2 injection. When 20.0 PV of CO_2 is injected into the model, water cut is decreased to 5.8%, 0.8% and 0.3% for Scenarios #1, #2, and #3, respectively. This means that CO_2 moves quickly in the channels that are generated during waterflooding, while the injected CO_2 contacts heavy oil along these channels and displaces oil out. In addition,

CO_2 shows its preference to displace heavy oil, though there still exists a significant amount of water in the porous media (Rojas and Farouq Ali, 1986). This results in very low water cut at the late stage of CO_2 injection. Obviously, there is a singular point for the measured water cut in Scenario #1 (See Figure 3.7). This may be ascribed to the fact that water that is previously trapped and/or bypassed by CO_2 at early stage has now been mobilized and produced with the heavy oil. Then, water cut keeps decreasing and remains almost constant after 62.0 PV CO_2 is injected. Also, there exist similar points at 1.1 PV and 11.3 PV of CO_2 injections for Scenarios #2 and #3, respectively, though they are much less obvious.

Oil recovery during CO_2 injection process has also been plotted in Figure 3.6. It can be seen from this figure that CO_2 injection has a favourable impact on pressure maintenance and oil recovery. CO_2 injection increases oil production, though waterflooding has been implemented. In addition, oil recovery is found to be strongly dependent on well configuration during CO_2 injection process. After CO_2 injection, oil recovery is measured to be 19.5% for Scenario #1, 32.2% for Scenario #2, and 38.6% for Scenario #3, respectively. Furthermore, Scenarios #2 and #3 show a later breakthrough than that of Scenario #1, though breakthrough occurs at early stage of all three scenarios. Such a large difference of oil recovery is due to a better sweep efficiency resulting from the well configuration with a horizontal well. In general, a horizontal well controls a large area than that of a vertical well. The presence of the horizontal producer located at the bottom of the physical model alleviates CO_2 override and delays early CO_2 production, leading to gas accumulating at the top of the model and exerting an extra force to drive heavy oil from top to the producer. The poor sweep efficiency of Scenario #1 implies that

CO_2 override is severe, resulting in early gas breakthrough and minor effect of mass transfer between CO_2 and heavy oil (Tüzünoğlu and Bagci, 2000).

Figure 3.8 shows the cumulative gas-oil ratio during CO_2 injection process for Scenarios #1 to #3, respectively. The cumulative gas-oil ratio for Scenario #1 is extremely high, which is another indication for poor sweep efficiency of the five-spot well configuration. As for Scenarios #2 and #3, the relatively low cumulative gas-ratio also implies that the well configurations of 4VI-HP and HI-HP can produce much more oil at the same PV injection of CO_2 due to the advantages of horizontal wells.

3.3.2 Waterflooding-CO_2 WAG process

The results of previous three scenarios (Scenarios #1 to #3) indicate that well configuration imposes a strong impact on oil recovery for CO_2 injection in waterflooded heavy oil reservoirs. The well configurations (HI-HP and 4VI-HP) associated with horizontal well have better sweep efficiency. Therefore, the following two scenarios (Scenarios #4 and #5) are conducted to examine the performance of CO_2 WAG in heavy oil reservoirs under the well configurations associated with horizontal well for the purpose of pressure maintenance and improving oil recovery. As for Scenarios #4 and #5, waterflooding is first initiated, then several cycles of water and CO_2 injection are alternatively implemented to examine performance of CO_2 WAG for pressure maintenance and improving oil recovery in heavy oil reservoirs, respectively.

During CO_2 WAG processes, the BPR is used to maintain the pressure of the 3D model at 3860 kPa, while the CO_2 injection pressure of 3900 kPa is controlled by the gas

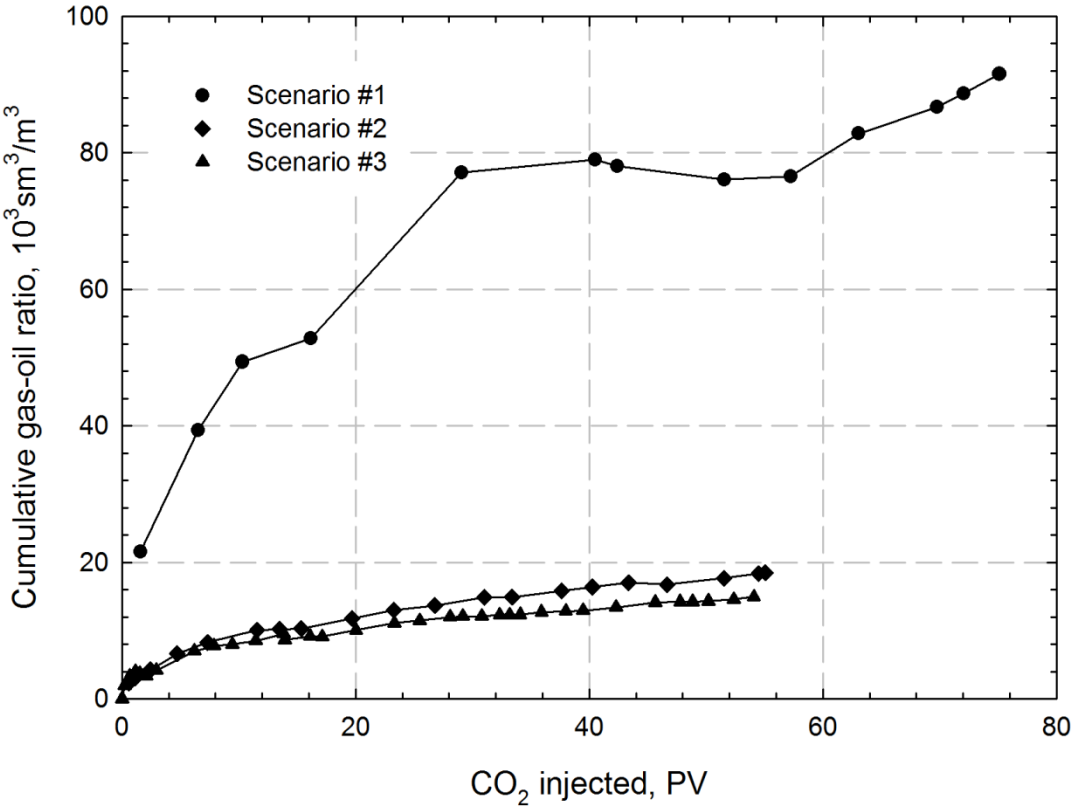

Figure 3.8 Cumulative gas-oil ratios for CO_2 injection processes.

regulator connected with the CO_2 cylinder. For Scenario #4, the same slug sizes (0.40 PV) of water and CO_2 are used (i.e., the WAG ratio is 1:1). The slug sizes of water and CO_2 of Scenario #5 are 0.25 and 1.00 PV, respectively, resulting in a WAG ratio of 1:4.

The oil recovery profiles for Scenarios #4 and #5 are shown in Figure 3.9, respectively. The waterflooding processes in these two scenarios show similar performance as that of Scenarios #2 to #3. As can be seen, after 1.0 PV of water injection, oil recoveries of 24.3% and 23.1% are achieved for Scenarios #4 and #5, respectively. For these two scenarios, water cut approximates 60% at 0.15 PV of injected water, while water cut for Scenarios #4 and #5 is measured to be 95.6% and 97.5% at 1.0 PV of injected water, respectively.

It can also be found that oil recoveries of the two scenarios remain close at the early stage. With a further increase of injected water PV, the well pattern of HI-HP (Scenario #4) tends to yield a higher oil recovery compared with Scenario #5. For instance, oil recovery of Scenario #4 is about 1.3% higher than that of Scenario #5 when 1.0 PV of water is injected. This can be attributed to the fact that two horizontal wells are efficient to achieve a better sweep efficiency.

Figure 3.9 illustrates that majority of the produced oil in the CO_2 WAG processes is recovered during the first cycle. After the second cycle, there is no significant increment in oil recovery. Similar results are also documented in the literature (Sohrabi *et al*., 2000). Obviously, the oil recovery of Scenario #4 levels out during the third cycle, while an additional 2.0% in oil recovery is achieved during the third cycle for Scenario #5. As depicted in Figure 3.9, CO_2 injection during all WAG cycles yields a minor increase in oil production, while the subsequent water injection contributes to the majority of oil

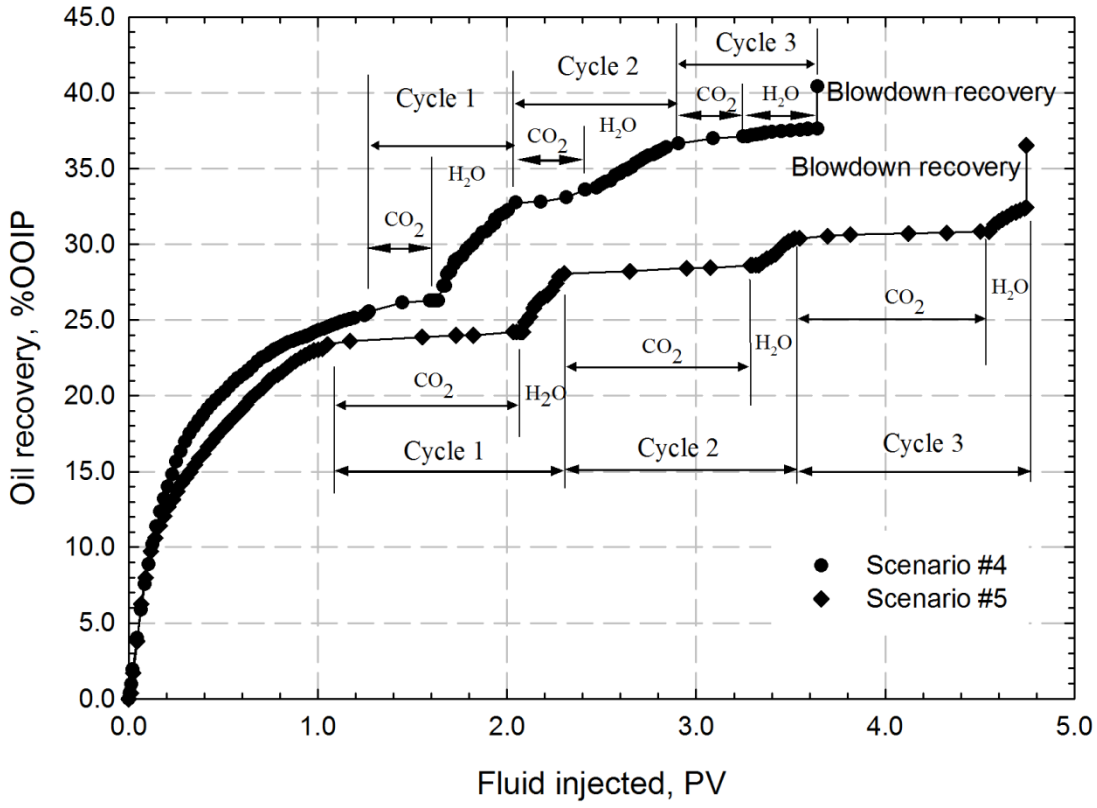

Figure 3.9 Oil recoveries during displacement experiments for Scenarios #4 and #5, respectively.

production, especially in the first two cycles. This is mainly attributed to the fact that gas flooding has high microscopic displacement efficiency than that of waterflooding. The injected CO_2 changes the distribution of liquids in the pores and mobilizes much more oil that is not previously contacted by water. Subsequently, the injected water displaces the mobilized oil to the producer. In this study, Scenario #4 with a larger water slug size achieves a higher oil recovery than Scenario #5 with a smaller water slug size when 3.0 PV of fluids is injected. Oil recovery of Scenario #4 reaches its plateau in a short period, illustrating that it reaches production limit quickly. As for Scenario #5, oil is still produced in the third cycle, indicating that production can be sustained for a much longer time.

The water cut profiles of the produced liquids during CO_2 WAG processes are shown in Figure 3.10. It is noticeable that water cut decreases during the CO_2 injection processes, especially in the first cycle. After CO_2 injection, water cut increases as the water injection is implemented, while it oscillates rather than keeps an approximately constant value during the subsequent water injection processes. This is because CO_2 injection has better microscopic displacement efficiency than that of waterflooding. The heavy oil that is not contacted by water is mobilized by CO_2, while CO_2 shows a slight preference for displacing heavy oil even though high water saturation exists in porous media.

3.3.3 Continuous CO_2 injection

In this study, continuous CO_2 injection is conducted to exploit the heavy oil reservoirs with the purpose of pressure maintenance and improving oil recovery via CO_2

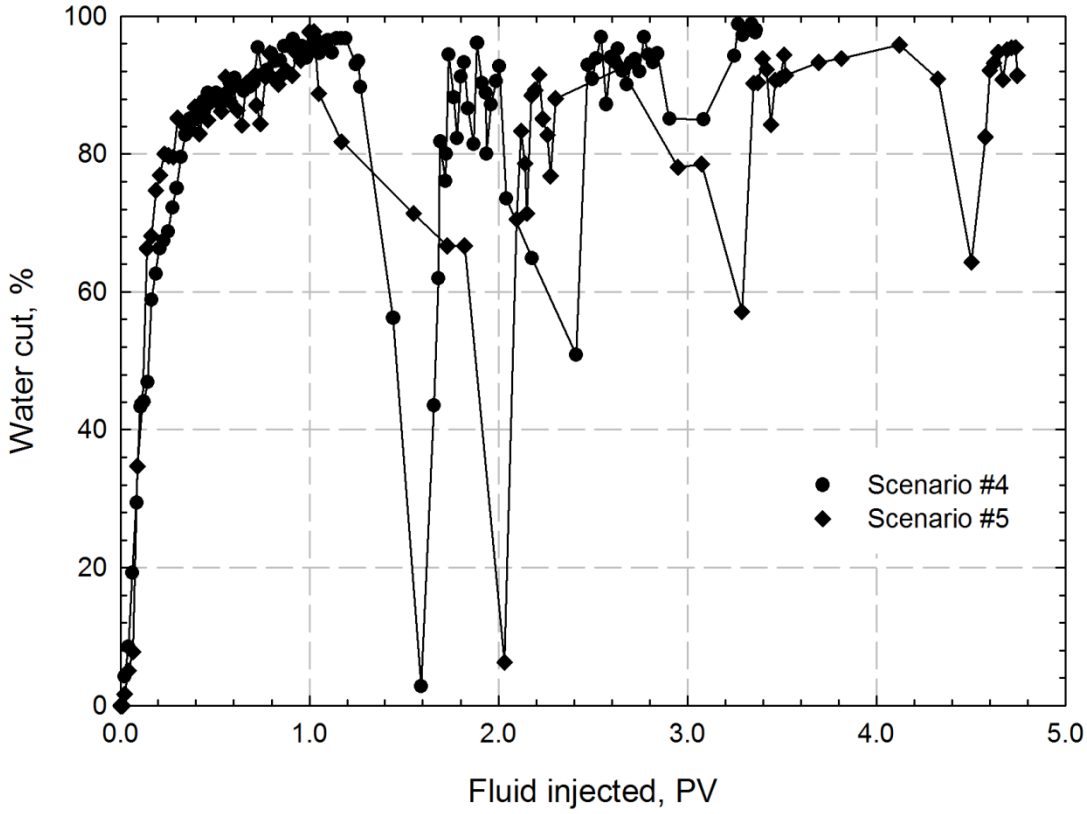

Figure 3.10 Water cut during displacement experiments for Scenarios #4 and #5, respectively.

injection alone. As for Scenario #6, CO_2 injection is first performed under five-spot well configuration, subsequently the well configuration is changed to the pattern of 4VI-HP. The oil recovery profile of Scenario #6 is shown in Figure 3.11.

It is obvious to distinguish two displacement stages (i.e., five-spot and 4VI-HP) from Figure 3.11. As for the well configuration of five-spot, oil recovery quickly reaches its plateau with the oil recovery of 3.6%; however, after converting the well configuration from five-spot to 4VI-HP, oil recovery keeps increasing until about 250 PV of CO_2 injection. This means once again that well configuration significantly affects oil recovery during a CO_2 injection process. It can be ascribed to the fact that the horizontal producer located at the bottom of 3D model alleviates the gas override and gas fingering in the top layer, leading to a better sweep efficiency (Zheng and Yang, 2012). For the whole CO_2 injection process, the final oil recovery of 32.5% is achieved. A satisfactory oil recovery can be obtained through a large amount of CO_2 injection, though the displacement efficiency is low. It is essential that CO_2 mobility control techniques should be taken to alleviate gas fingering, improve sweep efficiency, and extend the contact time between injected CO_2 and heavy oil during the process of CO_2 injection with the purpose of pressure maintenance and improving oil recovery in heavy oil reservoirs.

3.3.4 Blowdown recovery

After termination of CO_2 injection or CO_2 WAG cycles, the pressure inside the model is deceased to atmospheric pressure for blowdown recovery. As shown in Figures 3.6, 3.9, and 3.11, blowdown process contributes an incremental oil recovery of 6.7%, 5.1%, 2.3%, 2.8%, 4.1%, and 4.7% for Scenarios #1 to #6, respectively. The blowdown

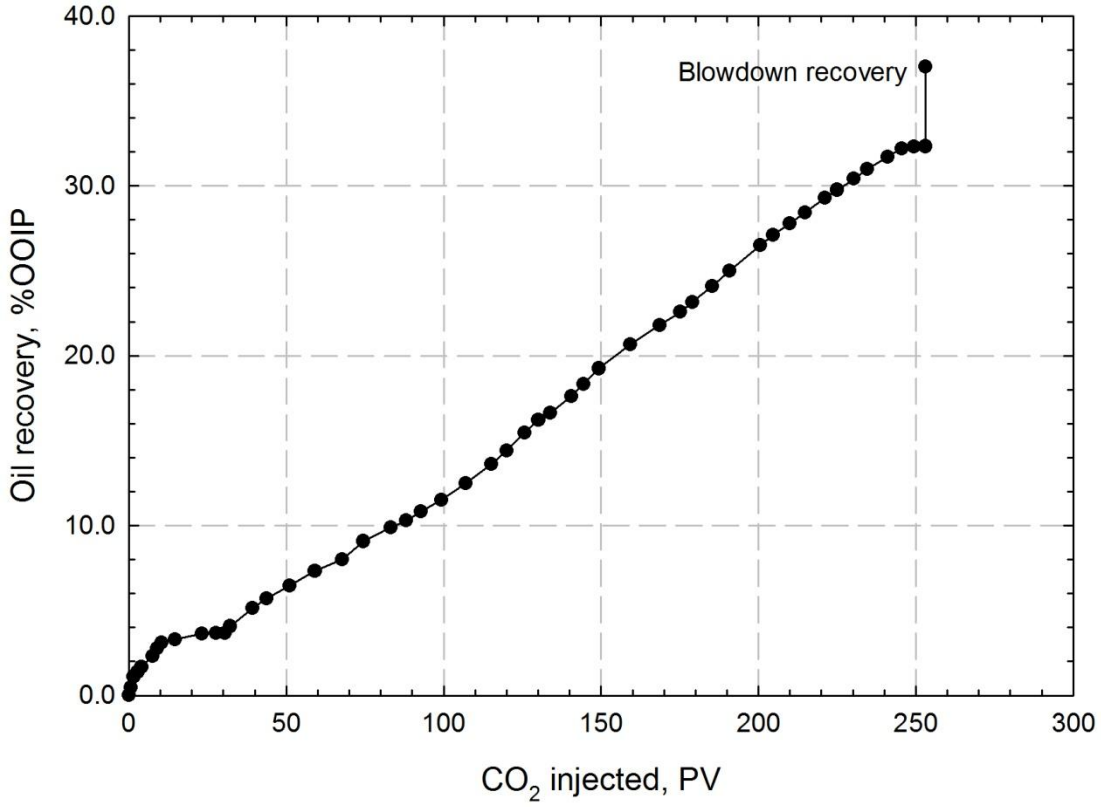

Figure 3.11 Oil recovery during CO_2 injection process for Scenario #6.

recovery is mainly resulted from the solution gas drive mechanism (Jha, 1986). CO_2 is a gas that has a good ability to dissolve into oil, while energy stored by CO_2 dissolution is then released and continues to drive the oil to the wellbore during the blowdown processes (Mangalsingh and Jagai, 1996). When pressure is decreased, fluids (heavy oil, CO_2, and water) tend to expand in the porous media. Such expansion of fluids also agitates the heavy oil in porous media. In addition to the fact that the expanded gas exerts a displacement force to drive oil to producers, such a high efficiency of solution gas drive in viscous oil is mainly due to: 1) a significant reduction in oil viscosity because small gas bubbles are formed in the oil, and 2) simultaneous flow of continuous oil phase and discontinuous gas phase in the form of tiny bubbles (Smith, 1988). Scenarios #1 and #2 yield a higher blowdown recovery, resulting from the fact that there exists a larger quantity of CO_2 injection and higher residual oil saturation after displacement processes.

It is experimentally found that little fluids are produced when pressure is decreased from 3800 kPa to 2000 kPa, whereas most of fluids are produced at pressure below 1500 kPa. The blowdown process is found to last for a relatively long period (i.e., more than 2 h) in this study. Approximately 100 L CO_2 is produced at ambient temperature and atmospheric pressure during blowdown process for Scenarios #1, #2, #3, and #6, while about 40 L CO_2 for Scenarios #4 and #5. During the blowdown process, gas is still producing even though the pressure of physical model approximates to the atmospheric pressure, while tiny bubbles evolve from the produced liquid. The produced CO_2 with a large volume and the evolved tiny bubbles indicate that CO_2 storage also occurs as the injected CO_2 dissolves into reservoir fluids, displaces the fluids from formation, and occupies some of pore spaces that are previously filled by reservoir fluids.

Figure 3.12 illustrates water cut versus oil recovery during blowdown processes for Scenarios # 2 to #5. As for Scenarios #2 and #3, it can be seen that water cut is low at early stage, then increases; rapidly to reach its peak, and finally decreases. This implies that heavy oil is preferential to be displaced at a relatively low pressure (Rojas and Farouq Ali, 1986). As for Scenarios # 4 and #5, water cut decreases from its high value (higher than 90%) to a low value less than 20%. This is partially because water saturation is high after three cycles of WAG and partially because water is first produced during blowdown process. Subsequently, more oil is mobilized towards producer(s), leading to a decreasing trend of water cut (Zheng and Yang, 2012).

3.3.5 Distribution of residual oil saturation

After a blowdown process, the steel lid on the top of the 3D model is removed so that distribution of residual oil saturation in the top layer can be observed directly. Digital images of the top layer for six scenarios are shown in Figure 3.13, respectively. As for Scenario #2 (see Figure 3.13b) where four vertical injectors (Wells #1 to #4) that are located in the corner of the model and a horizontal producer (Well #5) are used, it is clear that colour of sands along the horizontal producer is light, demonstrating that heavy oil along the horizontal well has been displaced effectively. It can also be found that the area along the horizontal producer shows light colour in Scenarios #3 and #4 (see Figures 3.13c and 3.13d) where a horizontal producer is used, respectively. The bottom-left portion of Scenarios #3 and #4 is much darker than its top-right portion, indicating that it is difficult to establish a stable displacement front along the horizontal injector. A large portion of the injected fluids invades the sandpack through the heel of the horizontal

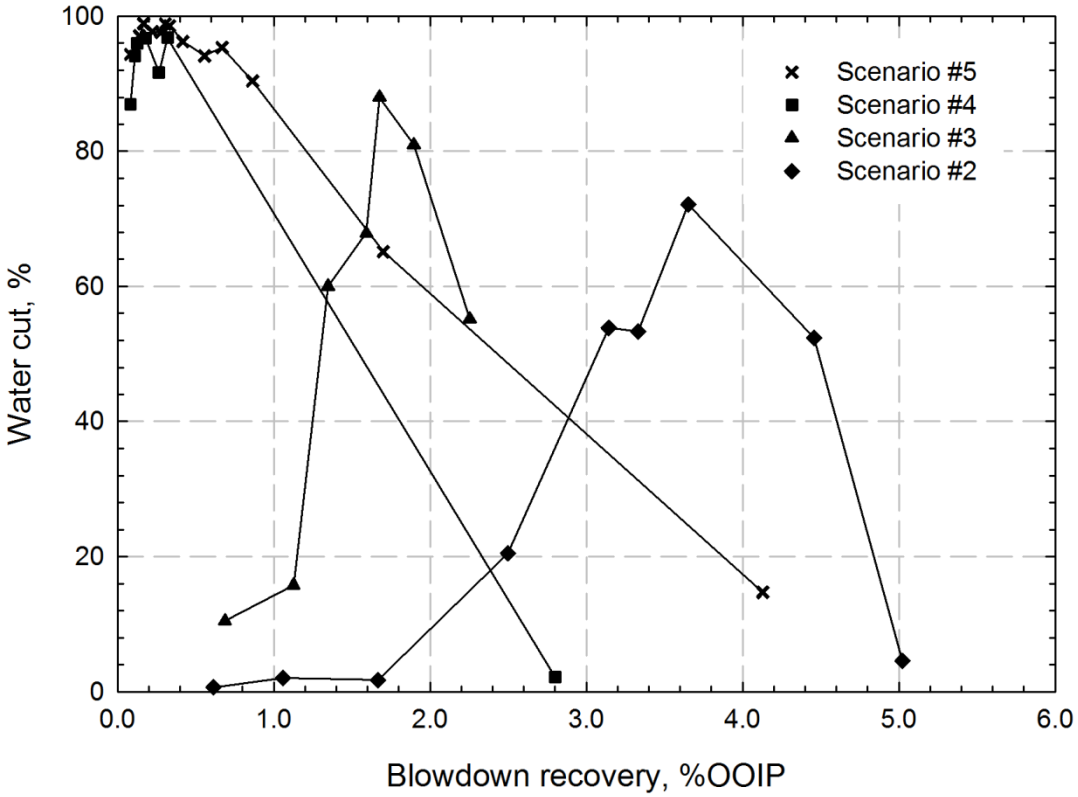

Figure 3.12 Water cut as a function of blowdown recovery for Scenarios #2 to #5, respectively.

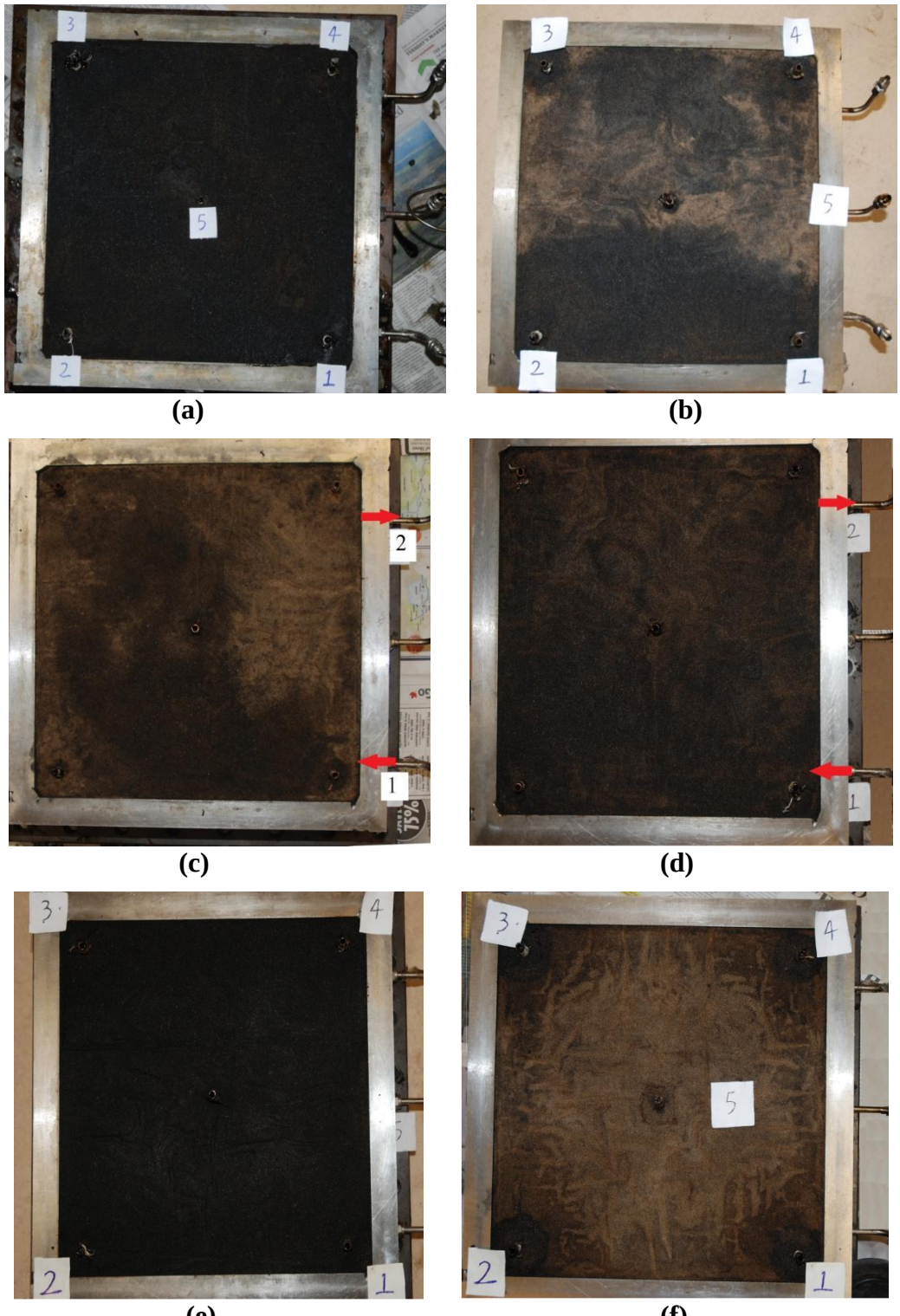

Figure 3.13 Distribution of residual oil saturation on the top layer: **(a)** Scenario #1; **(b)** Scenario #2; **(c)** Scenario #3; **(d)** Scenario #4; **(e)** Scenario #5; and **(f)** Scenario #6.

injector, and then displaces the heavy oil to the producer, resulting in a well-displaced triangle area (i.e., top-right portion). This observation implies that it is possible to improve the sweep efficiency by changing the position of heels and toes of these two parallel horizontal wells. By contrast, there still exists much oil in the top layer for Scenario #1, though a large amount of CO_2 has been injected. Such observed dark sand distribution in the 3D model is consistent with its low oil recovery as observed previously. This means that displacement efficiency is low under the well configuration of five-spot, leading to high residual oil saturation in hydrocarbon reservoirs.

Scenarios #2 and #5 are conducted under the same well configuration (4VI-HP). However, the sand colour of Scenario #5 along the horizontal producer is not light as that of Scenario #2. This is because the volume of injected fluids for Scenario #5 is much less than the injected volume for Scenario #2. As for Scenario #6 (see Figure 3.13f), the heavy oil in the top layer around the vertical producer has been effectively displaced, while much oil is left near the four vertical injectors.

In order to examine the residual oil saturation in the physical model, distributions of residual oil saturation in the sandpack for Scenarios #1 to #6 are measured and illustrated in Figures 3.14 to 3.19, respectively. A total of 13 samples are collected from different locations for each layer marked by the circle symbols in these figures. Then, the residual oil saturation contours are generated based on the measured values.

As previously mentioned, waterflooding is first implemented in Scenarios #1 to #3, followed by CO_2 injection under different well configurations, respectively. As for Scenario #1 where waterflooding and CO_2 injection processes are conducted under the well configuration of five-spot, residual oil saturation in Layer #4 is much higher than

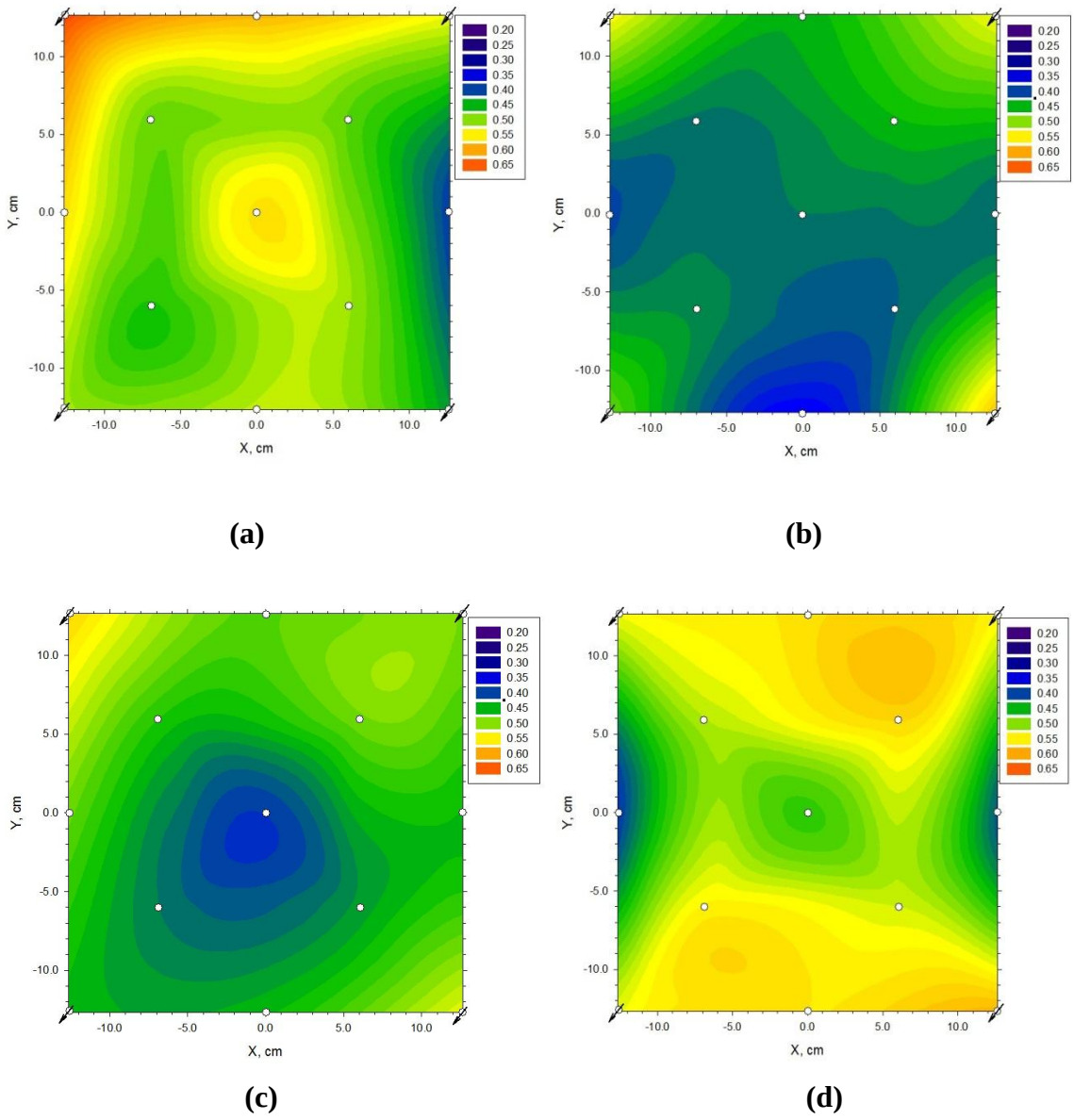

Figure 3.14 Distribution of residual oil saturation for Scenario #1 in **(a)** Layer #1, **(b)** Layer #2, **(c)** Layer #3, and **(d)** Layer #4.

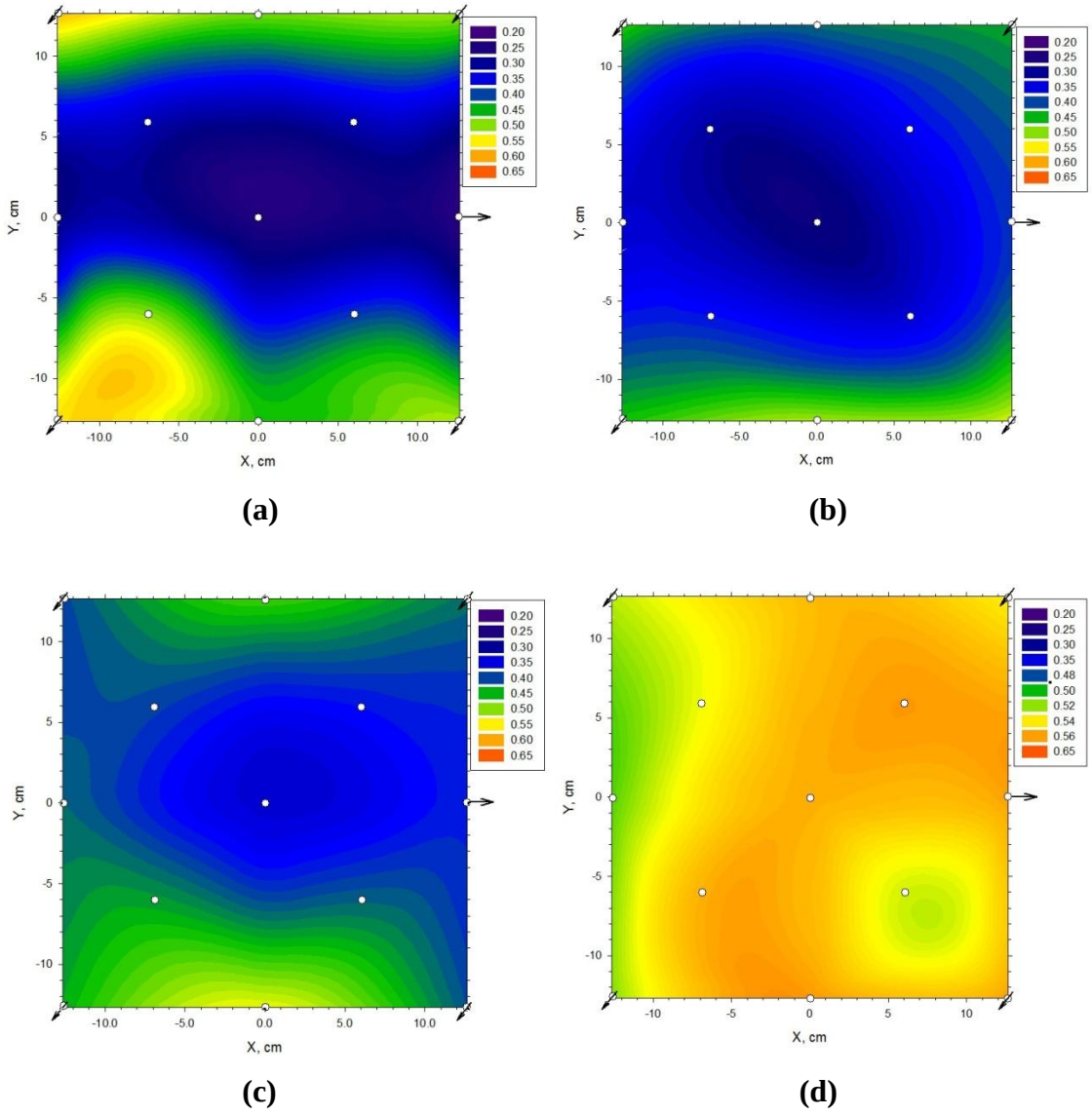

Figure 3.15 Distribution of residual oil saturation for Scenario #2 in **(a)** Layer #1, **(b)** Layer #2, **(c)** Layer #3, and **(d)** Layer #4.

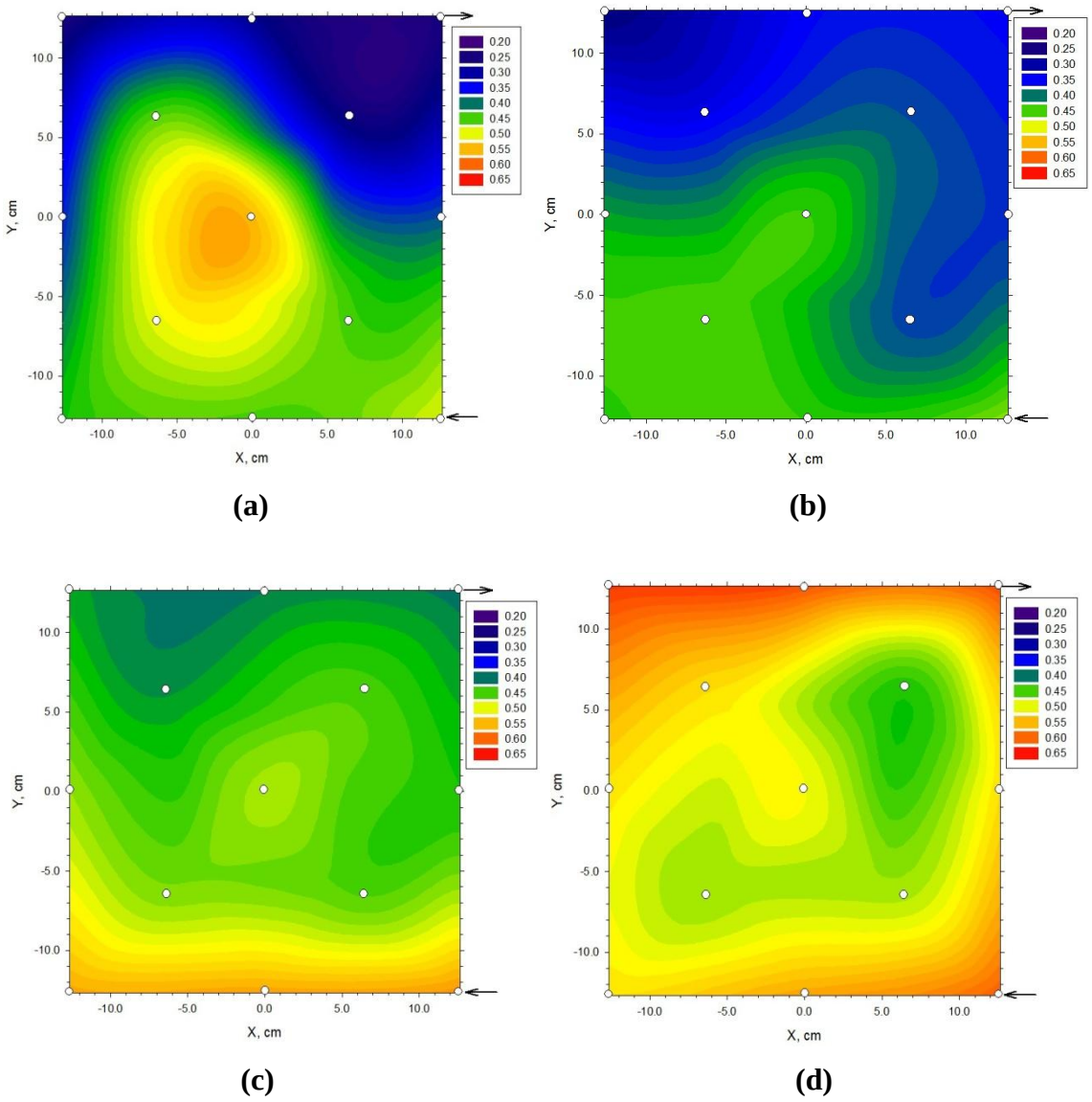

Figure 3.16 Distribution of residual oil saturation for Scenario #3 in **(a)** Layer #1, **(b)** Layer #2, **(c)** Layer #3, and **(d)** Layer #4.

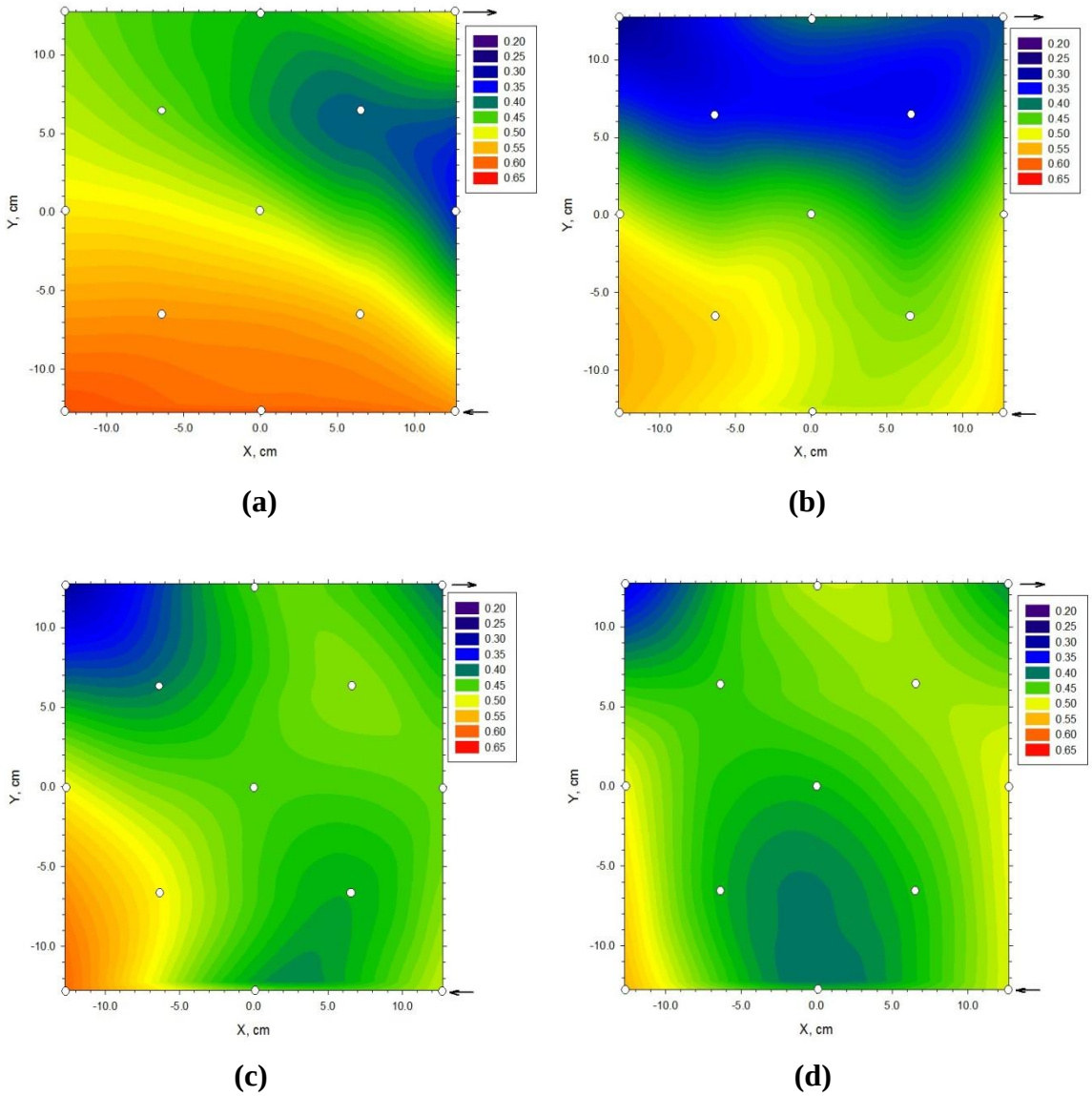

Figure 3.17 Distribution of residual oil saturation for Scenario #4 in **(a)** Layer #1, **(b)** Layer #2, **(c)** Layer #3, and **(d)** Layer #4.

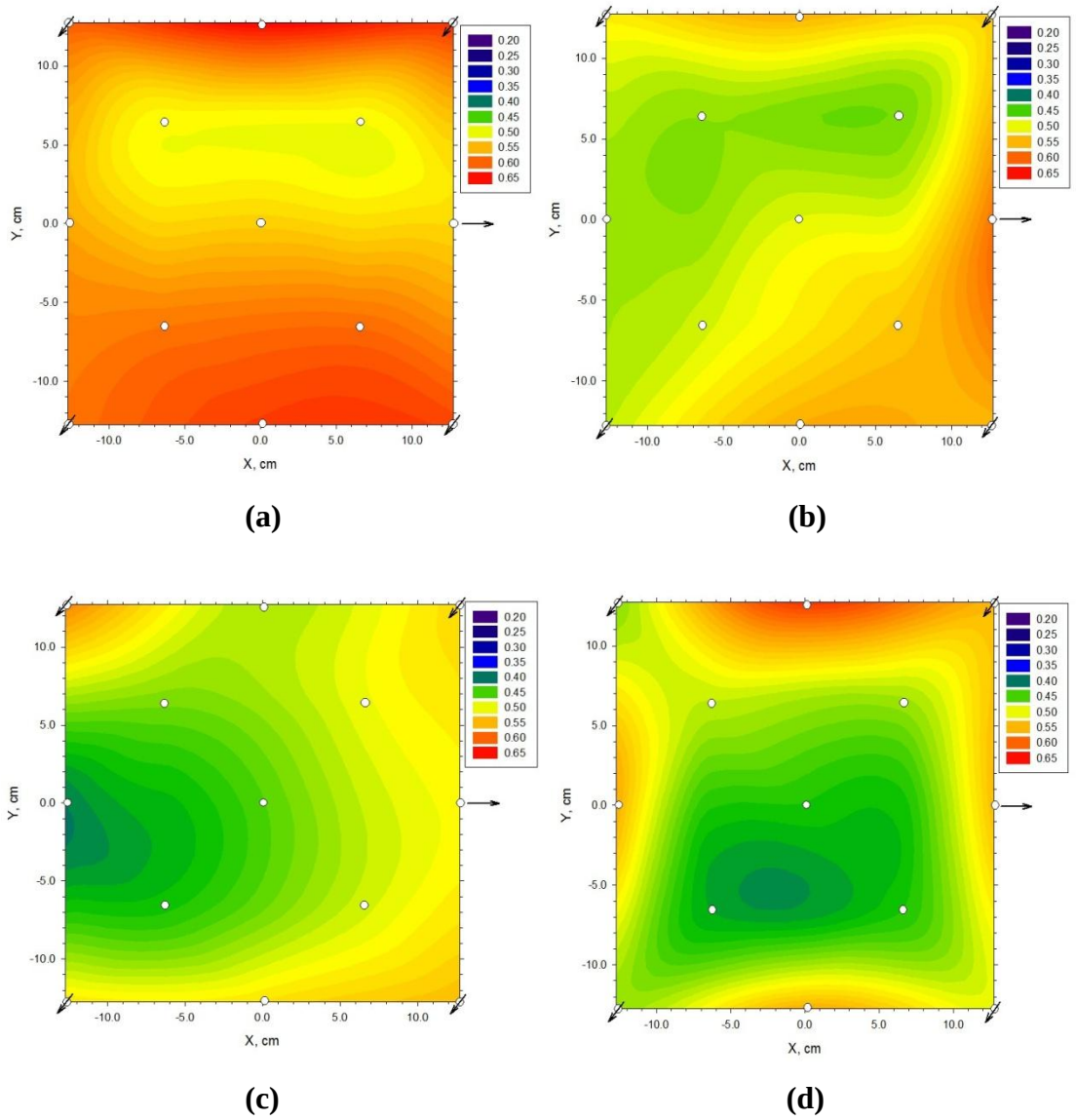

Figure 3.18 Distribution of residual oil saturation for Scenario #5 in **(a)** Layer #1, **(b)** Layer #2, **(c)** Layer #3, and **(d)** Layer #4.

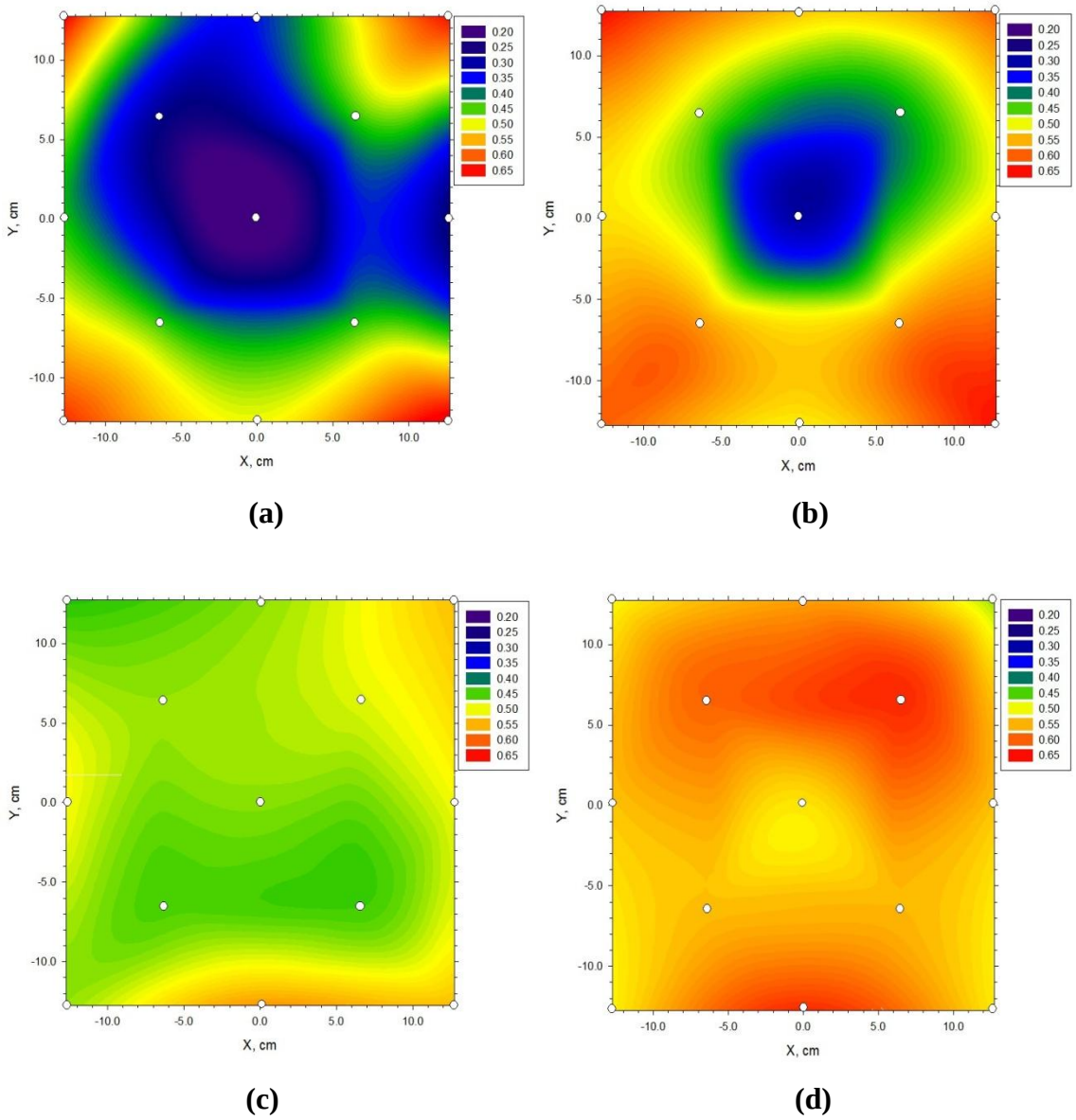

Figure 3.19 Distribution of residual oil saturation for Scenario #6 in **(a)** Layer #1, **(b)** Layer #2, **(c)** Layer #3, and **(d)** Layer #4.

that of Layers #1 and #2 (see Figure 3.14). This implies that bottom of the model has not been well swept by CO_2 so that a high residual oil saturation is resulted from gas override. This finding is consistent with the phenomena of early breakthrough and high gas-oil ratio discovered during the displacement process of Scenario #1.

Figure 3.15 shows the residual oil saturation distribution of four layers for Scenario #2. As shown in Figure 3.15, distribution of residual oil saturation is well depicted and consistent with the colour as observed in Figure 3.13b. Residual oil saturation along the horizontal producer is low in Layers #1 to #3, respectively. This indicates that the horizontal producer controls a large area and results in a better sweep efficiency. Layer #4 (see Figure 3.15d) shows higher residual oil saturation than that of Layers #1 to #3. This is ascribed to gas override (Zheng *et al*., 2011).

Figure 3.16 shows the residual oil saturation of Scenario #3 under the well configuration of HI-HP. It is obviously found that the stripe area along the horizontal producer has low residual oil saturation, while the residual oil saturation along the horizontal injector is much higher. The reservoir area near the horizontal producer has been efficiently swept by injected fluids. The average oil saturation in the bottom layer is higher than that of top layers.

As for waterflooding-CO_2 injection processes (Scenarios #1 to #3) under different well configurations, it can be observed that there exists a conspicuous difference that the reservoir area along horizontal producer shows light colour, while the sand around the vertical producer is still dark. This indicates that the area controlled by horizontal producer has been well swept, leading to low residual oil saturation. By contrast, the well configuration of five-spot shows poor sweep efficiency. These profiles of residual oil

saturation distribution demonstrate that well configuration has a strong effect on oil recovery during the process of pressure maintenance with CO_2 injection in heavy oil reservoirs. The well configurations associated with horizontal well(s) have advantages of controlling a large reservoir area and dominating high sweep efficiency.

Waterflooding-CO_2 WAG processes are performed in Scenarios #4 and #5, respectively. Scenario #4 is under the well configuration of HI-HP that is the same as Scenario #3, while the well configuration of Scenario #5 is the same as that of Scenario #2 (4VI-HP). As shown in Figure 3.17 (Scenario #4), for Layer #1, the bottom-left portion shows a higher residual oil saturation, which is consistent with that of the digital image of the top layer for Scenario #4 (see Figure 3.13d). As for Layer #2 of Scenario #4, the residual oil saturation along the horizontal producer is low, indicating that the horizontal producer controls a large reservoir area, while heavy oil along the producer has been efficiently displaced after three CO_2 WAG cycles.

The average residual oil saturation of Layers #3 and #4 for Scenario #5 is relatively low (see Figure 3.18). This is ascribed to the fact that two parallel horizontal wells are located at the bottom of the physical model, leading to high sweep efficiency in the bottom layers of the model. As can also be seen from Figure 3.18, Layer #1 shows that there is high residual oil saturation in the top layer, while the average residual oil saturation decreases from top to bottom layers. Layer #4 illustrates low residual oil saturation, while a clear displacement front from four vertical injectors to the horizontal producer is formed due to the fact that the horizontal producer is located at the bottom of the model. Therefore, the horizontal producer located at the bottom layer is beneficial for recovering the bottom heavy oil in reservoirs with gas cap drive.

The residual oil saturation of Scenario #6 is shown in Figure 3.19. Obviously, the residual oil saturations around the four vertical injectors are much higher than that of central part. That is because the central vertical well and horizontal well is used as producers in sequence. The displacement profiles from the injectors to the producer are well depicted in Figure 3.19. The residual oil saturation of bottom layer (Figure 3.19d) is also high, implying that much oil in bottom layers has not been displaced.

3.3.6 Numerical simulation and performance optimization

Waterflooding-CO_2 injection (Scenarios #1 to #3) and waterflooding-WAG processes (Scenario #4 to #5) have been history matched in this study. As previously mentioned, Scenario #6 is an experimental attempt for continuous CO_2 injection since primary production, while the history matching for Scenario #6 is not included in this thesis study. Since the relative permeabilities cannot be directly measured from experiments, they are to be determined by using the history matching techniques instead (Watson *et al*., 1980; Eydinov *et al*., 2009; Li *et al*., 2009; Li and Yang, 2011). The oil viscosity also affects the heavy oil-water relative permeability curves. With an increase in oil viscosity, residual oil saturation is increased and relative permeabilities are decreased at a higher water saturation range (Wang *et al*., 2006; Nejad *et al*., 2011). Numerical simulation of the displacement processes is conducted with injection rate, injection pressure, and production pressure as input constraints. The relative permeability curves determined by history matching for Scenarios #1 to #5 are shown in Figures 3.20 to 3.24.

As can be seen from figures for water-oil relative permeability curves, water relative permeability increases slightly when the water saturation is less than 0.3. With an

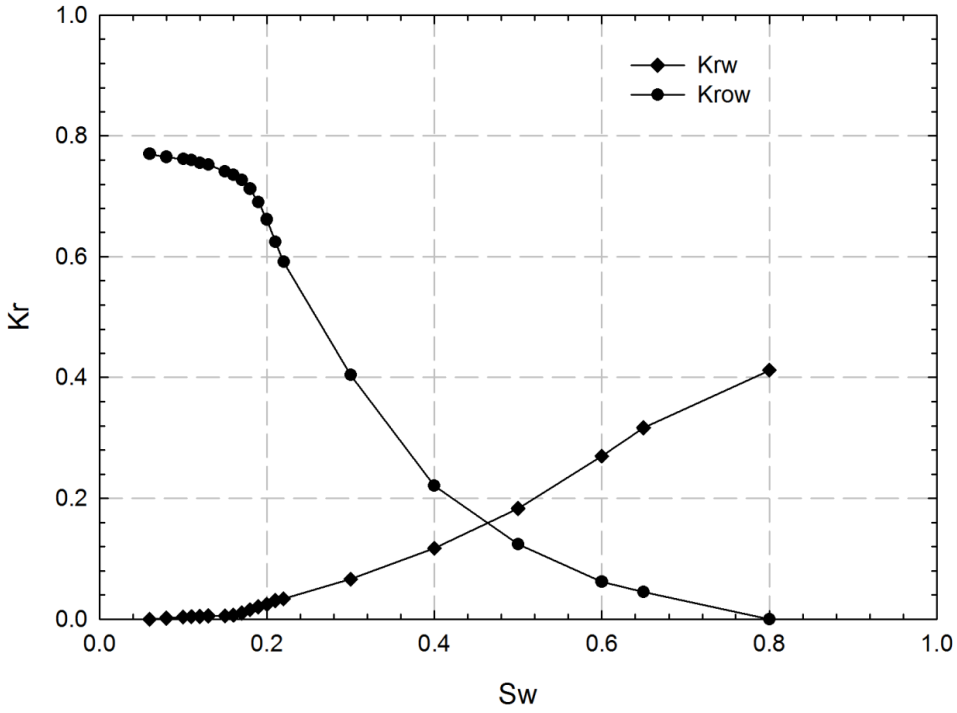

(a)

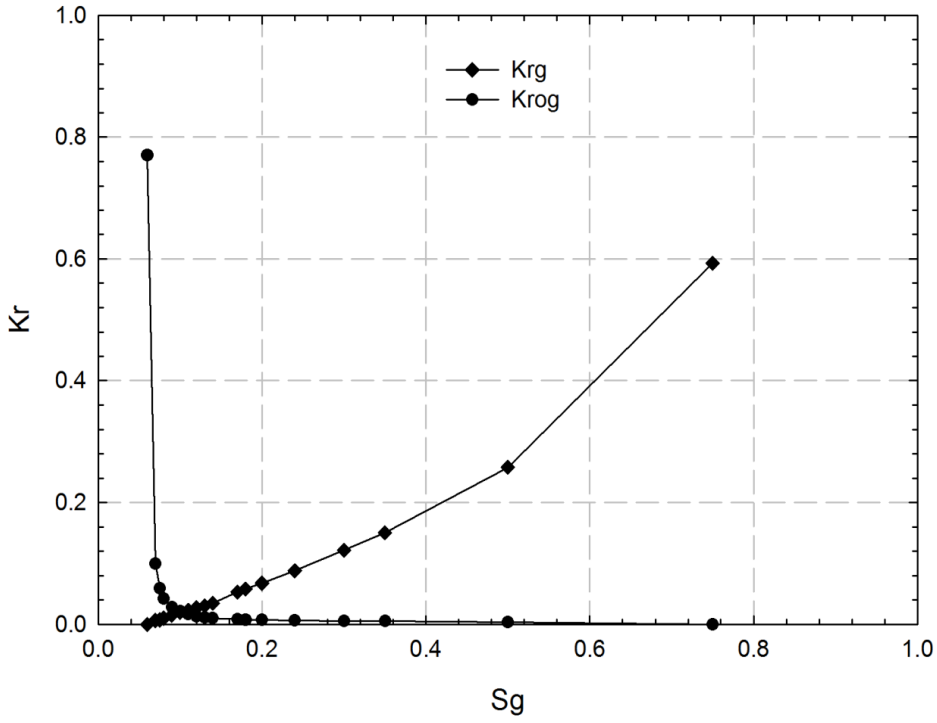

(b)

Figure 3.20 Relative permeability curves for Scenario #1: **(a)** water-oil system and **(b)** liquid-gas system.

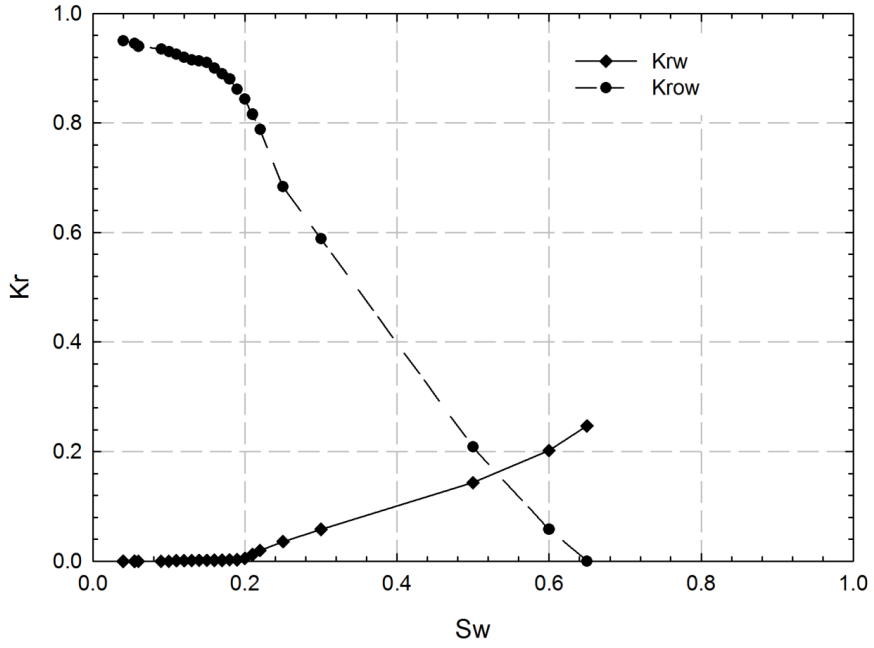

(a)

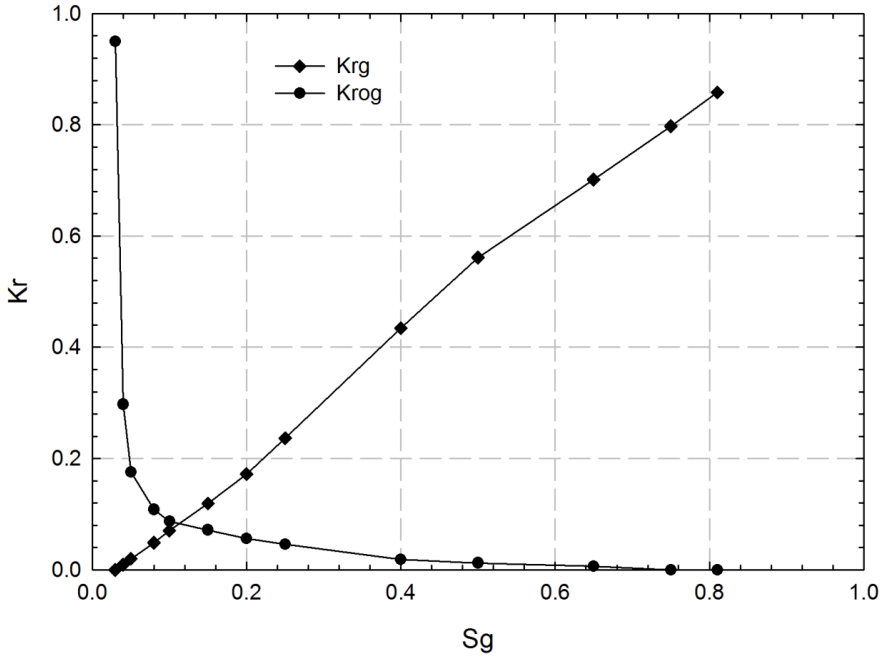

(b)

Figure 3.21 Relative permeability curves for Scenario #2: **(a)** water-oil system and **(b)** liquid-gas system.

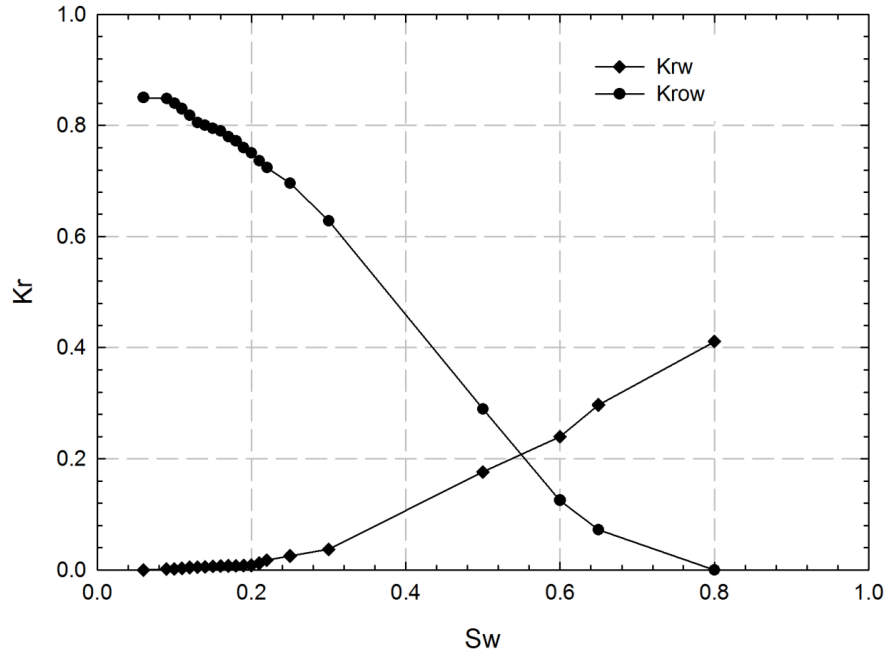

(a)

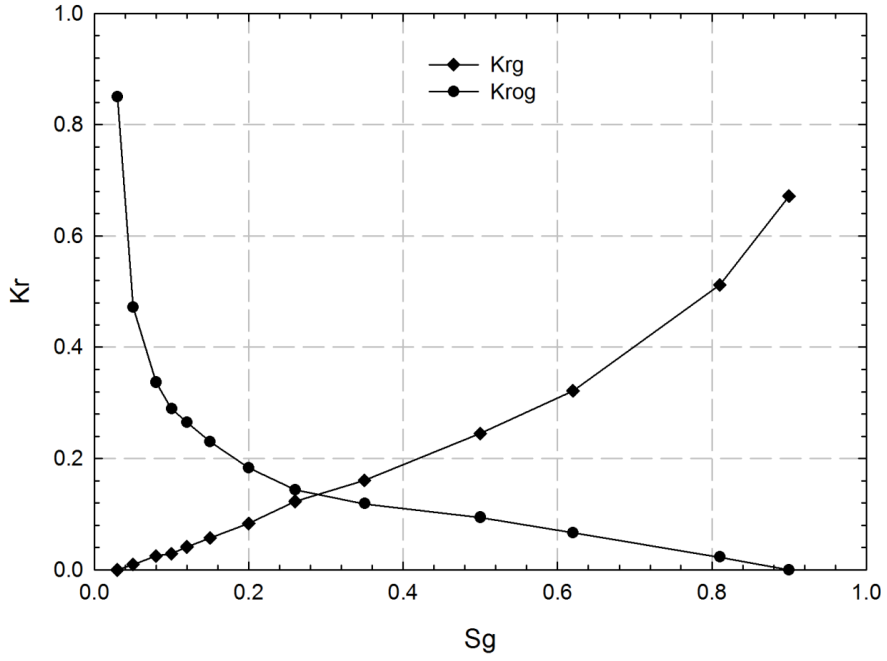

(b)

Figure 3.22 Relative permeability curves for Scenario #3: **(a)** water-oil system and **(b)** liquid-gas system.

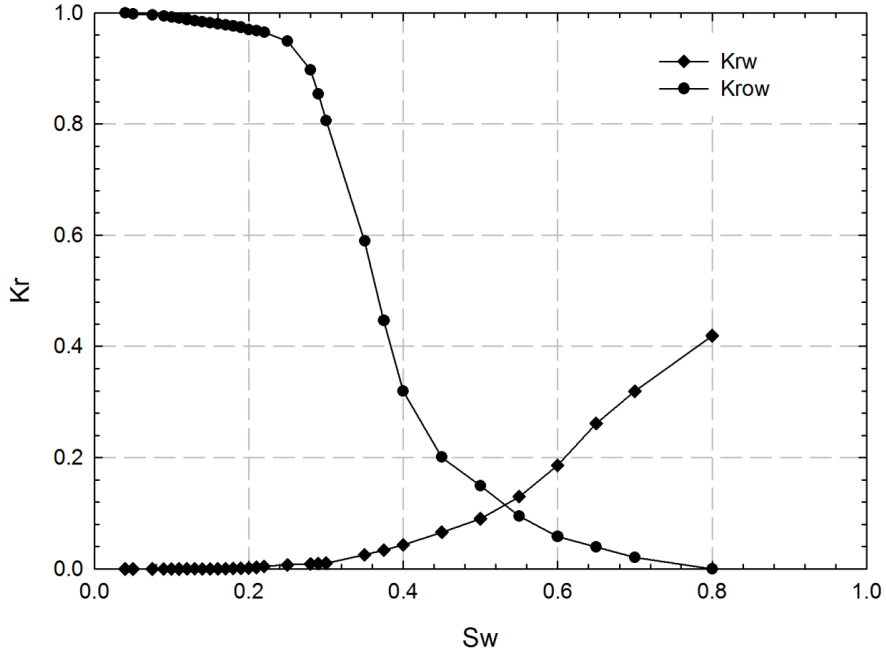

(a)

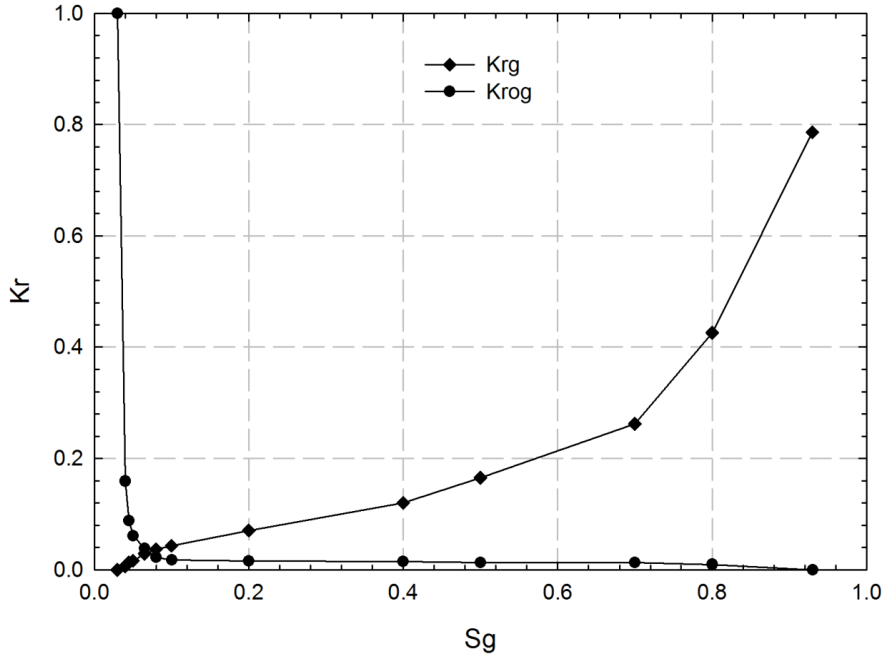

(b)

Figure 3.23 Relative permeability curves for Scenario #4: **(a)** water-oil system and **(b)** liquid-gas system.

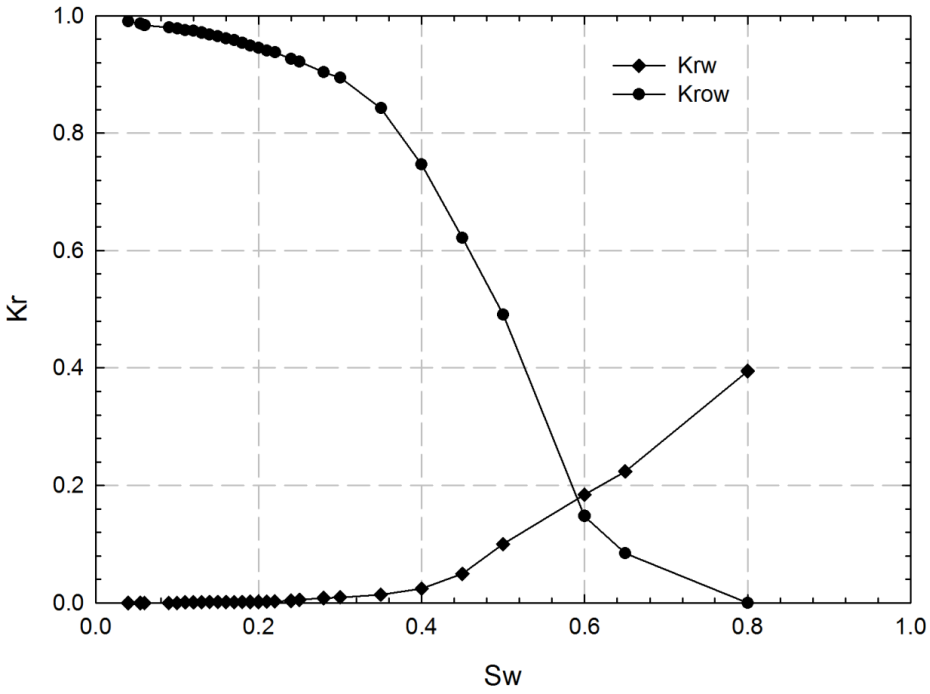

(a)

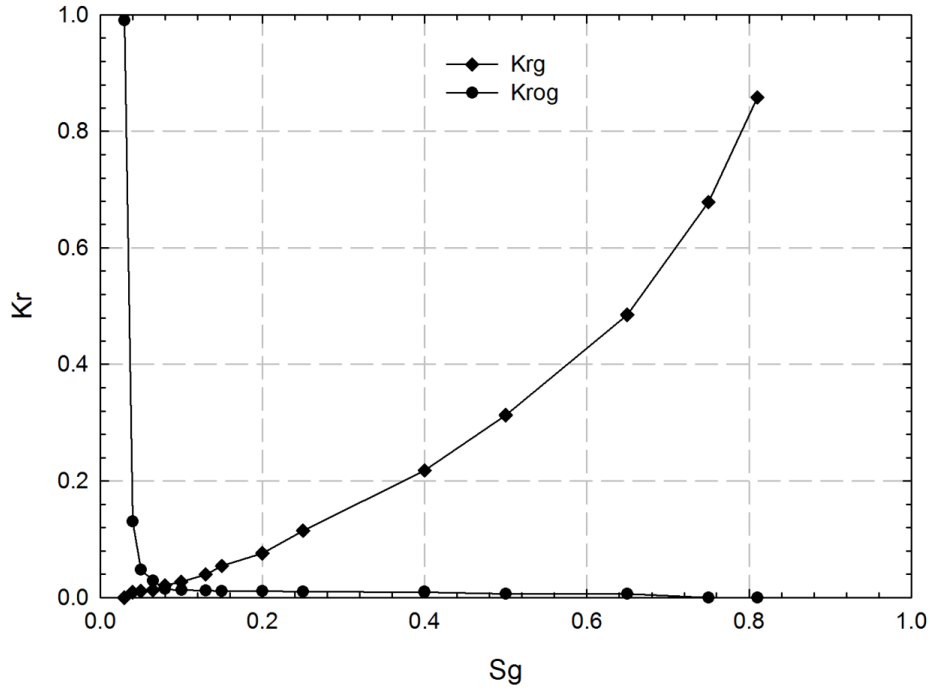

(b)

Figure 3.24 Relative permeability curves for Scenario #5: **(a)** water-oil system and **(b)** liquid-gas system.

increase in water saturation, oil relative permeability decreases rapidly. The relative permeability values are low at high water saturation range. The performance of waterflooding is very sensitive to the relative permeability values at low water saturation range (less than 0.2). As for liquid-gas relative permeability curves, liquid and gas relative permeabilities change dramatically in low gas saturation range (less than 0.1). The relative permeability of oil reduces sharply as gas saturation increases, while gas relative permeability increase quickly. This implies that gas has high mobility in heavy oil, leading to adverse gas-oil mobility ratio and severe gas fingering.

The cumulative oil production of simulation is compared with the experimental data in Figures 3.25 to 3.29, respectively. The good matching results show that the numerical simulation captured the overall behaviour of both the waterflooding-CO_2 injection process and waterflooding-CO_2 WAG processes. As shown in Figures 3.25 to 3.29, oil recovery approaches its plateau after 1.0 PV injection (2000 min), indicating that the waterflooding becomes less efficient afterwards. These are consistent with the high water cut after 1.0 PV of water injection shown in Figures 3.7 and 3.10. For waterflooding-CO_2 injection processes (see Figures 3.25 to 3.27), CO_2 injection following the waterflooding process enhances oil production, especially in the scenarios associated with horizontal wells.

As for a waterflooding-WAG process, it is worthwhile mentioning that, after CO_2 injection, a large amount of oil is still produced during the subsequent water injection process, though the oil recovery reaches its plateau at the first stage of waterflooding. This is attributed to the fact that the injected CO_2 with high microscopic sweep efficiency can swell the heavy oil, reduce oil viscosity, and mobilize the heavy oil in the pores,

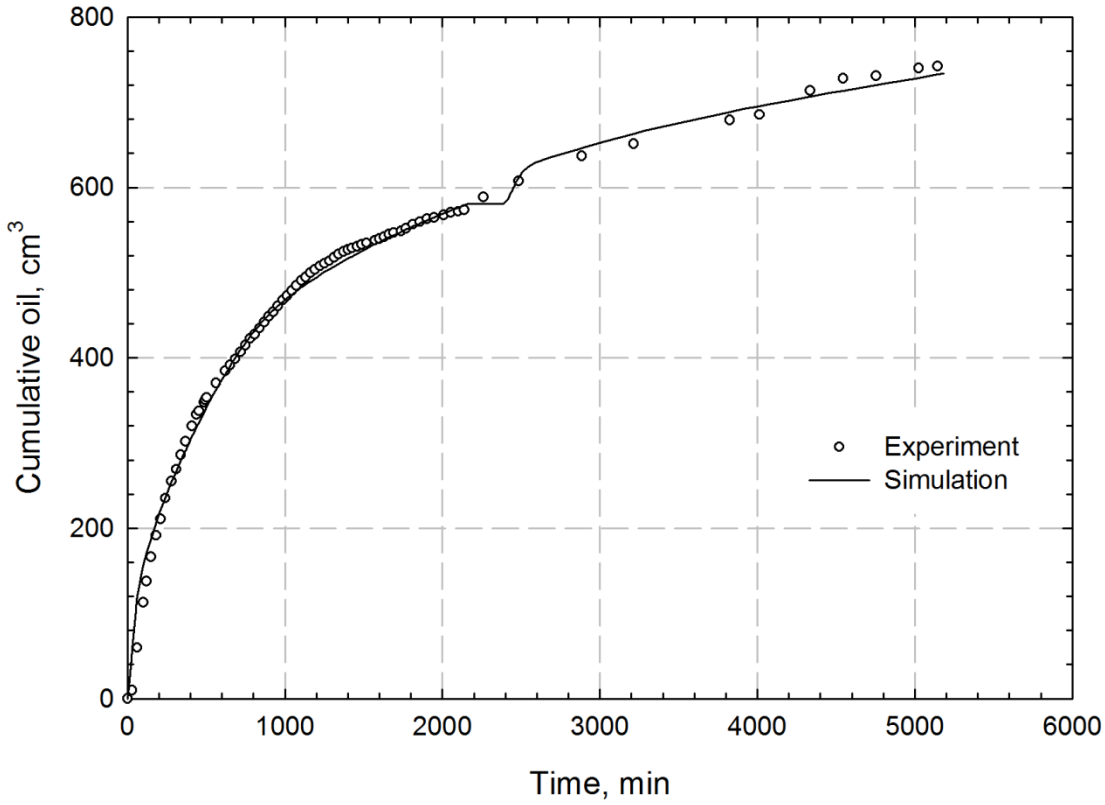

Figure 3.25 Measured and simulated cumulative oil production for Scenario #1.

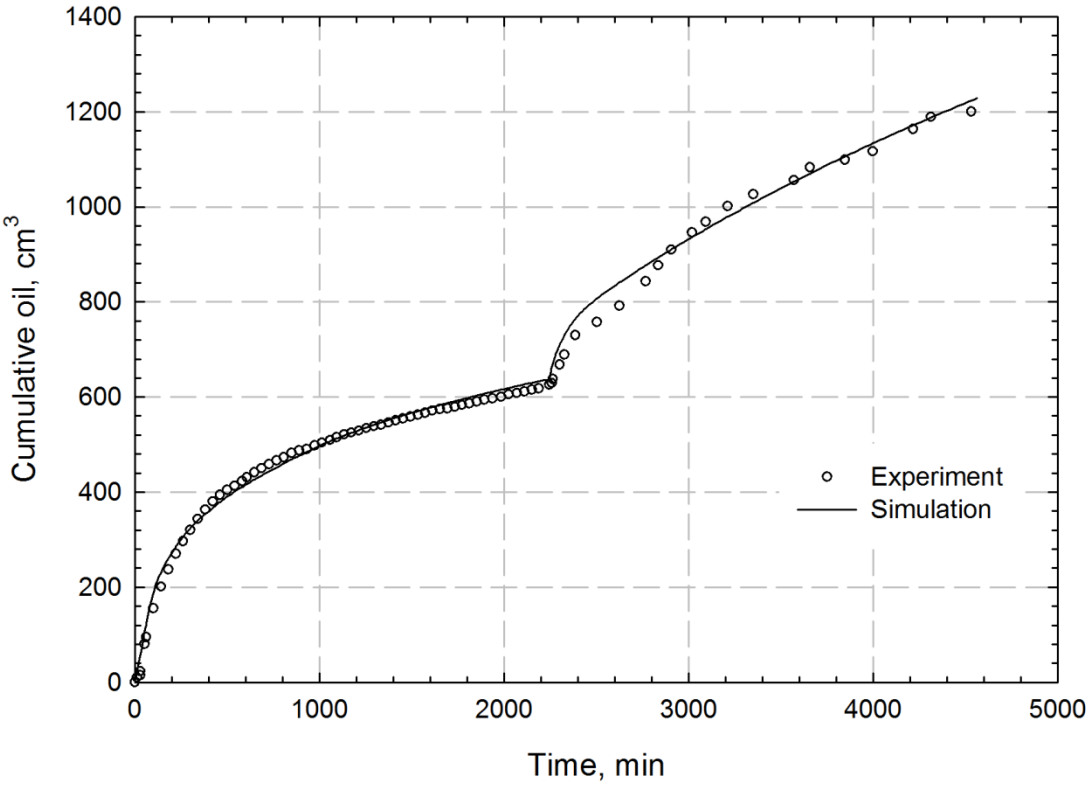

Figure 3.26 Measured and simulated cumulative oil production for Scenario #2.

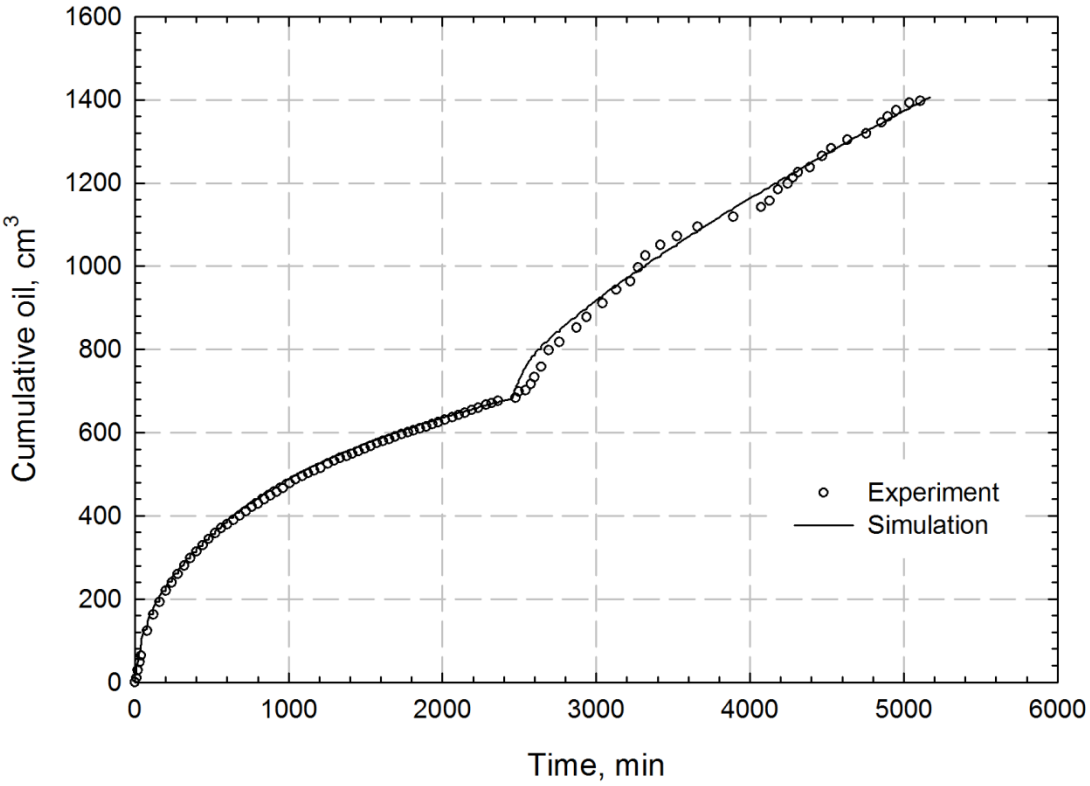

Figure 3.27 Measured and simulated cumulative oil production for Scenario #3.

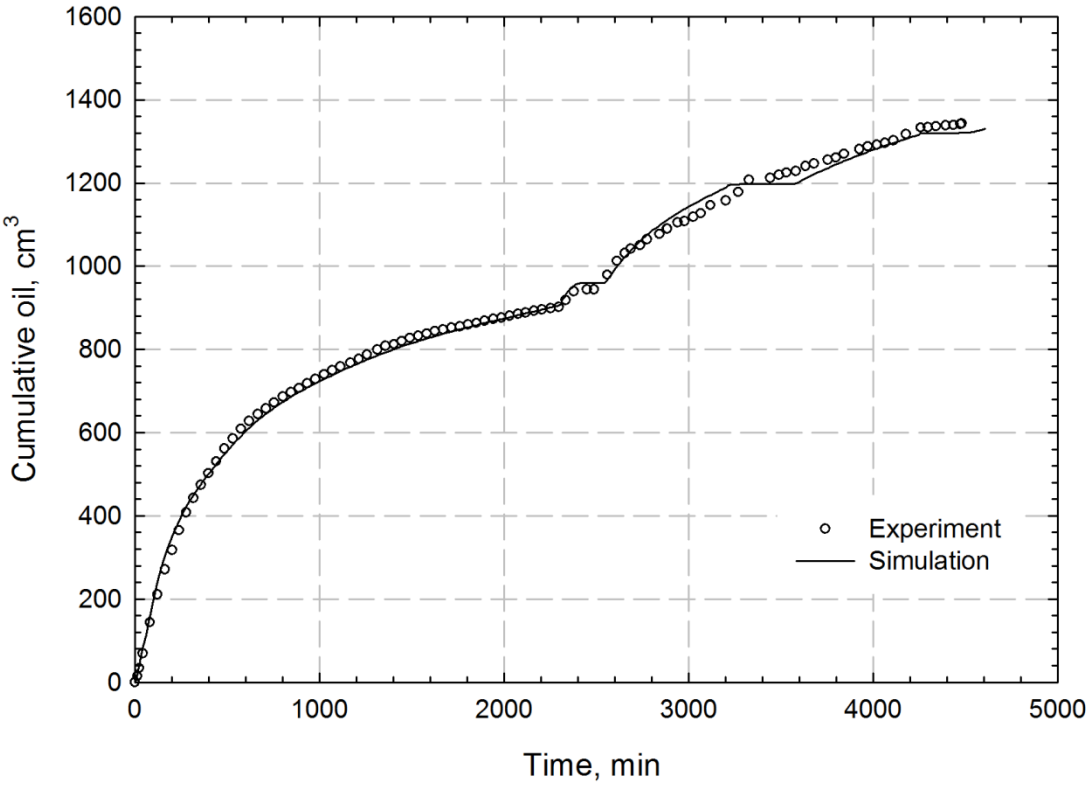

Figure 3.28 Measured and simulated cumulative oil production for Scenario #4.

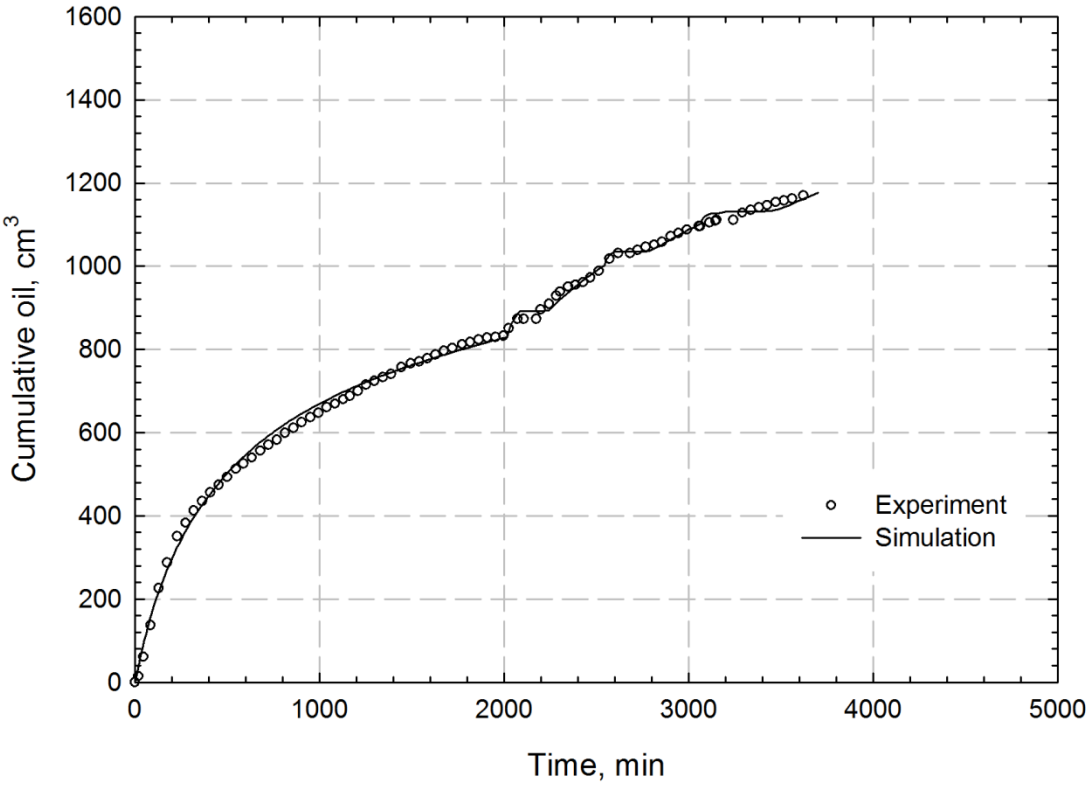

Figure 3.29 Measured and simulated cumulative oil production for Scenario #5.

resulting in a higher oil recovery with the subsequent water injection that displaces the mobilized heavy oil. Therefore, the CO_2 WAG process is a promising approach to maintain pressure and improve oil recovery in heavy oil reservoirs because of the positive and synergetic effects of oil swelling and viscosity reduction by CO_2 dissolution, high microscopic sweep efficiency of CO_2, and good macroscopic sweep efficiency of water.

As discussed previously, oil is mainly produced during the water injection process for each CO_2 WAG cycle. In this study, effects of water slug size are examined by using the history matched reservoir models for Scenarios #4 and #5, respectively, see Figures 3.30 to 3.33. As for Scenario #4, the slug size of CO_2 is kept to be 0.4 PV for each cycle, while the slug size of water is changed from 0.1 to 0.8 PV (i.e., WAG ratio varies from 0.25 to 2.00). For the purpose of convenient comparison, the continuous waterflooding is used as reference case.

As shown in Figure 3.30, compared to other schemes, the scheme with a WAG ratio of 0.25 produces less oil, though 4.0 PV of fluids has been injected. This is attributed to the fact, compared with the CO_2 slug size, the water slug size is too small to effectively control the CO_2 mobility in heavy oil reservoirs (Zheng and Yang, 2012). As for the same CO_2 slug size, a larger water slug size yields a higher oil recovery. As can be seen from Figure 3.31, if the water slug size is very large, the extra amount of water injection leads to trapping of oil and high cumulative water-oil ratios (WORs) (Rojas and Farouq Ali, 1986). It should be noted that oil recovery increases when the WAG ratio is increased from 0.50 to 2.00, while the cumulative WOR at WAG ratio of 0.75 remains close to the value at WAG ratio of 0.5. As such, WAG ratio of 0.75 leads to a relatively higher oil recovery and a lower cumulative WOR.

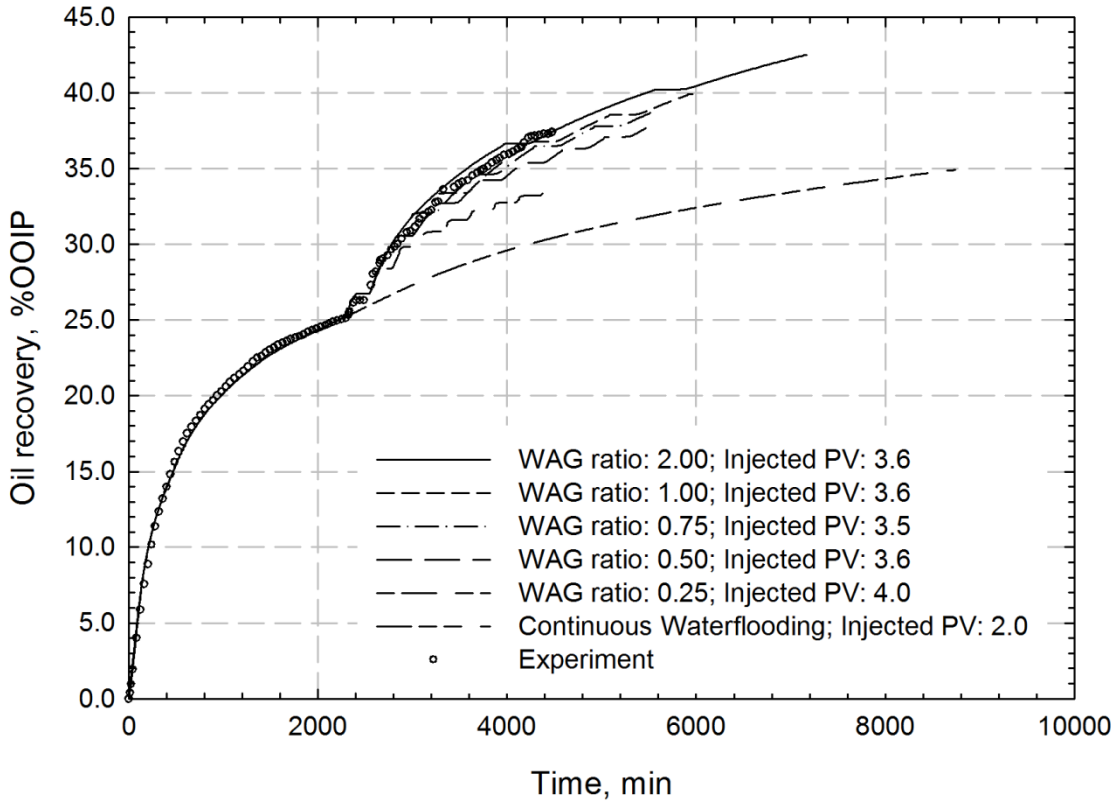

Figure 3.30 Production profiles with different water slug sizes for Scenario #4.

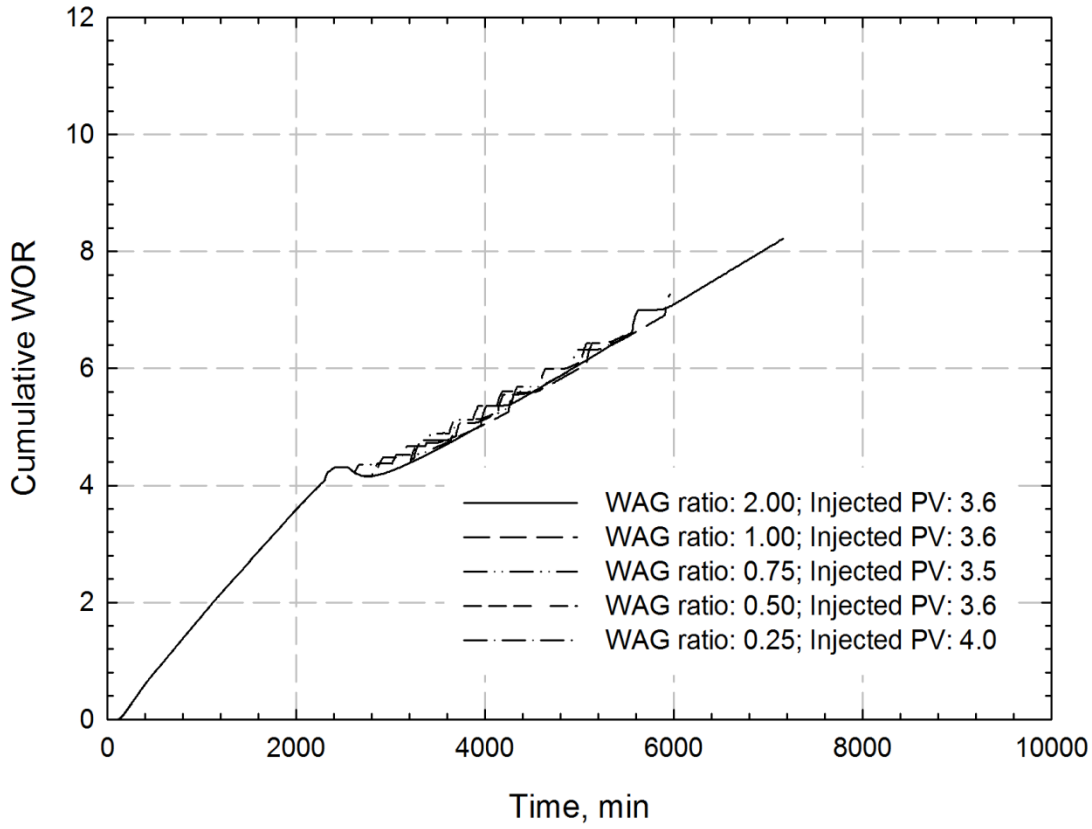

Figure 3.31 Cumulative WOR with different water slug sizes for Scenario #4.

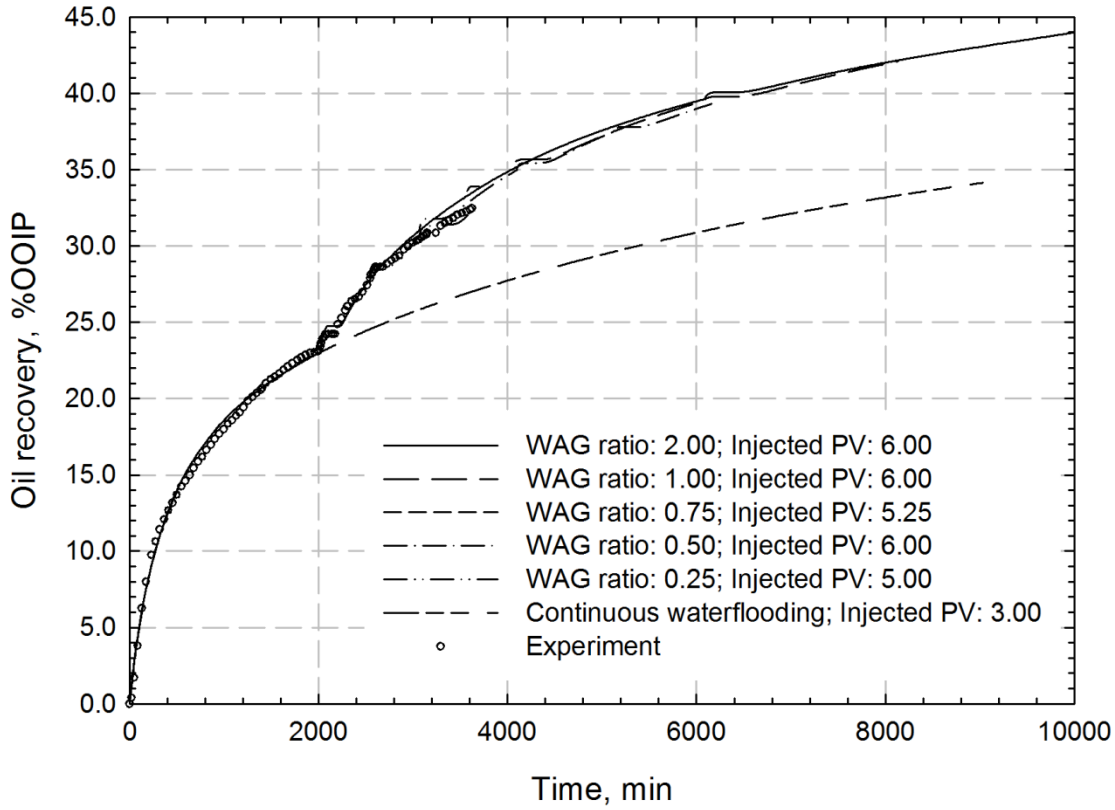

Figure 3.32 Production profiles with different water slug sizes for Scenario #5.

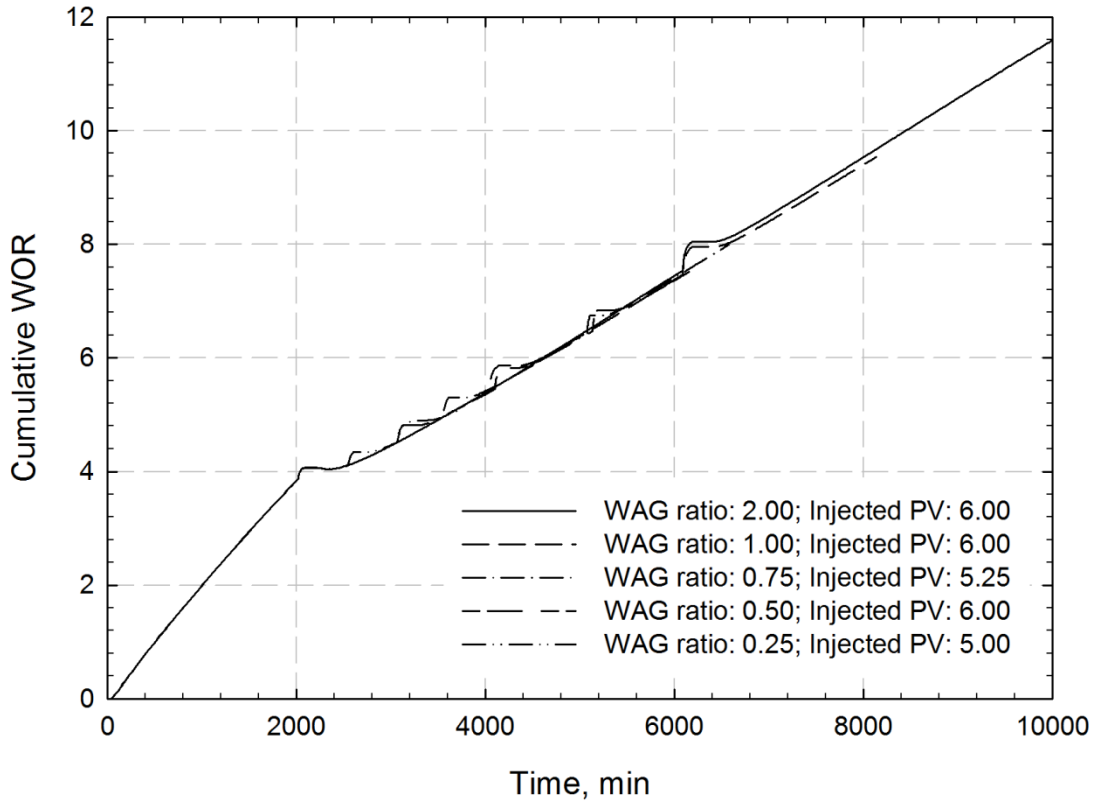

Figure 3.33 Cumulative WOR with different water slug sizes for Scenario #5.

As for Scenario #5, the slug size of CO_2 is set to be 1.0 PV for all cases (see Figures 3.32 and 3.33). The production profiles for different WAG ratios follow a similar trend, while a higher water slug size yields a higher oil recovery. The water slug sizes of 1.0 PV and 2.0 PV (i.e., WAG ratios of 1.0 and 2.0) are sufficient to control the mobility of CO_2 to achieve high oil recovery. However, the WAG ratio of 1.0 can keep a lower cumulative WOR than that of WAG ratio of 2.0 when the same PV of fluids is injected (6.0 PV). Therefore, the WAG ratios of 0.75 and 1.00 are determined to be the optimum values for Scenarios #4 and #5, respectively.

3.4 Summary

A 3D displacement model with five vertical wells and three horizontal wells has been developed and used to evaluate performance of pressure maintenance and improving oil recovery with CO_2 injection in heavy oil reservoirs. The effects of well configuration on pressure maintenance and oil recovery are examined by using three well configurations (i.e., five-spot, 4VI-HP, and HI-HP). Waterflooding-CO_2 injection processes, waterflooding-CO_2 WAG process and continuous CO_2 injection are examined, respectively. The well configurations associated with horizontal well(s) are found to have advantages of controlling a larger reservoir area and dominating a better sweep efficiency. CO_2 injection and CO_2 WAG can mobilize heavy oil and promotes oil recovery in waterflooded heavy oil reservoirs, though breakthrough occurs early. Numerical simulations are performed to history match the experimental results. There exists a good agreement between numerical and experimental results, demonstrating that numerical simulation has captured the overall behaviors of both the waterflooding-CO_2 injection

process and waterflooding-CO_2 WAG process. The optimum WAG ratio is determined to be 0.75 and 1.00 for Scenarios #4 and #5, respectively.

CHAPTER 4 SCREENING CRITERIA FOR PRESSURE MAINTENANCE WITH CO_2 INJECTON

A number of screening criteria have been proposed in tabular forms in which the suitable ranges of oil and formation properties for CO_2 injection are recommended in light and medium oil reservoirs (Taber, 1983; Taber, 1997a; 1997b; Thomas, 1998; Adasani and Bai, 2011). As for the tabulated criteria, reservoirs whose parameters comply with the recommended values will be selected; otherwise, they will be rejected. A parametric method was proposed to take into account synergistic effects of reservoir properties on CO_2 flooding performance (Rivas *et al*., 1994), while the similar screening technique was used to investigate the technical feasibility of CO_2 miscible displacement in light oil reservoirs and rank the Alberta oil reservoirs for CO_2 EOR and sequestration, respectively (Diaz *et al*., 1996; Shaw and Bachu, 2002). For the parametric screening methods, the reservoirs whose parameters are close to the fictitious optimum reservoir will be assigned high scores; otherwise, the score will be low.

CO_2 injection is a promising technique to enhance heavy oil reservoirs where other EOR techniques are not applicable. As mentioned in Chapter 3, it has been experimentally found that CO_2 injection is beneficial for oil recovery in heavy oil reservoirs by using a 3D experimental displacement system. Few attempts have been made to screen heavy oil reservoirs for pressure maintenance and improving oil recovery with CO_2 injection. To facilitate screening a right candidate for CO_2 EOR, it is essential that corresponding criteria need to be developed for such purpose in heavy oil reservoirs. In this Chapter, the response surface methodology (RSM) (Box and Wilson, 1951) has

been used to develop the screening criteria for selecting right candidates and subsequently evaluating the performance of CO_2 injection in heavy oil reservoirs for pressure maintenance and improving oil recovery.

4.1 Methodology

4.1.1 Response surface model

Response surface methodology (RSM) was introduced by Box and Wilson (1951), which explores the relationships between several input variables and one or more response variables. It comprises a set of statistical techniques for empirical model construction and model application. Based on effective design and analysis of experiments, response surface model can be used to reveal the relationship between the performance of heavy oil reservoirs and reservoir parameters, such as reservoir pressure, temperature, API gravity, when CO_2 injection is implemented for the purpose of pressure maintenance.

As a widely used response surface model, quadratic model is first chosen to evaluate reservoir performance, which has been successfully applied in reservoir engineering to approximate the reservoir response (Vanegas Prada and Cunha, 2008; Wood *et al.*, 2008).

$$f(x) = a_0 + \sum_{i=1}^{n} a_i x_i + \sum_{i=1}^{n} a_{ii} x_i^2 + \sum_{i=1}^{n} \sum_{j=1, i \neq j}^{n} a_{ij} x_i x_j \qquad [4.1]$$

where a_0 is the intercept term, x_i are linear terms, x_i^2 are quadratic terms, $x_i x_j$ are interaction terms, and a_i, a_{ii}, and a_{ij} are coefficients.

In this study, the linear terms and quadratic terms show the influence of a reservoir parameter on oil recovery, while the interaction terms display the synergistic effect of two reservoir parameters on oil recovery. As shown in Figure 4.1, the procedure of screening a reservoir candidate by using the response surface methodology can be briefly summarized as follows.

1). Select input parameters and their ranges on the basis of geological and geophysical properties, fluid properties, and production history.
2). Specify details on experimental design. The number of runs and levels of factors used in the simulation work should be defined. In this study, the central composite design (CCD) is used to achieve such purpose.
3). Perform the designed simulations. Based on the simulation results, the response surface model can be constructed by using the linear regression, while effects of parameters can also be analyzed.
4). Screen and rank the reservoir candidate with the proposed response surface model.

There are many characteristics for a certain reservoir, such as reservoir pressure, temperature, depth, permeability, oil saturation. But it is impractical to include all the reservoir parameters to construct the response surface model. Therefore, several crucial reservoir parameters should be screened and selected prior to establishing the response surface model.

Oil viscosity is not a necessary screening parameter, since it is not an independent parameter which mainly depends on API gravity and temperature. Depth is not considered as a crucial screening parameter because the former two parameters (i.e.,

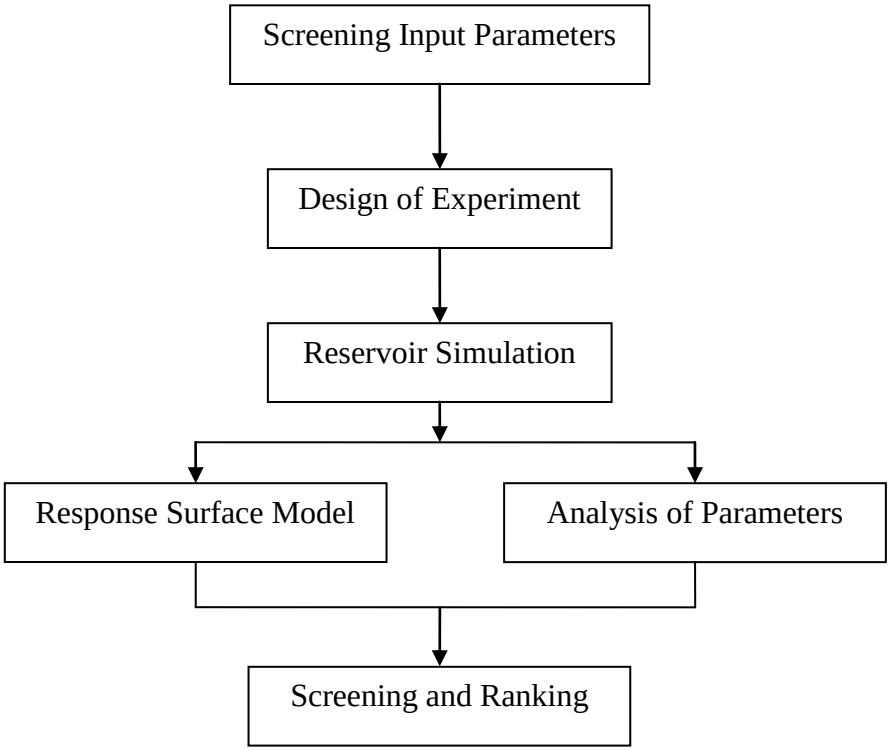

Figure 4.1 Flowchart of screening reservoir candidates for CO_2 injection with the response surface methodology.

reservoir temperature and pressure) are associated with depth. In other words, depth can be estimated by reservoir temperature and pressure if its respective gradient is known. Porosity is not taken as a critical screening parameter, because there is no significant difference in porosity for most of heavy oil reservoirs that have relatively high porosity. For different heavy oil reservoirs, permeability that represents the difficulty of fluid flowing in porous media is of remarkable difference. Thus, due to the independence and importance, reservoir temperature, pressure, API gravity, oil saturation, net pay thickness and permeability are chosen as crucial screening parameters to construct the response surface model and screen oil reservoirs for pressure maintenance with CO_2 injection.

According to the properties of heavy oil reservoirs (Meyer, 1997; Dusseault, 2001; Hinkle and Batzle, 2006; James *et al*., 2008), the variation ranges of the screening reservoir parameters are summarized and listed in Table 4.1. It is worthwhile mentioning that these screening parameters should be normalized when they are used as input factors to construct the response surface models. The input factors are normalized because possible values for different factors vary by several orders of magnitude, and thus the coefficients for response surface model vary by several orders of magnitude as well. Normalization improves the fairness of regressions by preventing an input factor with a large value from overwhelming other input factors that are important for the response result but with small values. Normalization implies that each factor has the same order of magnitude. In this way, the most influential coefficient is simply the largest coefficient that will impose the most impact on the value obtained by the response surface model. This also applies to the quadratic and interaction terms due to the fact that -1 and +1 are selected as the normalization endpoints (Wood *et al*., 2008). The normalization can be

Table 4.1 Variation range of the screening parameters

Parameter	Minimum	Maximum
Temperature, °C	15.0	45.0
Pressure, MPa	5.0	17.0
API gravity, °API	10.0	20.0
Oil saturation, %	40.0	70.0
Net pay thickness, m	3.0	50.0
Permeability, mD	500.0	3000.0

achieved by using the following equation:

$$x_{ni} = \frac{x_{oi} - \frac{x_{oi,max} + x_{oi,min}}{2}}{\frac{x_{oi,max} - x_{oi,min}}{2}} \quad [4.2]$$

where x_{ni} is the normalized value for parameter i; x_{oi} is the original value for parameter i, $x_{oi,max}$ and $x_{oi,min}$ are maximum and minimum original values for parameter i, respectively.

4.1.2 Central composite design

Numerous cases and levels of parameters are required to evaluate and analyze for determining the screening criteria associated with CO_2 injection in a heavy oil reservoir. The selected cases should be sufficient to determine all coefficients in the response surface model, and have more than two levels to characterize the non-linear behavior of the response parameters (Vanegas Prada and Cunha, 2008).

The central composite design (CCD) technique that is one of the most frequently used experimental design methods is selected in this study. It is comprised of three parts: 1) cube points, 2^k cube points come from two-level factorial design, where k is the number of parameters; 2) axial points, the number of axial point is always twice the number of factors, i.e., $2k$ axial points; 3) central point, representing one experiment where all control parameters are set to their nominal values (Ryan, 2007). In this study, oil recoveries for different cases are determined by reservoir simulation, and then they are used to construct the response surface model. The selected cases and normalized input

parameters are listed in Table 4.2. As shown in the table, the values of -1 and 1 mean minimum and maximum values for the input parameters, respectively, while the value of 0 indicates the nominal value of input parameters.

4.1.3 Reservoir simulation

There are three well configurations, Pattern #1, Pattern #2, and Pattern #3 in this section. Pattern #1 is five-spot well pattern, Pattern #2 is one horizontal injector combining with four vertical producers, and Pattern #3 is one horizontal producer integrating with four vertical injectors. For three different well configurations, three synthetic reservoir models are built, respectively. Each of them is a square unit covering an area of 6.25×10^4 m^2. The reservoirs are modeled using the Cartesian grids, with 25 grids in i direction, j direction, and 10 layers in k direction, respectively. The reservoir models are homogeneous, and there is no temperature change during CO_2 injection process for each case. In addition, no bottom aquifer and gas cap are considered. The horizontal well is located at bottom layer of the reservoir, while the vertical wells are fully perforated through the net pay zone. It is assumed that all the reservoir models have the same porosity in this study. The value of porosity is set to be 0.3 in reservoir models, which is a typical value of porosity reported in literatures (Meyer, 1997; Dusseault, 2001; Hinkle and Batzle, 2006; James *et al*., 2008). The performances of continuous CO_2 injection of 10 years are evaluated with a reservoir simulator (CMG GEM, Version 2009.13).

Table 4.2 Selected cases for model analysis

Case #	A	B	C	D	E	F	Case #	A	B	C	D	E	F
1	-1	-1	-1	-1	-1	-1	40	1	1	1	-1	-1	1
2	1	-1	-1	-1	-1	-1	41	-1	-1	-1	1	-1	1
3	-1	1	-1	-1	-1	-1	42	1	-1	-1	1	-1	1
4	1	1	-1	-1	-1	-1	43	-1	1	-1	1	-1	1
5	-1	-1	1	-1	-1	-1	44	1	1	-1	1	-1	1
6	1	-1	1	-1	-1	-1	45	-1	-1	1	1	-1	1
7	-1	1	1	-1	-1	-1	46	1	-1	1	1	-1	1
8	1	1	1	-1	-1	-1	47	-1	1	1	1	-1	1
9	-1	-1	-1	1	-1	-1	48	1	1	1	1	-1	1
10	1	-1	-1	1	-1	-1	49	-1	-1	-1	-1	1	1
11	-1	1	-1	1	-1	-1	50	1	-1	-1	-1	1	1
12	1	1	-1	1	-1	-1	51	-1	1	-1	-1	1	1
13	-1	-1	1	1	-1	-1	52	1	1	-1	-1	1	1
14	1	-1	1	1	-1	-1	53	-1	-1	1	-1	1	1
15	-1	1	1	1	-1	-1	54	1	-1	1	-1	1	1
16	1	1	1	1	-1	-1	55	-1	1	1	-1	1	1
17	-1	-1	-1	-1	1	-1	56	1	1	1	-1	1	1
18	1	-1	-1	-1	1	-1	57	-1	-1	-1	1	1	1
19	-1	1	-1	-1	1	-1	58	1	-1	-1	1	1	1
20	1	1	-1	-1	1	-1	59	-1	1	-1	1	1	1
21	-1	-1	1	-1	1	-1	60	1	1	-1	1	1	1
22	1	-1	1	-1	1	-1	61	-1	-1	1	1	1	1
23	-1	1	1	-1	1	-1	62	1	-1	1	1	1	1
24	1	1	1	-1	1	-1	63	-1	1	1	1	1	1
25	-1	-1	-1	1	1	-1	64	1	1	1	1	1	1
26	1	-1	-1	1	1	-1	65	-1	0	0	0	0	0
27	-1	1	-1	1	1	-1	66	1	0	0	0	0	0
28	1	1	-1	1	1	-1	67	0	-1	0	0	0	0
29	-1	-1	1	1	1	-1	68	0	1	0	0	0	0
30	1	-1	1	1	1	-1	69	0	0	-1	0	0	0
31	-1	1	1	1	1	-1	70	0	0	1	0	0	0
32	1	1	1	1	1	-1	71	0	0	0	-1	0	0
33	-1	-1	-1	-1	-1	1	72	0	0	0	1	0	0
34	1	-1	-1	-1	-1	1	73	0	0	0	0	-1	0
35	-1	1	-1	-1	-1	1	74	0	0	0	0	1	0
36	1	1	-1	-1	-1	1	75	0	0	0	0	0	-1
37	-1	-1	1	-1	-1	1	76	0	0	0	0	0	1
38	1	-1	1	-1	-1	1	77	0	0	0	0	0	0
39	-1	1	1	-1	-1	1							

Note:
A: Temperature; B: Pressure; C: API; D: Oil saturation; E: Net pay thickness;
F: Permeability

The simulation strategies are designed according to the CCD technique. For each well configuration, a total of 77 cases are utilized for regression of response surface model. In total, 231 simulation cases are performed in this study. As shown in the Table 4.2, the first 64 cases are determined by the two-level factorial design of six factors, which are used to estimate the linear and two-factor interaction terms of the regression model. Cases #65 to #76 are the twelve face centered axial points, which contributes to estimation of the quadratic terms. Finally, one central point (Case #77) is selected in this study. The reservoir and fluid data used in simulations are obtained from the literature (Spivak and Chima, 1984; Sankur *et al*., 1986; McKean *et al*., 1999; Guler *et al*., 2001; Krejbjerg and Pedersen, 2006).

4.2 Results and Discussion

4.2.1 Effects of screening parameters

Based on the simulation results, effects of screening parameters on recovery factor for each well configuration can be observed through the Pareto plots (see Figures 4.2 to 4.4). Ten terms that impose important impact on oil recovery are shown in Pareto plots, respectively. Based on three Pareto plots, it can be seen that pressure and API gravity are found to be the most crucial parameters that significantly affect oil recovery during CO_2 injection for pressure maintenance in heavy oil reservoirs. Temperature and permeability impose their moderate impact on oil recovery, while reservoir thickness shows its minor effect. The interaction term of pressure and permeability leads to a more dominant effect on the oil recovery factor for Patterns #2 and #3 than that for Pattern #1. This indicates that the interaction term of pressure and permeability plays a more important role in the

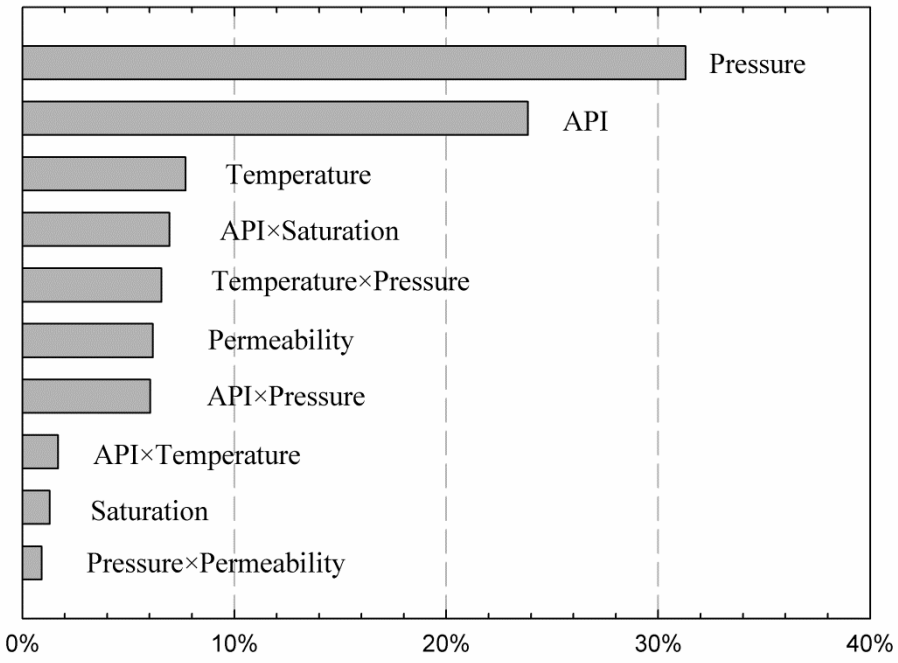

Figure 4.2 Pareto plot for oil recovery of Pattern #1.

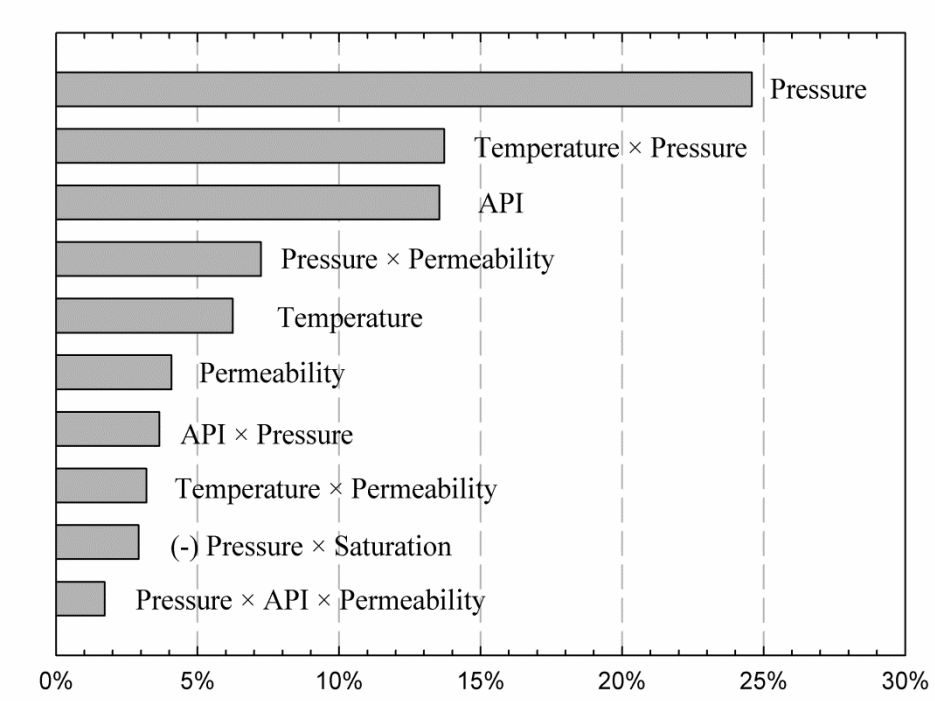

Figure 4.3 Pareto plot for oil recovery of Pattern #2.

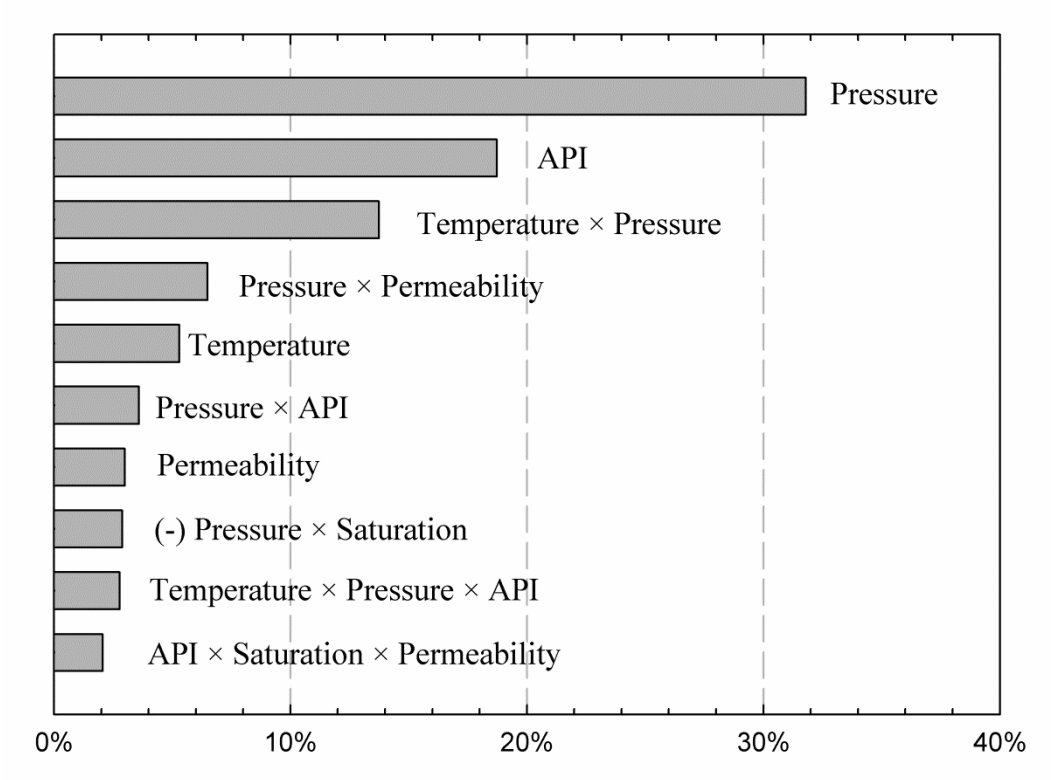

Figure 4.4 Pareto plot for oil recovery of Pattern #3.

well configuration associated with horizontal well. For Pattern #2 and Pattern #3, the interaction term of temperature and pressure shows a little more important effect on recovery factor for Pattern #2 than Pattern #3, while the interaction term of API and pressure imposes more significant influence on recovery factor for Pattern #3 than Pattern #2. Integrating response surface of screening parameters, the synergistic effect of screening parameters on oil recovery have been revealed sufficiently.

Pressure: Obviously, reservoir pressure shows a prominent influence on recovery factor. The dissolution of CO_2 into heavy oil, which causes the oil swelling, viscosity reduction, and interfacial tension reduction, is dependent on pressure. It has been found that viscosity is decreased with an increase in pressure at the first stage, and then the viscosity is increased slightly (Hao *et al.*, 2004). More CO_2 can be dissolved into heavy oil at a higher pressure during CO_2 injection, which is beneficial for oil recovery. Thus, pressure imposes a significantly positive impact on recovery factor when the reservoir pressure is maintained sufficiently. This is consistent with the experimental findings presented in Chapter 3.

API gravity: API gravity is found to be the other one of the most influential parameter during the process of pressure maintenance with CO_2 injection in heavy oil reservoirs. API gravity represents the characteristics of heavy oil. Low API gravity means that heavy components account for a large portion in heavy oil and thus the heavy oil has a high potential of viscosity. As previously mentioned, CO_2 can enhance heavy oil recovery due to inducing oil swelling, reducing oil viscosity and interfacial tension. However, it is difficult for CO_2 to reduce oil viscosity significantly and displace oil in the oil reservoirs with low API gravity. An increase in viscosity of heavy oil and thus a

decrease in CO_2-mass transfer leads to a marked reduction in heavy oil recovery by CO_2 injection (Rojas and Farouq Ali, 1986). By contrast, CO_2 plays a great role in acting as a pressure maintenance agent and displacing oil in heavy oil reservoirs with a higher API gravity for the purpose of pressure maintenance and improving oil recovery. Therefore, the performance of pressure maintenance with CO_2 injection in a heavy oil reservoir mainly depends on API gravity, and a higher API gravity benefits a higher oil recovery.

Temperature: It is also shown in Pareto plots that temperature imposes a positive influence on oil recovery. In fact, temperature has two-side effects during the process of CO_2 injection in heavy oil reservoirs. A high temperature is not favorable for the dissolution of CO_2 into heavy oil. However, heavy oil viscosity is very sensitive to temperature. In this study, the temperature ranges from 15°C to 45°C. In this range, the increase of temperature contributes to low viscosity (McCain Jr., 1991), which offsets the negative effect of high temperature on reducing the dissolution of CO_2 in heavy oil. As a result, the favourable effect of temperature on oil recovery is observed through the Pareto plots.

Permeability: It can be seen that permeability is a crucial parameter that imposes a noticeably impact on oil recovery. The difficulty of fluid flowing in porous media can be represented by permeability. A reservoir with high permeability means that the formation allows reservoir fluids flowing from reservoir into wellbore with low resistance and less energy consumption. In heavy oil reservoirs, high permeability is beneficial for CO_2 displacing oil to producers, leading to a high oil recovery during CO_2 injection in heavy oil reservoirs with the purpose of pressure maintenance.

API×Pressure: Figures 4.5 to 4.7 show the response surface of API×Pressure for three different well configurations, respectively. It is found that the recovery factor is low when the value of this interaction term of API×Pressure is low, while the recovery factor increases with the increase of API gravity and pressure. This interaction term with a higher value results in a higher recovery factor because a high API gravity indicates that less heavy components are contained in heavy oil, which is great of benefit to oil recovery. Furthermore, the dissolution of CO_2 is high in such heavy oil at a higher pressure, leading to a higher oil recovery. It can also be found that recovery factor is increased much more remarkably with the increase of pressure, although it increases with API gravity as well.

Pressure×Permeability: The response surfaces of Pressure×Permeability for Pattern #1, Pattern #2, and Pattern #3 are shown in Figures 4.8 to 4.10, respectively. Based on the response surfaces of Pressure×Permeability, it can be found that oil recovery factor increases with the increase of pressure and permeability. In addition, with the increase of pressure, oil recovery increases significantly, indicating that pressure exerts a more important effect on recovery factor than permeability. This result is in good agreement with the fact shown in Pareto plots.

Temperature×Pressure: Figures 4.11 to 4.13 show the response surfaces of Temperature×Pressure for three well configurations, respectively. This interaction term imposes a positive effect on recovery factor. The higher value of this term, the higher oil recovery can be obtained through CO_2 injection in heavy oil reservoirs. This is attributed to the fact that the positive synergistic effects of these two parameters (i.e., a high dissolution of CO_2 in heavy oil at a higher pressure and a decrease in oil viscosity at a

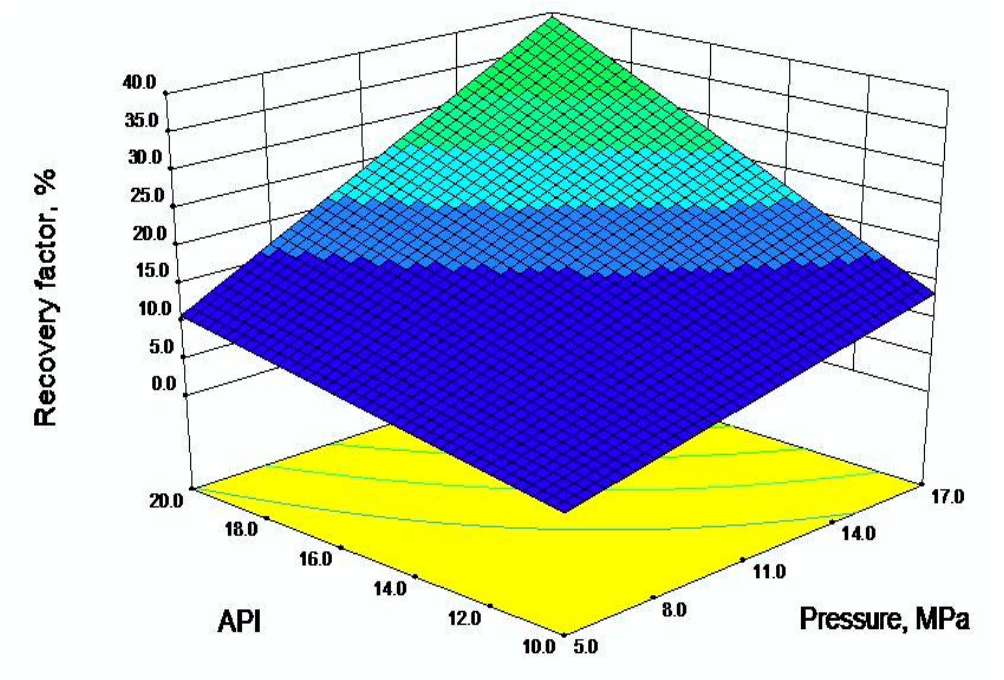

Figure 4.5 Response Surface of API×Pressure for Pattern #1.

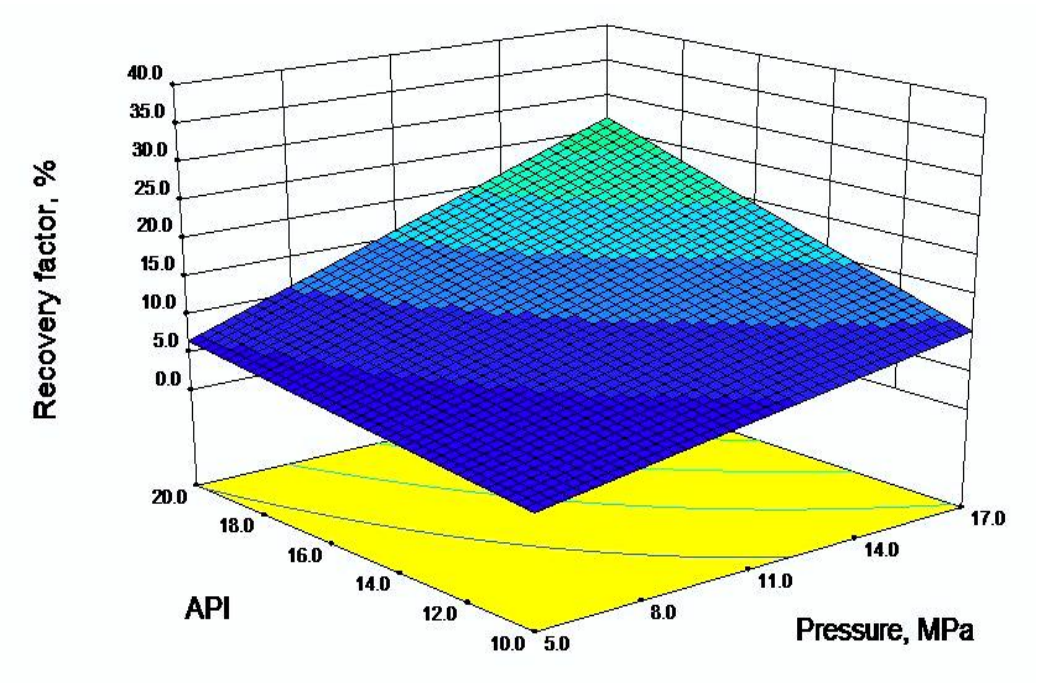

Figure 4.6 Response Surface of API×Pressure for Pattern #2.

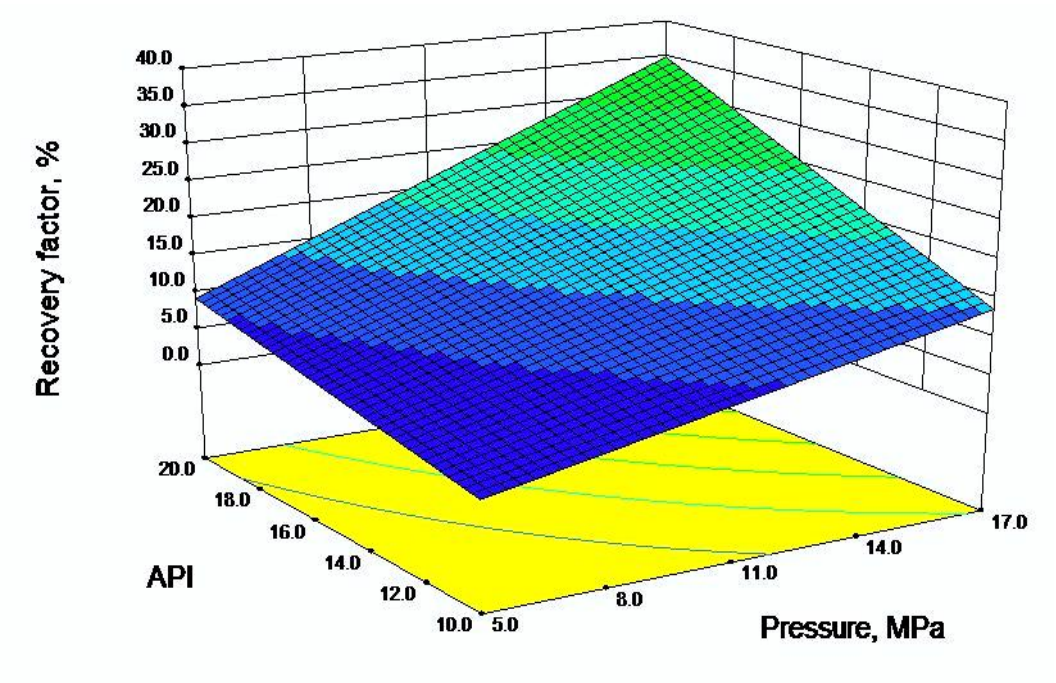

Figure 4.7 Response Surface of API×Pressure for Pattern #3.

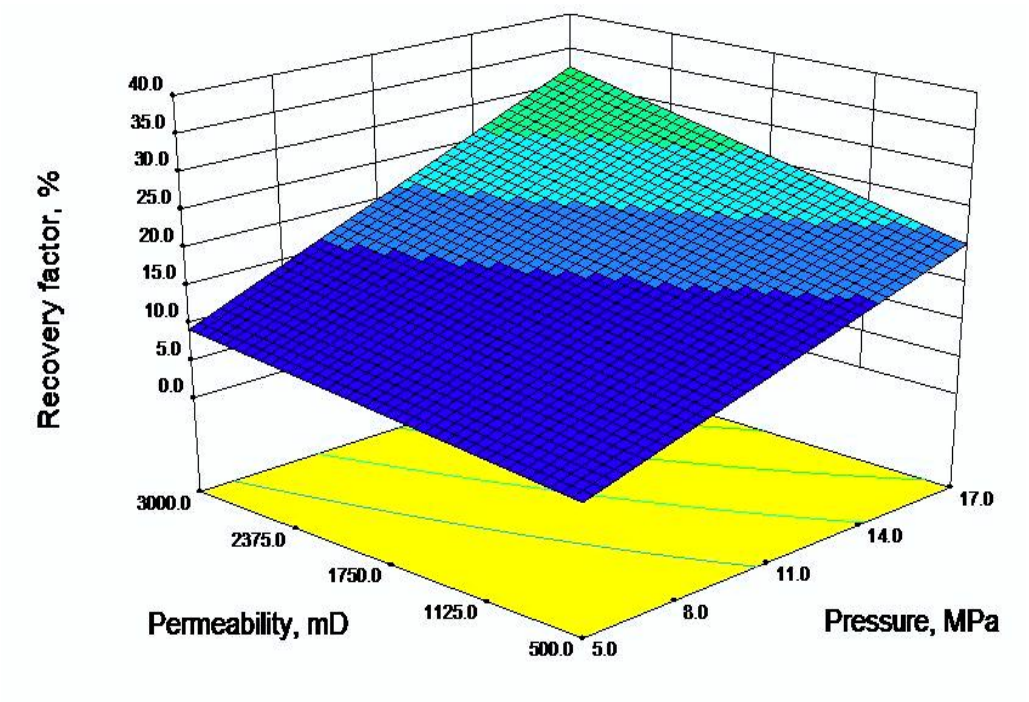

Figure 4.8 Response Surface of Pressure×Permeability for Pattern #1.

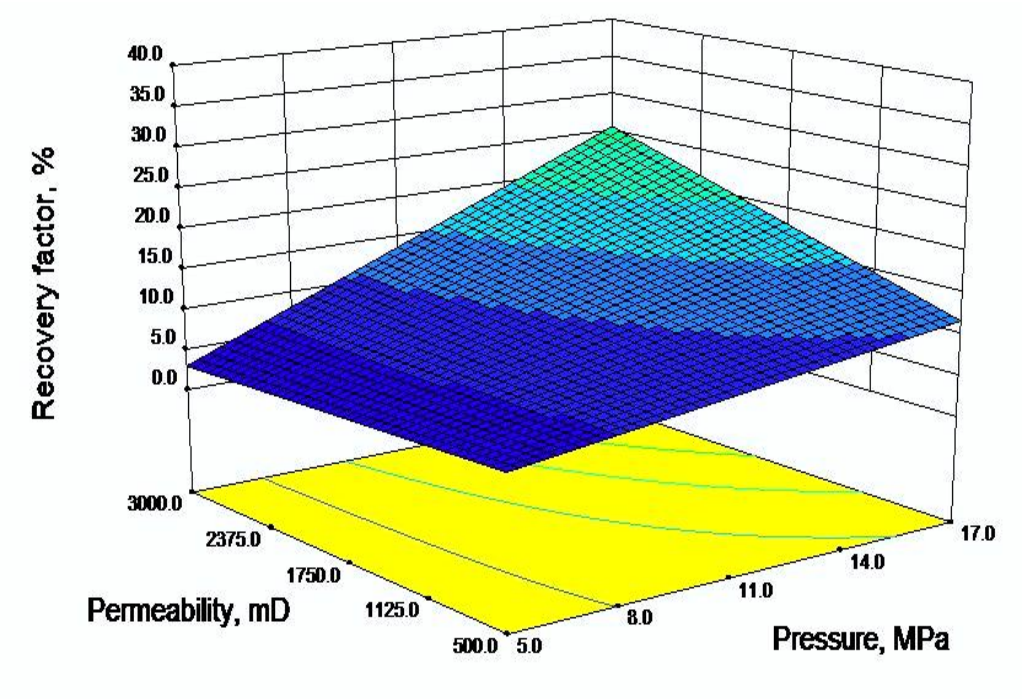

Figure 4.9 Response Surface of Pressure×Permeability for Pattern #2.

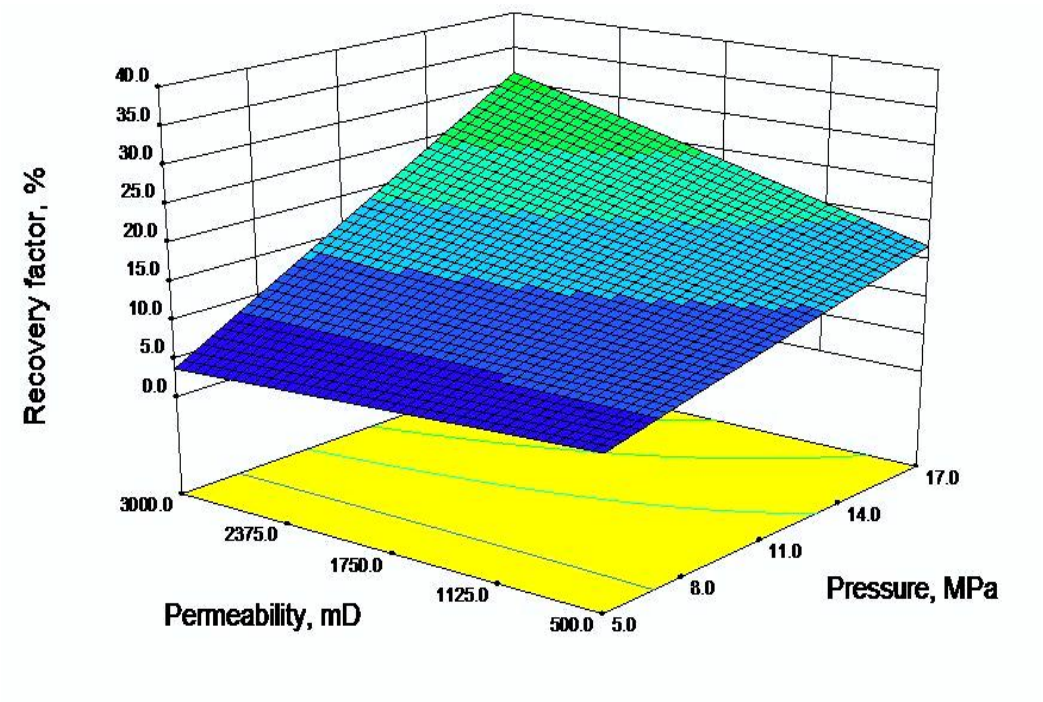

Figure 4.10 Response Surface of Pressure×Permeability for Pattern #3.

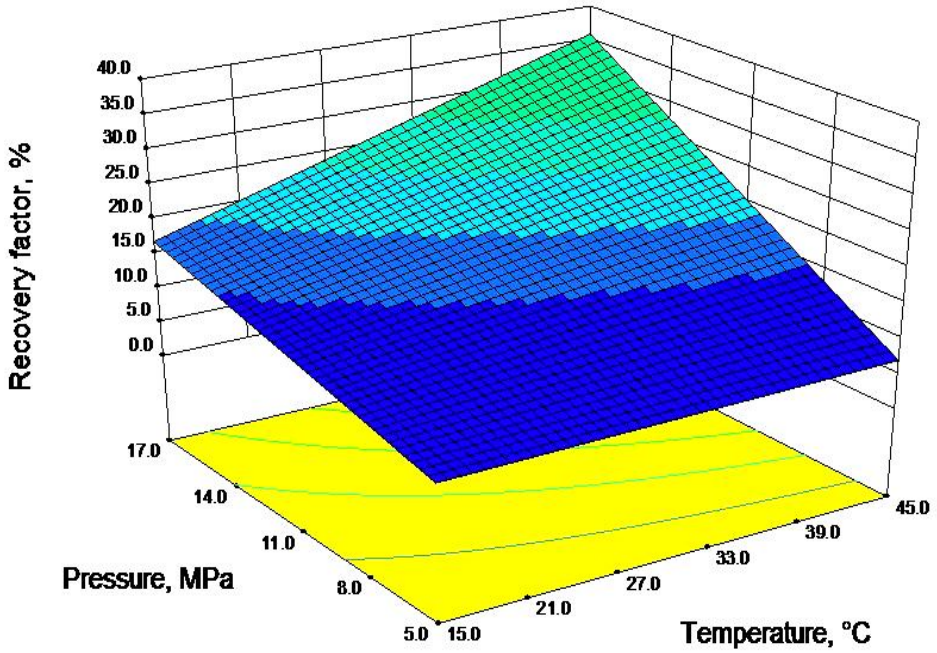

Figure 4.11 Response Surface of Temperature×Pressure for Pattern #1.

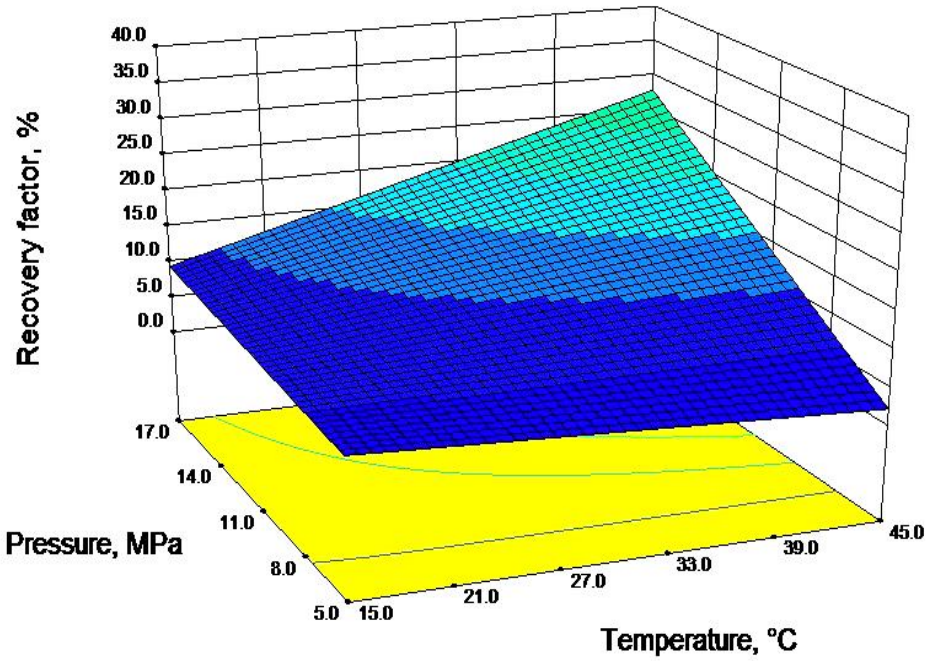

Figure 4.12 Response Surface of Temperature×Pressure for Pattern #2.

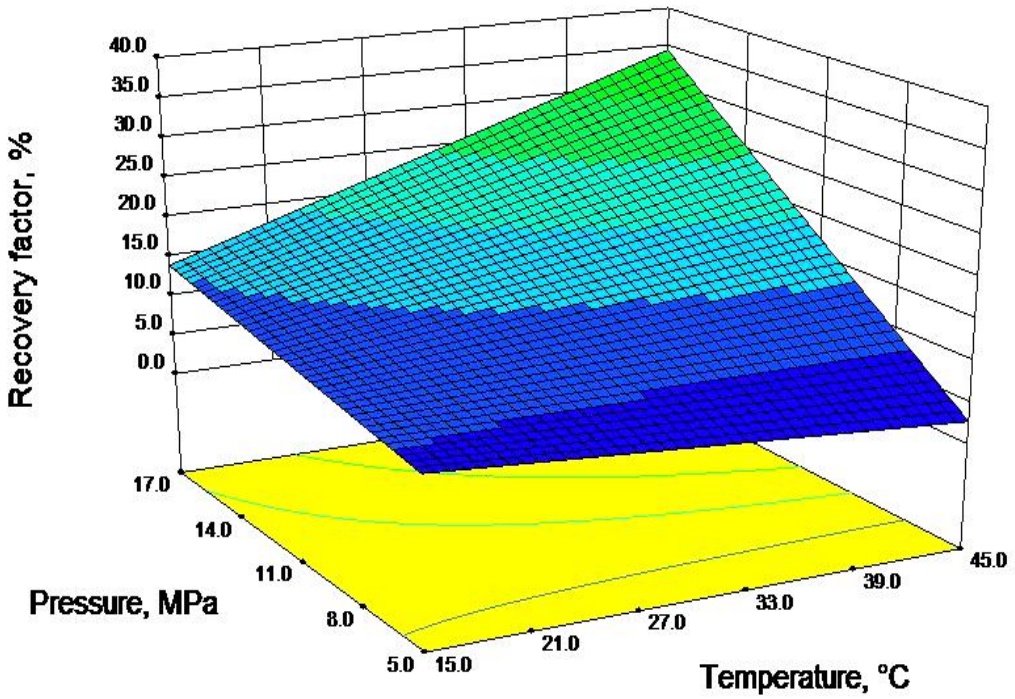

Figure 4.13 Response Surface of Temperature×Pressure for Pattern #3.

higher temperature). The figures also show that the impact of pressure on recovery factor is more significant. It is worthwhile mentioning that the performance of pressure maintenance with CO_2 injection in heavy oil reservoirs mainly depends on pressure and API gravity. The heavy oil reservoir with a higher pressure and API gravity provides a better response of CO_2 injection, while CO_2 injection in a heavy oil reservoir with a lower API gravity is not very attractive. The interaction terms of temperature and permeability impose greater positive effects on oil recovery. Reservoir net pay thickness does not show a significant effect on oil recovery.

4.2.2 Proposed response surface model

The response surface model is constructed by using a statistical tool (Design-Expert, Version 8, Stat-Ease, Inc., Minneapolis, USA) based on the results obtained from reservoir simulations. As for Pattern #1, a quadratic model with $R^2 = 0.9293$, adjusted $R^2 = 0.8904$, predicted $R^2 = 0.8172$ and adequate precision of 21.29 that measures the signal to noise ratio, and a ratio greater than 4.0 is desirable, is first obtained.

Through further analysis, it is found that the three-factor interaction terms are not included in the quadratic model. As a result, the information obtained from simulations has not been taken full advantage. In addition, for Pattern #1, the Pareto plot and the analysis of variance for the quadratic model indicate that API gravity, reservoir pressure, temperature, and permeability show great influence on the performance of pressure maintenance with CO_2 injection in a heavy oil reservoir. Therefore, the response surface model is re-formulated. Some two-factor interaction terms are eliminated, while several

three-factor interaction terms are added with the purpose of improving the response surface model. Eventually, a reduced cubic response model with one intercept term, six linear terms, sixteen quadratic terms and four three-factor interaction terms has been established. The statistics of this new model are: $R^2 = 0.9445$, adjusted $R^2 = 0.9157$, predicted $R^2 = 0.8589$, and adequate precision is 23.75. This indicates that the new model is better than the quadratic one. The response surface model for the CO_2 injection with Pattern #1 is shown as follows:

$$\begin{aligned} r(T,P,API,So,h,k) = {} & 19.76 + 4.67\times T + 9.85\times P + 8.87\times API + 2.06\times So + 0.44\times h \\ & + 4.36\times k + 4.53\times T\times P + 2.29\times T\times API + 0.54\times T\times So \\ & + 0.60\times T\times k + 4.34\times P\times API - 1.49\times P\times So + 1.69\times P\times k \\ & + 4.65\times API\times So - 0.48\times API\times h + 0.70\times API\times k \\ & + 0.85\times So\times k - 0.35\times h\times k - 3.59\times T^2 + 11.09\times API^2 \\ & + 1.65\times h^2 - 7.18\times k^2 - 1.60\times T\times P\times So + 0.98\times T\times P\times k \\ & - 0.95\times P\times So\times h + 0.95\times API\times So\times h \end{aligned}$$

[4.3]

where r is oil recovery, %; T is normalized temperature; P is normalized pressure; API is normalized API gravity; S_o is normalized oil saturation; h is normalized net pay thickness; k is normalized permeability.

Similarly, the response models for Pattern #2 and Pattern #3 are obtained, respectively. For Pattern #2, the response surface model with $R^2 = 0.9253$, adjusted $R^2 = 0.8792$, predicted $R^2 = 0.7902$, and adequate precision of 22.55 is expressed as follows.

$$
\begin{aligned}
r(T,P,API,So,h,k) = {} & 19.98 + 3.43\times T + 7.45\times P + 5.12\times API - 2.74\times So - 1.03\times h \\
& + 2.97\times k + 5.51\times T\times P - 0.18\times T\times API - 1.70\times T\times So \\
& - 0.10\times T\times h + 2.66\times T\times k + 2.84\times P\times API - 2.55\times P\times So \\
& - 1.12\times P\times h + 4.00\times P\times k + 0.24\times API\times So - 1.39\times API\times h \\
& + 0.63\times API\times k + 1.00\times So\times k - 6.20\times T^2 - 4.91\times P^2 \\
& + 7.28\times API^2 + 1.46\times T\times P\times API - 2.83\times T\times P\times So \\
& - 1.09\times T\times API\times h - 1.04\times T\times So\times k - 1.58\times P\times API\times h \\
& + 1.95\times P\times API\times k + 1.22\times API\times So\times k
\end{aligned}
\qquad [4.4]
$$

For Pattern #3, the response surface model with $R^2 = 0.9702$, adjusted $R^2 = 0.9538$, predicted $R^2 = 0.9189$, and adequate precision of 30.33 is expressed as follows.

$$
\begin{aligned}
r(T,P,API,So,h,k) = {} & 22.52 + 3.71\times T + 9.48\times P + 7.38\times API - 1.89\times So + 0.12\times h \\
& + 2.93\times k + 6.30\times T\times P + 0.50\times T\times API - 1.20\times T\times So \\
& + 1.95\times T\times k + 3.22\times P\times API - 2.89\times P\times So + 4.33\times P\times k \\
& + 1.94\times API\times So - 0.35\times API\times k + 1.27\times So\times k - 5.15\times T^2 \\
& - 5.34\times P^2 + 8.52\times API^2 + 3.87\times So^2 - 6.40\times h^2 \\
& + 2.84\times T\times P\times API - 2.02\times T\times P\times So + 0.92\times T\times API\times k \\
& + 0.96\times P\times API\times So + 0.96\times P\times API\times k + 2.44\times API\times So\times k
\end{aligned}
\qquad [4.5]
$$

The proposed response surface models act as proxy functions to the reservoir simulator. These three models with good statistical results allow us to evaluate the performance of pressure maintenance with CO_2 injection in a heavy oil reservoir without performing reservoirs simulation for the mentioned well configurations. Six key reservoir parameters are use to estimate the performance of CO_2 injection in heavy oil reservoirs through the response surface models, which is practical for new heavy oil reservoirs when less reservoir properties are known.

4.3 Screening Criteria

For preliminary screening the heavy oil reservoirs to implement CO_2 injection for the purpose of pressure maintenance, a heavy oil reservoir with high pressure and API gravity is preferred for conducting CO_2 injection due to the fact that the performance of pressure maintenance with CO_2 injection mainly depends on pressure and API gravity. Higher pressure and API gravity are beneficial for oil recovery. In addition, a heavy oil reservoir with high temperature and permeability is also appropriate to implement CO_2 injection because higher temperature and permeability contribute to higher oil recovery.

For further screening, the performance of pressure maintenance with CO_2 injection in heavy oil reservoirs can be evaluated by using the proposed response surface models once the values of reservoir temperature, pressure, API gravity, oil saturation, net pay thickness and permeability are known and in the range as listed in the Table 4.1. In other words, the oil recovery for a specific heavy oil reservoir with CO_2 injection is estimated through the response surface model, and then the candidate reservoirs are screened and ranked based on the estimated oil recoveries.

4.4 Summary

The screening criteria for pressure maintenance with CO_2 injection in heavy oil reservoirs have been developed. The criteria are associated with reservoir temperature, pressure, API gravity, oil saturation, net pay thickness and permeability. It is found that pressure and API gravity are the most influential reservoir properties on the performance of CO_2 injection in heavy oil reservoirs. Higher pressure and API gravity are beneficial

for higher oil recovery. The interaction terms associated with pressure also show a prominent influence on oil recovery factor. The heavy reservoirs with high API gravity, pressure and temperature are preferred for conducting the pressure maintenance with CO_2 injection.

The CCD technique has been used to design the simulation strategies. The reduced cubic response surface models with good statistics have also been developed. By using the proposed response surface model, it is convenient and efficient to estimate the reservoir response in terms of oil recovery factor. The candidate reservoirs can be screened and ranked based on the estimated oil recovery.

CHAPTER 5 CONCLUSIONS AND RECOMMENDATIONS

5.1 Conclusions

In the course of this thesis study, comprehensive studied have been conducted on utilization of CO_2 for pressure maintenance and improving oil recovery in heavy oil reservoirs. A 3D displacement model with five vertical wells and three horizontal wells has been established at the Petroleum Technology Research Centre (PTRC), University of Regina, to study the performance of pressure maintenance with CO_2 injection in heavy oil reservoirs. Three well configurations, i.e., five-spot, four vertical injectors and one horizontal producer (4VI-HP), and one horizontal injector and one horizontal producer (HI-HP), are designed to examine effect of well configurations on oil recovery under different flooding processes. Subsequently, numerical simulations are performed to history match the experimental results of waterflooding-CO_2 injection and waterflooding-CO_2 WAG processes. Finally, the central composite design (CCD) technique is applied to design simulation strategies for determining the screening criteria for CO_2 injection in heavy oil reservoirs.

The major conclusions that can be drawn from this thesis study are summarized as follows.

1. Utilization of CO_2 for pressure maintenance is beneficial for heavy oil recovery because the injected CO_2 not only acts as a pressure maintenance agent, but also enhances oil recovery. As for waterflooding-CO_2 injection processes, oil recoveries are measured to be 19.5% for Scenario #1, 32.2% for Scenario #2,

and 38.6% for Scenario #3, respectively. The incremental oil recoveries of 12.4% and 8.9% through three water-alternating-CO_2 cycles are experimentally achieved for Scenarios #4 and #5, respectively, and continuous CO_2 injection contributes to oil recovery of 32.5% for Scenario #6.

2. Well configuration imposes a strong impact on oil recovery. Gas override is severe under well configuration of five-spot, while the well configurations with horizontal well(s) are found to efficiently control a larger reservoir area, alleviate gas override, and initiate a better sweep efficiency, leading to higher oil recovery.
3. For CO_2 WAG processes, water slug facilitates the displacement of CO_2. It is experimentally found that majority of the produced oil in the CO_2 WAG process is recovered during the first cycle. After the second cycle, there is no significant increment in oil recovery. The optimum WAG ratio is determined to be 0.75 and 1.00 for two CO_2 WAG processes, respectively.
4. During a blowdown process, it is experimentally found that little fluids are produced when pressure is decreased from 3800 kPa to 2000 kPa, whereas most of fluids are produced at pressure below 1500 kPa. The blowdown process is found to last for a relatively long period (i.e., more than 2 h) in this study. Blowdown process contributes to the incremental oil recoveries of 6.7%, 5.1%, 2.3%, 2.8%, 4.1%, and 4.7% for Scenarios #1 to #6, respectively.
5. There exists an excellent agreement between numerically simulated and experimentally measured oil recoveries, demonstrating that numerical simulation has captured the overall behaviours of both the waterflooding-CO_2

injection process and waterflooding-CO_2 WAG process. Viscous forces are found to dominate the displacement process, while CO_2 breakthrough occurs early due to the adverse mobility ratio of CO_2 to heavy oil.

6. The CCD technique has been successfully used to design reservoir simulation strategies. A total of 231 simulation cases are well designed and sufficient to construct response surface models with good statistics, which are convenient and efficient to initially evaluate the oil recovery associated with CO_2 injection in heavy oil reservoirs.
7. The screening criteria for pressure maintenance with CO_2 injection in heavy oil reservoirs have been developed. Such screening criteria are associated with reservoir temperature, pressure, API gravity, oil saturation, net pay thickness and permeability. Pressure and API gravity are found to be the most influential reservoir properties on performance of CO_2 injection in heavy oil reservoirs. Higher pressure and API gravity are beneficial for higher oil recovery. The candidate reservoirs for pressure maintenance with CO_2 injection can be screened and ranked with the associated response surfaces.

5.2 Recommendations

Based on this thesis study, the following recommendations for future studies are made:

1. Due to the adverse mobility ratio, not only does CO_2 breakthrough occur early, but also gas channelling is severe when CO_2 is injected into heavy oil reservoirs. Effective CO_2 mobility control techniques, such as polymer and foam injection,

which are conventionally used to alleviate gas fingering, improve sweep efficiency, and extend the contact time between injected CO_2 and heavy oil, should be investigated with the 3D displacement model, and subsequently implemented during the developed process of CO_2 injection in heavy oil reservoirs.

2. The effects of well spacing for conventional well pattern comprising of vertical wells and the well patterns associated with horizontal wells shall be examined and optimized, while position of heels and toes for horizontal wells need to be investigate to alleviate gas fingering and improve CO_2 sweep efficiency.
3. Pressure distribution among injectors and producers shall be examined by using well-designed pressure sensors when the 3D displacement model is used to evaluate performance of CO_2 injection in heavy oil reservoirs. It will be practical to capture the behaviours of CO_2 displacement and simulate the displacement process based on the pressure distribution.
4. Comprehensive phase behaviours of CO_2 and solvents should be studied, while various impurities or rich solvents can be added to the CO_2 stream to investigate the synergistic effects of CO_2 and solvents on heavy oil under various well configurations and reservoirs conditions.
5. Comprehensive field-scale reservoir simulations should be performed to examine the performance of CO_2 injection for pressure maintenance in a targeted heavy oil reservoir. Effect of reservoir heterogeneity on oil recovery and sequestration of CO_2 can be investigated, while economic analysis and

sensitivity analysis shall be performed to guide the field application of CO_2 injection in heavy oil reservoirs.

6. Due to the high content of asphaltene in heavy oils and dissolution of CO_2 in heavy oil, both effect of CO_2 on asphaltene precipitation and effect of asphaltene on oil recovery should be investigated.

REFERENCES

Adams, D.M. Experiences with Waterflooding Lloydminster Heavy-Oil Reservoirs. *J. Pet. Technol*., 34 (8):1643-1650, 1982.

Adasani, A.A. and Bai, B. Analysis of EOR Projects and Updated Screening Criteria. *J. Pet. Sci. Eng.*, 79 (1-2): 10-24, 2011.

Akin, S. and Kovscek, A.R. Heavy-oil Solution Gas Drive: A Laboratory Study. *J. Pet. Sci. Eng.*, 35 (1-2): 33-48, 2002.

Ala, K.K. and Earlougher, R.C. CO_2 Injection as an Immiscible Application for Enhanced Recovery in Heavy Oil Reservoirs. Paper SPE 9928, presented at SPE California Regional Meeting, Bakersfield, CA, March 25-27, 1981.

Alberta Energy and Utilities Board (AEUB) ST98-2007. Alberta's Energy Reserves and Supply/Demand Outlook 2007-016. ISSN 1910-4235, Farhood Rahnama, Coord., Alberta Energy and Utilities Board, Calgary, AB, Canada, 2007.

Alberta Energy Resources Conservation Board (ERCB) ST98-2011. Alberta's Energy Reserves 2010 and Supply/Demand Outlook 2011-2020. ISSN 1910-4235, Carol Crowfoot, Coord., Energy Resources Conservation Board, Calgary, AB, 2011.

Arshad, A., AI-Majed, A.A., Maneouar, H., Muhammadain, A., and Mtawaa, B. Carbon Dioxide (CO_2) Miscible Flooding in Tight Oil Reservoirs: A Case Study. Paper SPE 127616, presented at the SPE Kuwait International Petroleum Conference and Exhibition, Kuwait City, Kuwait, December 14-16, 2009.

Asghari, K., Dong, M., Shire, J., Coleridge, T., Nagrampa, J., and Grassick, J. Development of a Correlation between Performance of CO_2 Flooding and the Past

Performance of Waterflooding in Weyburn Oil Field. *SPE Prod. Oper.*, 22 (2): 260-264, 2007.

ASTM D2007-03. Standard Test Method for Characteristic Groups in Rubber Extender and Processing Oils and Other Petroleum-Derived Oils by the Clay-Gel Absorption Chromatographic Method. ASTM International: West Conshohocken, PA, 2007.

Bagci, A.S. Immiscible CO_2 Flooding through Horizontal Wells. *Energy Sources Part A*, 29 (1): 85-95, 2007.

Bagci, S. and Tuzunoglu, E. 3D Model Studies of the Immiscible CO_2 Process Using Horizontal Wells for Heavy Oil Recovery. Paper 98-74, presented at the Annual Technical Meeting of CIM, Calgary, AB, June 8-10, 1998.

Beecher, C.E. and Parkhurst, I.P. Effect of Dissolved Gas upon the Viscosity and Surface Tension of Crude Oil. *Pet. Trans.* AIME, G-26: 51-69, 1926.

Beggs, H.D. and Robinson, J.R. Estimating the Viscosity of Crude Oil Systems. *J. Pet. Technol*., 27 (9): 1140-1141, 1975.

Bennett, E.O. Pressure Maintenance. Paper SPE 113, presented at the Eighth SPE Mid-year Meeting, Wichita, KS, May 24, 1938.

Bon, J. and Sarma, H.K. A Technical Evaluation of a CO_2 Flood for EOR Benefits in the Cooper Basin, South Australia. Paper SPE 88451, presented at the SPE Asia Pacific Oil and Gas Conference and Exhibition, Perth, Australia, October 18-20**,** 2004.

Bora, B., Maini, B.B., and Chakma, A. Flow Visualization Studies of Solution Gas Drive Process in Heavy Oil Reservoirs Using a Glass Micromodel. *SPE Reservoir Eval. Eng.*, 3 (3): 224-229, 2000.

Boustani, A. and Maini, B.B. The Role of Diffusion and Convective Dispersion in Vapour Extraction Process. *J. Can. Pet. Technol*., 40 (4): 68-77, 2001.

Boutette, M.J., Stephen, C.M.K., and Withers, R.L. Waterflooding in a Small Pinnacle Reef Reservoir with a Single Wellbore. *J. Can. Pet. Technol.*, 29 (1): 72-77, 1990.

Box, G.E.P. and Wilson, K.B. On the Experimental Attainment of Optimum Conditions. *J. Roy. Statistical Society, Series B*, 13 (1): 1-45, 1951.

Butler, R.M. and Mokrys, I.J. A New Process (VAPEX) For Recovering Heavy Oils Using Hot Water and Hydrocarbon Vapour. *J. Can. Pet. Technol*., 30 (1): 97-106, 1991.

Butler, R.M., Mcnab, G.S., and Lo, H.Y. Theoretical Studies on the Gravity Drainage of Heavy Oil during In-Situ Steam Heating. *Can. J. Chem. Eng.*, 59 (4): 455-460, 1981.

Chatzis, L. and Morrow, N.R. Correlation of Capillary Number Relationship for Sandstone. *SPE J.*, 24 (5): 555-562, 1984.

Chen, S., Li, H., Yang, D., and Tontiwachwuthikul, P. Optimal Parametric Design for Water-Alternating-Gas (WAG) Process in a CO_2-Miscible Flooding Reservoir. *J. Can. Pet. Technol.*, 49 (10): 75-82, 2010.

Chew, J. and Connally Jr., C.A. A Viscosity Correlation for Gas-Saturated Crude Oils. *Pet. Trans.* AIME, 216: 23-25, 1959.

Christensen, J.R., Stenby, E. H., and Skauge, A. Review of WAG Field Experience. *SPE Reservoir Eval. Eng.*, 4 (2): 97-106, 2001.

Chung, F.T.H., Jones, R.A., and Nguyen, H.T. Measurements and Correlations of the Physical Properties of CO_2/Heavy-Crude-Oil Mixtures. *SPE Reservoir Eng.*, 3 (3): 822-828, 1988.

Cobanoglu, M. A Numerical Study to Evaluate the Use of WAG as an EOR Method for Oil Production Improvement at B.Kozluca Field, Turkey. Paper SPE 72127, presented at the SPE Asia Pacific Improved Oil Recovery Conference, Kuala Lumpur, Malaysia, October 6-9, 2001.

Crawford, P.B. Pressure Maintenance Needed Here. *J. Pet. Technol*., 19 (11): 1449-1452, 1967.

Das, S.K. and Butler, R.M. Effect of Asphaltene Deposition on the Vapex Process: A Preliminary Investigation Using a Hele-Shaw Cell. *J. Can. Pet. Technol*., 33 (6): 39-45, 1994.

Das, S.K. Vapex: An Efficient Process for the Recovery of Heavy Oil and Bitumen. *SPE J.*, 3 (3): 232-237, 1998.

David, H.S. Disposal of Carbon Dioxide, a Greenhouse Gas, for Pressure Maintenance in a Steam-Based Thermal Process for Recovery of Heavy Oil and Bitumen. Paper SPE 86958, presented at the SPE International Thermal Operations and Heavy Oil Symposium and Western Regional Meeting, Bakersfield, CA, March 16-18, 2004.

Dello, L., Miyake, S., Kawaguchi, K., and Kimoto, M. Improved Oil Recovery by Pattern Gas Injection Using Horizontal Wells in a Tight Carbonate Reservoir. Paper SPE

36247, presented at the SPE Abu Dhabi International Petroleum Exhibition and Conference, Abu Dhabi, United Arab Emirates, October 13-16, 1996.

Denbina, E.S., Boberg, T.C., and Rottor, M.B. Evaluation of Key Reservoir Drive Mechanisms in the Early Cycles of Steam Stimulation at Cold Lake. *SPE Reservoir Eng.*, 6 (2): 207-211, 1991.

Diaz, D., Bassiouni, Z., Kimbrell, W., and Wolcott, J. Screening Criteria for Application of Carbon Dioxide Miscible Displacement in Waterflooded Reservoirs Containing Light Oil. Paper SPE 35431, presented at the SPE/DOE Improved Oil Recovery Symposium, Tulsa, OK, April 21-24, 1996.

Dong, M. and Dullien, F.A.L. Porous Media Flows. In: Multiphase Flow Handbook (Crowe, C.T., Ed), Taylor & Francis Group, New York, 2006.

Dong, M. and Huang, S. Fuel Gas Injection for Heavy Oil Recovery. *J. Can. Pet. Technol.*, 41 (9): 44-50, 2002.

Dong, M., Huang, S., and Hutchence, K. Methane Pressure-Cycling Process with Horizontal Wells for Thin Heavy-Oil Reservoirs. *SPE Reservoir Eval. Eng.*, 9 (2): 154-164, 2006.

Dusseault, M.B. Comparing Venezuelan and Canadian Heavy Oil and Tar Sands. Paper CIPC 2001-061, presented at the Canadian International Petroleum Conference, Calgary, AB, June 12-14, 2001.

Dyer, S.B. and Farouq Ali, S.M. The Potential of the Immiscible Carbon Dioxide Flooding Process for the Recovery of Heavy Oil. Paper SPE SS-89-27, presented at Technical Meeting/Petroleum Conference of the South Saskatchewan Section, Regina, SK, September 25-27, 1989.

Dyer, S.B., Huang, S.S., Farouq Ali, S.M., and Jha, K.N. Phase Behaviour and Scaled Model Studies of Prototype Saskatchewan Heavy Oils with Carbon Dioxide. *J. Can. Pet. Technol.*, 33 (8): 42-48, 1994.

Emera, M.K. and Sarma, H.K. A Genetic Algorithm-Based Model to Predict CO_2-Oil Physical Properties for Dead and Live Oil. *J. Can. Pet. Technol.*, 47 (2): 52-60, 2008.

Enayati, M., Heidaryan, E., and Mokhtari, B. New Investigations into Carbon Dioxide Flooding by Focusing on Viscosity and Swelling Factor Changes. Paper CIPC 2008-064, presented at the Canadian International Petroleum Conference, Calgary, AB, June 17-19, 2008.

Enick, R.M., Beckman, E.J., Shi, C., Huang, Z., Xu, J., and Kilic, S. Direct Thickeners for Carbon Dioxide. Paper SPE 59325, presented at the SPE/DOE Improved Oil Recovery Symposium, Tulsa, OK, April 3-5, 2000.

Etminan, S.R., Maini, B.B., and Kharrat, R. The Role of Connate Water Saturation in VAPEX Process. *J. Can. Pet. Technol*., 47 (2): 8-12, 2008.

Eydinov, D., Gao, G., Li, G., and Reynolds, A.C. Simultaneous Estimation of Relative Permeability and Porosity/Permeability Fields by History Matching Production Data. *J. Can. Pet. Technol*., 48 (12): 13-25, 2009.

Farouq Ali, S.M. Heavy oil-Evermore Mobile. *J. Pet. Sci. Technol.*, 37 (2003): 5-9, 2002.

Firoozabadi, A. Mechanisms of Solution Gas Drive in Heavy Oil Reservoirs. *J. Can. Pet. Technol.*, 40 (3): 15-20, 2001.

Forth, R., Slevinsky, B., Lee, D., and Fedenczuk, L. Application of Statistical Analysis to Optimize Reservoir Performance. *J. Can. Pet. Technol.*, 35 (8): 36-42, 1996.

Garcia, FM. and Meneven S.A. A Successful Gas-Injection Project in a Heavy Oil Reservoir. Paper SPE 11988, presented at the SPE Annual Technical Conference and Exhibition, San Francisco, CA, October 5-8, 1983.

Gasem, K.A.M., Dickson, K.B., Shaver, R.D., and Robinson Jr., R.L. Experimental Phase Densities and Interfacial Tensions for a CO_2/Synthetic-Oil and a CO_2/Reservoir-Oil System. *SPE Reservoir Eng.*, 8 (3): 170-174, 1993.

Guan, L., Du, Y., and Wang, Z. Water Injectivity-What We Have Learned in the Past 30 Years. *J. Can. Pet. Technol.*, 45 (5): 9-13, 2006.

Hadia, N. Chaudhari, L., Mitra, S.K., Vinjamur, M., and Singh, R. Experimental Investigation of Use of Horizontal Wells in Waterflooding. *J. Pet. Sci. Eng.*, 56 (4): 303-310, 2007.

Hao, Y., Wu, Z., Ju, B., Chen, Y., and Luo, X. Laboratory Investigation of CO_2 Flooding. Paper SPE 88883, presented at the SPE Nigeria Annual International Conference and Exhibition, Abuja, Nigeria, August 2-4, 2004.

Hatzignatiou, D.G. and Lu, Y. Feasibility Study of CO_2 Immiscible Displacement Process in Heavy Oil Reservoirs. Paper 94-90, presented at the Annual Technical Meeting of CIM, Calgary, AB, June 12-15, 1994.

Hinkle, A. and Batzle, M. Heavy Oils: A Worldwide Overview. *The Leading Edge*, 25 (6): 742-749, 2006.

Holm, L.W. and Josendal, V.A. Mechanisms of Oil Displacement by Carbon Dioxide. *J. Pet. Technol.*, 26 (12): 1427-1438, 1974.

Holm, L.W. and O'Brien, L.J. Carbon Dioxide Test at the Mead-Strawn Field. *J. Pet. Technol.*, 23 (4): 431-442, 1971.

Holm, L.W. Carbon Dioxide Solvent Flooding for Increased Oil Recovery. *Pet. Trans.* AIME, 216: 225-231, 1959.

Horner, W.L. Pressure Maintenance by Water Injection, Midway Field, Arkansas. Paper SPE 45-027, presented at the Twenty-fifth SPE Annual Meeting, Chicago, IL, November, 1945.

Huang, E.T.S. and Holm, L.W. Effect of WAG Injection and Rock Wettability on Oil Recovery during CO_2 Injection. *SPE Reservoir Eng.*, 3(1): 119-129, 1988.

Huang, S.S, Pappas, E.S., and Jha, K.N. The Carbon Dioxide Immiscible Recovery Process and Its Potential for Saskatchewan Reservoirs. Paper SS-87-1, presented at the Technical Meeting/Petroleum Conference of the South Saskatchewan Section, Regina, SK, October 6-8, 1987.

James, L.A., Rezaei, N., and Chatzis, I. Vapex, Warm Vapex and Hybrid Vapex-The State of Enhanced Oil Recovery for In Situ Heavy Oils in Canada. *J. Can. Pet. Technol*., 47 (4): 1-7, 2008.

Jha, K.N. A Laboratory Study of Heavy Oil Recovery with Carbon Dioxide. *J. Petrol. Technol.*, 25 (2): 54-63, 1986.

Jha, K.N. and Chakma, A. Nitrogen Injection with Horizontal Wells for Enhancing Heavy-Oil Recovery: 2D and 3D Model Studies. Paper SPE 23029, presented at the SPE Asia-Pacific Conference, Perth. Australia, November 4-7, 1991.

Kantar, K., Karaoguz, D., Issever, K., and Varana, L. Design Concepts of a Heavy-Oil Recovery Process by an Immiscible CO_2 Application. *J. Pet. Technol*., 37 (2): 275-283, 1985.

Kantzas, A. and Brook, G. Preliminary Laboratory Evaluation of Cold and Post-Cold Production Methods for Heavy Oil Reservoirs Part B: Reservoir Conditions. *J. Can. Pet. Technol.*, 43 (10): 39-48, 2004.

Karaoguz, D., Issever, K., Pamir, N., and Tirek, A. Performance of a Heavy-Oil Recovery Process by an Immiscible CO_2 Application, Bati Raman Field. Paper SPE 18002, presented at the SPE Middle East Oil Technical Conference and Exhibition, Manama, Bahrain, March 11-14, 1989.

Kelly, P. and Kennedy, S.L. Thirty Years of Effective Pressure Maintenance by Gas Injection in the Hilbig Field. *J. Pet. Technol*., 17 (3): 279-281, 1965.

Kesler M.G. and Lee, B.I. Improve Predictions of Enthalpy of Fractions. *Hydro. Prod.*, 55 (3): 153-158, 1976.

Klins, M.A. and Farouq Ali, S.M. Heavy Oil Production by Carbon Dioxide Injection. *J. Can. Pet. Technol.*, 21 (5): 64-72, 1982.

Kuhlman, M. Expanded Uses of Nitrogen, Oxygen and Rich Air for Increased Production of Both Light Oil and Heavy Oil. Paper SPE 86954, presented at the SPE International Thermal Operations and Heavy Oil Symposium and Western Regional Meeting, Bakersfield, CA, March 16-18, 2004.

Lederer, E.L. Viscosity of Mixtures with and without Diluents. *Proc. World Pet. Cong.*, 2: 526-528, 1933.

Li, H. and Yang, D. Estimation of Multiple Petrophysical Parameters for the PUNQ-S3 Model Using Ensemble-Based History Matching. Paper SPE 143583, presented at the SPE EUROPEC/EAGE Annual Conference and Exhibition, Vienna, Austria, May 23-26, 2011.

Li, H., Chen, S., Yang, D., and Tontiwachwuthikul, P. Estimation of Relative Permeability by Assisted History Matching Using the Ensemble Kalman Filter Method. *J. Can. Pet. Technol*., 51 (3): 205-214, 2012.

Li, H., Yang, D., and Tontiwachwuthikul, P. Experimental and Theoretical Determination of Equilibrium Interfacial Tension for the Solvent(s)-CO_2-Heavy Oil Systems. *Energy Fuels*, 26 (3): 1776-1786, 2012.

Li, J., Jiang, T., Xiao, L., Yang, M., Zhao, J. Field Study of Enhancing Oil Recovery by Gas Recycling Injection in Ultra Deep Heavy Oil Reservoirs. Paper SPE 115877, presented at SPE Asia Pacific Oil and Gas Conference and Exhibition, Perth, Australia, October 20-22, 2008.

Lim, G.B., Kry, R.P., Harker, B.C., and Jha, K.N. Cyclic Stimulation of Cold Lake Oil Sand with Supercritical Ethane. Paper SPE 30298, presented at SPE International Heavy Oil Symposium, Calgary, AB, June 19-21, 1995.

Lin, F.F.J. Oil Recovery by Carbon Dioxide Injection into Consolidated and Unconsolidated Sandstone. Paper 83-34-16, presented at Annual Technical Meeting, Banff, AB, May 10-13, 1983.

Lobe, V.M. A Model for the Viscosity of Liquid-Liquid Mixture. MASc. Thesis, University of Rochester, Rochester, NY, 1973.

Loomis, A.G. and Shea, G.B. Secondary Recovery of Oil in California. Paper WPC 4141, presented at the Third World Petroleum Congress, Hague, Netherlands, May 28-June 6, 1951.

Mai, A. and Kantzas, A. Heavy Oil Waterflooding: Effects of Flow Rate and Oil Viscosity. *J. Can. Pet. Technol*., 48 (3): 42-51, 2009.

Maini, B.B. and Okazawa, T. Effects of Temperature on Heavy-oil-water Relative Permeability of Sand. *J. Pet. Technol*., 26 (3): 33-41, 1987.

Mangalsingh, D. and Jagai, T. A Laboratory Investigation of the Carbon Dioxide Immiscible Process. Paper SPE 36134, presented at the SPE Latin America/ Caribbean Petroleum Engineering Conference, Port-of-Spain, Trinidad, April 23-26, 1996.

McDonald, S., Mandybura, F., and Sparks, N. Carbon Dioxide for Enhanced Oil Recovery in Canada. *J. Can. Pet. Technol*., 24 (1): 66-70, 1985.

Mehrotra, A.K. and Svrcek, W.Y. Correlations for Properties of Bitumen Saturated with CO_2, CH_4 and N_2, and Experiments with Combustion Gas Mixtures. *J. Can. Pet. Technol.*, 21 (6): 95-104, 1982.

Meyer, R.F. World Heavy Crude Oil Resources. Paper WPC 29196, presented at the 15th World Petroleum Congress, Beijing, China, October 12-17, 1997.

Miller, K.A. State of the Art of Western Canadian Heavy Oil Water Flood Technology. Paper CIPC 2005-251, presented at the Canadian International Petroleum Conference, Calgary, AB, June 7-9, 2005.

Mokrys, I.J. and Butler R.M. The Rise of Interfering Solvent Chambers: Solvent Analog Model of Steam-Assisted Gravity Drainage. *J. Can. Pet. Technol*., 32 (3): 26-36, 1993.

Monger, T.G. Measurement and Prediction of Swelling Factors and Bubble Points for Paraffinic Crude Oils in the Presence of CO_2 and Contaminant Gases. *Ind. Eng. Chem. Res.*, 26 (6): 1147-1153, 1987.

Mullken, C.A. and Sandler, S.I. The Prediction of CO_2 Solubility and Swelling Factors for Enhanced Oil Recovery. *Ind. Eng. Chem. Process Des. Dev.*, 19 (4): 709-711, 1980.

Mungan, N. Carbon Dioxide Flooding Fundamentals. *J. Can. Pet. Technol*., 20 (1): 87-92, 1981.

Olenick, S., Schroeder, F.A., Haines, H.K., and Monger-Mcclure, T.G. Cyclic CO_2 Injection for Heavy-Oil Recovery in Halfmoon Field: Laboratory Evaluation and Pilot Performance. Paper SPE 24645, presented at the SPE Annual Technical Conference and Exhibition, Washington, DC, October 4-7, 1992.

Pariani, G.J., McColloch, K.A., Warden, S.L., and Edens, D.R. An Approach to Optimize Economics in a West Texas CO_2 Flood. *J. Pet. Technol.*, 44 (9): 984-988, 1992.

Park, R.A. Pressure Maintenance by Waterflooding North Virden Scallion Field, Manitoba. *J. Can. Pet. Technol.*, 5 (1): 7-13, 1966.

Patton, E.C. Jr. Evaluation of Pressure Maintenance by Internal Gas Injection in Volumetrically Controlled Reservoirs. *Pet. Trans.* AIME, 170: 112-155, 1947.

Paul D. Oil Recovery by Fluid Injection. Paper WPC 4140, presented at the Third World Petroleum Congress, Hague, Netherlands, May 28-June 6, 1951.

Peng, D.Y. and Robinson, D.B. A New Two-constant Equation of State. *Ind. Eng. Chem. Fundam.*, 15 (1): 58-64, 1976.

Poston, S.W., Ysrael, S., Hossain, A.K.M.S., Montgomery III, E.F., and Ramey Jr., H.J. The Effect of Temperature on Irreducible Water Saturation and Relative Permeability of Unconsolidated Sands. *SPE J.*, 10 (2): 171-180, 1970.

Puttagunta, V.R. and Miadonye, A. Correlation and Prediction of Viscosity of Heavy Oils and Bitumens Containing Dissolved Gases. Part II: Saskatchewan Heavy Oils Saturated with Gas Mixtures. *AOSTRA J. Res.*, 7 (4): 251-258, 1991.

Pyo, K., and Damian-Diaz, N., Powell, M., and Van Nieuwkerk, J. CO_2 Flooding in Joffre Viking Pool. Paper CIPC 2003-109, presented at Canadian International Petroleum Conference, Calgary, AB, June 10-12, 2003.

Quail, B., Gordon, A.H., and Jha, K.N. Correlations of Viscosity, Density and Gas Solubility for Saskatchewan Heavy Oils. Paper SS-87-6, presented at the Technical Meeting/Petroleum Conference of the South Saskatchewan Section, Regina, SK, October 6-8, 1987.

Righi, E.F. and Pascual, M. Water-Alternating-Gas Pilot in the Largest Oil Field in Argentina: Chihuido de la Sierra Negra, Neuquen Basin. Paper SPE 108031, presented at the Latin American & Caribbean Petroleum Engineering Conference, Buenos Aires, Argentina, April 15-18, 2007.

Rivas, O., Embid, S., and Bolivar, F. Ranking Reservoirs for Carbon Dioxide Flooding Processes. *SPE Advanced Technology Series*, 2 (1): 95-103, 1994.

Rogan, A.D. and Smith, B.R. Waterflood Pressure Maintenance of the Peejay Field-British Columbia. *J. Can. Pet. Technol.*, 4 (1): 36-41, 1965.

Rojas, G.A. and Farouq Ali, S.M. Dynamics of Subcritical CO_2/Brine Floods for Heavy-Oil Recovery. *SPE Reservoir Eng.*, 3 (1): 35-44, 1988.

Rojas, G.A. and Farouq Ali, S.M. Scaled Model Studies of Carbon Dioxide/Brine Injection Strategies for Heavy Oil Recovery from Thin Formations. *J. Pet. Technol.*, 25 (1): 85-94, 1986.

Romanov, A.S. and Zolnikova, E.F. Maintenance of Reservoir Pressure in Gas and Oil Deposit by Gas Injection. Paper SPE 117426, presented at the SPE Russian Oil and Gas Technical Conference and Exhibition, Moscow, Russia, October 28-30, 2008.

Ryan, T.P. Modern Experimental Design. *John Wiley & Sons, Inc*., Hoboken, New Jersey, 2007.

Sahin, S., Kalfa, U., and Celebioglu, D. Bati Raman Field Immiscible CO_2 Application: Status Quo and Future Plans. Paper SPE 106575, presented at the Latin American & Caribbean Petroleum Engineering Conference, Buenos Aires, Argentina, April 15-18, 2007.

Samane, M., Nobakht, M., and Gu, Y. Theoretical and Physical Modeling of a Solvent Vapour Extraction (VAPEX) Process for Heavy Oil Recovery. *J. Petrol. Sci. Eng.*, 65 (1-2): 93-104, 2009.

Sankur, V., Creek, J.L., Dijulio, S.S., and Emanuel, A.S. A Laboratory Study of Wilmington Tar Zone CO_2 Injection Project. *SPE Reservoir Eng.*, 1 (1): 95-104, 1986.

Saskatchewan Energy and Resources. *Oil and Gas Industry Facts*, Regina, SK, Canada, 2008.

Satter, A., Brugman, R.J., Yard, M.B., and Mims, D.S. The Role of Simulators in Reservoir Management. Paper SPE 25605, presented at the SPE Middle East Oil Technical Conference & Exhibition, Bahrain, April 3-6, 1993.

Settari, T. New Developments in Simulation. *J. Can. Pet. Technol*., 32 (1): 21-24, 1993.

Shaw, J. and Bachu, S. Screening, Evaluation, and Ranking of Oil Reservoirs Suitable for CO_2-Flood EOR and Carbon Dioxide Sequestration. *J. Can. Pet. Technol*., 41(9): 51-61, 2002.

Sheikha, H. and Pooladi-Darvish, M. The Effect of Pressure Decline Rate and Pressure Gradient on the Behaviour of Solution Gas Drive in Heavy Oil. *SPE Reservoir Eval. Eng.*, 12 (3): 390-398, 2009.

Shi, W., Corwith, J., Bouchard, A., Bone, R., and Reinhold, E. Kuparuk MWAG Project after 20 Years. Paper SPE 113933, presented at the SPE/DOE Symposium on Improved Oil Recovery, Tulsa, OK, April 20-23, 2008.

Shtepani, E. Experimental and Modeling Requirements for Compositional Simulation of Miscible CO_2-EOR Processes. Paper SPE 111290, presented at the SPE/EAGE Reservoir Characterization and Simulation Conference, Abu Dhabi, UAE, October 28-31, 2007.

Shu, W.R. A Viscosity Correlation for Mixtures of Heavy Oil, Bitumen, and Petroleum Fractions. *SPE J.*, 24 (6): 277-282, 1984.

Simon, R. and Graue, D.J., Generalized Correlations for Predicting Solubility, Swelling and Viscosity Behaviour of CO_2-Crude Oil Systems. *J. Pet. Technol*., 17 (1): 102-106, 1965.

Singhal, A.K., Sim, S., and Hawkins, B. Gas Return from Gas Injection Projects. Paper CIPC 2008-72, presented at the Canadian International Petroleum Conference, Calgary, AB, June 17-19, 2008.

Smith, G.E. Fluid Flow and Sand Production in Heavy-Oil Reservoirs under Solution-Gas Drive. *SPE Prod. Eng.*, 3 (2): 169-180, 1988.

Smith, G.E. Waterflooding Heavy Oils. Paper SPE 24367, presented at the SPE Rocky Mountain Regional Meeting, Casper, WY, May 18-21, 1992.

Sohrabi, M., Henderson, G.D., Tehrani, D.H., and Danesh, A. Visualisation of Oil Recovery by Water Alternating Gas (WAG) Injection Using High Pressure Micromodels-Water-Wet System. Paper SPE 63000, presented at the SPE Annual Technical Conference and Exhibition, Dallas, TX, October 1-4, 2000.

Sohrabi, M., Tehrani, D.H., Danesh, A., and Henderson, G.D. Visualisation of Oil Recovery by Water Alternating Gas (WAG) Injection Using High Pressure Micromodels Oil-Wet and Mixed-Wet Systems. Paper SPE 71494, presented at the SPE Annual Technical Conference and Exhibition, New Orleans, LA, September 30-October 3, 2001.

Sommerauer G. and Petersen, R. Implementation of Pressure Maintenance in Seria Field Using Limited Entry Fractured Water Injection. Paper SPE 84884, presented at the SPE International Improved Oil Recovery Conference in Asia Pacific, Kuala Lumpur, Malaysia, October 20-21, 2003.

Speight, J.G. Enhanced Recovery Methods for Heavy Oil and Tar Sands, Gulf Pub. Co., Houston, pp: 13-14, 2009.

Spivak, A. and Chima, C.M. Mechanisms of Immiscible CO_2 Injection in Heavy Oil Reservoirs, Wilmington Field, CA. Paper SPE 12667, presented at the SPE Enhanced Oil Recovery Symposium, Tulsa, OK, April 15-18, 1984.

Spivak, A., Karaoguz, D., Issever, K., and Nolen, J.S. Simulation of Immiscible CO_2 Injection in a Fractured Carbonate Reservoir, Bati Raman Field, Turkey. Paper

SPE 18765, presented at the SPE California Regional Meeting, Bakersfield, CA, April 5-7, 1989.

Srivastava, R. and Huang, S. Technical Feasibility of CO_2 Flooding in Weyburn Reservoir-A Laboratory Investigation. *J. Can. Pet. Technol*., 36 (10): 48-55, 1997.

Srivastava, R.K, Huang, S., and Dong, M. Laboratory Investigation of Weyburn CO_2 Miscible Flooding. *J. Can. Pet. Technol.*, 39 (2): 41-51, 2000.

Srivastava, R.K., Huang, S., and Dong, M. Comparative Effectiveness of CO_2, Produced Gas, and Flue Gas for Enhanced Heavy-Oil Recovery. *SPE Reserv. Eval. Eng.*, 2(3): 238-247, 1999.

Surguchev, L.M., Ragnhild, K., and Krakstad, O.S. Optimum Water Alternate Gas Injection Schemes for Stratified Reservoirs. Paper SPE 24646, presented at the SPE Annual Technical Conference and Exhibition, Washington, DC, October 4-7, 1992.

Taber, J.J. Technical Screening Guides for the Enhanced Recovery of Oil. Paper SPE 12069, presented at the SPE Annual Technical Conference and Exhibition, San Francisco, CA, October 5-8, 1983.

Taber, J.J., Martin, F.D., and Seright, R.S. EOR Screening Criteria Revisited-Part 1: Introduction to Screening Criteria and Enhanced Recovery Field Projects. *SPE Reservoir Eng*., 12 (3): 189-198, 1997.

Taber, J.J., Martin, R.S., and Seright, R.S. EOR Screening Criteria Revisited-Part 2: Applications and Impact of Oil Prices. *SPE Reservoir Eng*., 12 (3): 199-206, 1997.

Tavassoli, Z., Carter J.N., and King, P.R. Errors in History Matching. *SPE J.*, 9 (3): 352-361, 2004.

Tehrani, D.H., Danesh, A., Sohrabi, M., and Henderson, G. Improved Oil Recovery from Oil-wet and Mix-wet Reservoirs by Gas Flood, Alternate with Water. Presented at the 22nd Annual Workshop and Symposium Collaborative Project on Enhanced Oil Recovery International Energy Agency, Vienna, September**,** 2001.

Teja, A.S. and Sandler, A.I. A Corresponding States Equation for Saturated Liquid Densities. II. Applications to the Calculation of Swelling Factors of CO_2-Crude Oil Systems. *AICHE J.*, 26 (3): 341-345, 1980.

Thomas, B. Proposed Screening Criteria for Gas Injection Evaluation. *J. Can. Pet. Technol*., 37 (11): 14-20, 1998.

Todd, M.R. Modeling Requirements for Numerical Simulation of CO_2 Recovery Processes. Paper SPE 7998, presented at the SPE California Regional Meeting, Ventura, CA, April 18-20, 1979.

Turta, A.T., Singhal, A.K., Goldman, J., and Zhao, L. Toe-To-Heel Waterflooding. Part II: 3D Laboratory-Test Results. *SPE Reservoir Eval. Eng*., 9 (3): 202-208, 2006.

Tüzünoğlu, E. and Bağci, S. Scaled 3-D Model Studies of Immiscible CO_2 Flooding Using Horizontal Wells. *J. Pet. Sci. Eng.*, 26 (1-4): 67-81, 2000.

Vanegas Prada, J.W. and Cunha, L.B. Prediction of SAGD Performance Using Response Surface Correlations Developed by Experimental Design Techniques. *J. Can. Pet. Technol*., 47 (9): 58-64, 2008.

Vittoratos, E., Scott, G.R., and Beatie, C.I. Cold Lake Cyclic Steam Stimulation: A Multiwell Process. *SPE Reservoir Eng.*, 5 (1):19-24, 1990.

Wang, G.C. and Locke, D.C. A Laboratory Study of the Effects of CO_2 Injection Sequence on Tertiary Oil Recovery. *SPE J.*, 20 (4): 278-280, 1980.

Watson, A.T., Seinfeld, J.H., Gavalas, G.R., and Woo, P.T. History Matching in Two-Phase Petroleum Reservoirs. *SPE J.*, 20 (6): 521-532, 1980.

Weinbrandt, R.M., Ramey Jr., H.J., and Casse, F.J. The Effect of Temperature on Relative and Absolute Permeability of Sandstones. *SPE J*., 15 (5): 376-384, 1975.

Welker, J.R. and Dunlop, D.D. Physical Properties of Carbonated Oils. *J. Pet. Technol*., 15 (8): 873-876, 1963.

Wilson, M.A. and Bennett, R.W. Heavy Oil Project-Evaluation of Saskatchewan's Heavy Oil Reserves. Saskatchewan Energy and Resources, SK, 1985.

Wood, D.J., Lake, L.W., Johns, R.T., and Nunez, V. A Screening Model for CO_2 Flooding and Storage in Gulf Coast Reservoirs Based on Dimensionless Groups. *SPE Reserv. Eval. Eng*., 11 (3): 513-520, 2008.

Wu, G.Q. and Kantzas, A. Experimental Study of Gas Solvent Flooding for Lloydminster Heavy Oil Reservoirs. Paper CIPC 2008-135, presented at Canadian International Petroleum Conference, June 17-19, Calgary, AB, 2008.

Yang, C. and Gu, Y. Diffusion Coefficient and Oil Swelling Factors of Carbon Dioxide, Methane, Ethane, Propane, and Their Mixture in Heavy Oil. *Fluid Phase Equilibr*., 243 (1-2): 64-73, 2006.

Yang, D. and Gu, Y. Interfacial Interactions between Crude Oil and CO_2 under Reservoir Conditions. *Pet. Sci. Technol*., 23 (9-10): 1099-1112, 2005.

Yang, D. and Gu, Y. Visualization of Interfacial Interactions of Crude Oil-CO_2 Systems under Reservoir Conditions. Paper SPE 89366, presented at the SPE/DOE Symposium on Improved Oil Recovery, Tulsa, OK, April 17-21, 2004.

Yang, D., Zhang, Q., Cui, H., Feng, H., and Li, L. Optimization of Multivariate Production-Injection System for Water-Alternating-Gas Miscible Flooding in Pubei Oil Field, Paper SPE 62856, presented at the SPE/AAPG Western Regional Meeting, Long Beach, CA, June 19-22, 2000.

Zhang, F., Fan, X., and Ding, J. Field Experiment of Enhancing Heavy Oil Recovery by Cyclic Fuel Gas Injection. Paper SPE 64724, presented at the SPE International Oil and Gas Conference and Exhibition, Beijing, China, November 7-10, 2000.

Zhang, Y., Huang, S. and Luo, P. Coupling Immiscible CO_2 Technology and Polymer Injection to Maximize EOR Performance for Heavy Oils. *J. Can. Pet. Technol.*, 49 (5): 25-33, 2010.

Zheng, S. and Yang, D. Pressure Maintenance and Improving Oil Recovery via Water-Alternating-CO_2 Process in Thin Heavy Oil Reservoirs. Paper SPE 157719, presented at the SPE Heavy Oil Conference Canada, Calgary, AB, June 12-14, 2012.

Zheng, S., Li, H., and Yang, D. Pressure Maintenance and Improving Oil Recovery with CO_2 Injection in Heavy Oil Reservoirs. Paper SPE 150169, presented at the SPE Heavy Oil Conference and Exhibition, Kuwait City, Kuwait, December 12-14, 2011.

Zhu, T., Strycker, A., Raible, C.J., and Vineyard, K. Foams for Mobility Control and Improved Sweep Efficiency in Gas Flooding. Paper SPE 39680, presented at the SPE/DOE Improved Oil Recovery Symposium, Tulsa, OK, April 19-22, 1998.

Zuo, Y. and Stenby, E.H. Prediction of Interfacial Tensions of Reservoir Crude Oil and Gas Condensate Systems. *SPE J.*, 3 (2): 134-145, 1998.